UNIVERSITA' VITA-SALUTE SAN RAFFAELE

CORSO DI DOTTORATO DI RICERCA INTERNAZIONALE IN MEDICINA MOLECOLARE

Curriculum in Basic and Applied Immunology and Oncology

Study the dynamics of HBsAg-specific B cells in mouse model of HBV pathogenesis

DoS: Prof. Matteo Iannacone

Second Supervisor: Prof. Ziv Shulman

Tesi di DOTTORATO DI RICERCA di Marta Grillo

Matr. 019205

Ciclo di Dottorato XXXVII

SSD BIO/13

Anno Accademico 2023/2024

UNIVERSITA' VITA-SALUTE SAN RAFFAELE

CORSO DI DOTTORATO DI RICERCA INTERNAZIONALE
IN MEDICINA MOLECOLARE

Curriculum in Basic and Applied Immunology and Oncology

Study the dynamics of HBsAg-specific B cells in mouse model of HBV pathogenesis

DoS: Prof. Matteo Iannacone

Second Supervisor: Prof. Ziv Shulman

Tesi di DOTTORATO DI RICERCA di Marta Grillo

Matr. 019205

Ciclo di Dottorato XXXVII

SSD BIO/13

Anno Accademico 2023/2024

CONSULTAZIONE TESI DI DOTTORATO DI RICERCA

I ***Marta Grillo***

Registration number: ***019205***

Born at: ***Roma (RM)***

On: ***09/12/1997***

Author of the PhD Thesis titled:

STUDY THE DYNAMICS OF HBSAG-SPECIFIC B CELLS IN MOUSE MODEL OF HBV PATHOGENESIS

AUTHORIZES the public release of the thesis

Copyright the contents of the thesis in whole or in part is forbidden

Date 25/10/2024

Signature …….....

DECLARATION

This thesis has been:

- composed by myself and has not been used in any previous application for a degree. Throughout the text I use both 'I' and 'We' interchangeably.

- has been written according to the editing guidelines approved by the University.

Permission to use images and other material covered by copyright has been sought and obtained. For the following images (Figure 1, Figure 2), it was not possible to obtain permission and are therefore included in thesis under the "fair use" exception (Italian legislative Decree no. 68/2003).

All the results presented here were obtained by myself, except for:

1) *qPCR experiments were performed by a senior technician of our lab, Dr. Leonardo Giustini, Dynamics of immune responses, San Raffaele Scientific Institute, Milan, Italy.*
2) *Serum alanine aminotransferase (sALT) activity was measured by Dr. Micol Ravà, Mouse Clinic, San Raffaele Scientific Institute, Milan, Italy.*
3) *Liver tissues for immunohistochemistry were processed by Dr. Amleto Fiocchi, Animal Histopathology Facility, San Raffaele Scientific Institute, Milan, Italy.*

All sources of information are acknowledged by means of reference.

ABSTRACT

Hepatitis B virus (HBV) infection remains a major global health challenge, affecting over 250 million people worldwide and contributing to severe liver diseases, including cirrhosis and hepatocellular carcinoma. Despite the availability of preventive vaccines, therapeutic options for chronic HBV infection are limited due to an incomplete understanding of the immune mechanisms underlying HBV pathogenesis. A key marker of immune control over HBV infection is Hepatitis B surface antigen (HBsAg) seroconversion. The presence of antibodies against the HBV surface antigen, in fact, signifies Hepatitis B infection resolution and seroconversion correlates with favourable clinical outcomes. However, the cellular and molecular mechanisms driving spontaneous HBsAg seroconversion are not fully elucidated.

With the aim of investigating the mechanisms of spontaneous seroconversion in HBV pathogenesis, we took advantage of HBV-replication competent transgenic mice (HBV Tg). Around ~60% of HBV Tg mice spontaneously develop anti-HBsAg antibodies which clear circulating virions and subviral particles, leading to seroconversion. Our findings show that, in HBV Tg mice that spontaneously lose HBsAg, anti-HBs-producing B cells are predominantly found in the spleen, liver, bone marrow, and colon, playing a crucial role in HBsAg clearance. This antibody-mediated clearance requires $CD4^+$ T cell help. HBV Tg mice lacking in CD40L or MHC-II expression, thus deficient in $CD4^+$ T cells, fail to generate anti-HBsAg antibodies and cannot clear HBsAg. Moreover, we find that adoptive transfer of $CD4^+$ T cells from seroconverted mice can restore the capacity for HBsAg clearance in antigen-persistent HBV Tg mice. Furthermore, the study explores the role of the intestinal microbiome in HBs seroconversion. By conducting faecal microbiota transplants (FMT) in HBV Tg mice, we observed that recipients of FMT from seroconverted donors exhibited significant reductions in serum HBsAg. Moreover, we showed that the intestinal microbiome alone could lead to HBs seroconversion, suggesting a direct role of the gut-liver axis in HBV immunity.

While the impact of these findings in humans requires further investigation, this research provides a foundational understanding of the immune and microbial mechanisms underpinning HBsAg seroconversion, with potentially broader implications for other viral infections. These insights could inform future therapeutic strategies aimed at enhancing HBV clearance and improving clinical outcomes in chronic HBV patients.

TABLE OF CONTENT

1. LIST OF FIGURES AND TABLE 7

2. INTRODUCTION 10

2.1. The Liver 10

2.1.1. Overview 10

2.1.2. Liver anatomy 11

2.1.3. Immunological features of the liver 12

2.1.4. Gut-Liver axis 13

2.2. Hepatitis B Virus (HBV) 15

2.2.1. HBV infection: generalities 15

2.2.2. Hepatitis B virus: virological features 16

2.2.3. HBV pathogenesis: acute and chronic infection 18

2.3. Liver immune response in HBV infection 20

2.3.1. B cell-mediated immunity in HBV infection 21

2.3.1.1. HBV-specific antibodies 22

2.3.1.2. HBV surface antigen (HBsAg) seroconversion 23

2.3.1.3. B cells and their immune response in HBV infection 24

2.3.1.4. $CD4^+$ T cell responses in HBV infection 25

2.3.1.5. Crosstalk between B cells and $CD4^+$ T cells 26

2.4. The role of gut microbiota in HBV infection 27

2.5. Experimental models to study HBV pathogenesis and HBsAg-seroconversion 28

3. AIM OF THE WORK 32

4. RESULTS 34

4.1. Aim I: Localisation and characterisation of endogenous HBsAg-Specific B cells in HBV-replication competent transgenic mice 34

4.1.1. Spontaneous HBsAg seroconversion in female HBV-replication competent transgenic mice *34*

4.1.2. HBsAg-Specific B cells localise to the spleen, liver, bone marrow, and colon following seroconversion in HBV transgenic mice *36*

4.1.3. Characterisation of global B cell populations in HBsAg$^+$ and HBsAg$^-$ HBV transgenic mice reveals no significant differences *40*

4.1.4. Summary Aim I *42*

4.2. Aim II: Study the role of CD4$^+$ T cell in promoting HBsAg seroconversion 44

4.2.1. CD40-CD40L and MHC-II pathways are essential for the anti-HBsAg antibody response in HBV transgenic mice *44*

4.2.2. Enhanced Tfh cell frequency and IFNɣ production characterise CD4$^+$ T cell responses in HBsAg$^-$ HBV transgenic mice *49*

4.2.3. Adoptive transfer of CD4$^+$ T cells from HBsAg$^-$ mice resolves HBsAg persistence 51

4.2.4. Summary of Aim II *53*

4.3. Aim III: Investigating the role of the microbiome in promoting the HBsAg seroconversion 55

4.3.1. Faecal microbiota transplant from HBsAg$^-$ mice leads to seroconversion *55*

4.3.2. Faecal Microbiota Transplantation fails to induce HBsAg clearance in HBV Tg x CD40L$^{-/-}$ mice *60*

4.3.3. Antibiotic treatment alone fails to induce HBsAg clearance without microbiome reconstitution *62*

4.3.4. Co-housing with seroconverted mice promotes HBsAg clearance in antigen-persistent HBV transgenic mice *64*

4.3.5. Summary of Aim III *66*

5. DISCUSSION 68

6. MATERIALS AND METHODS 79

6.1. Mouse models 79

6.2. Organ processing 79

6.2.1. Spleen 79

6.2.2. Liver 80

6.2.3. Bone marrow 80

6.2.4. Lymph node 80

6.2.5. Payer's patches 80

6.2.6. Colon 81

6.3. Cell culture and cell purification 81

6.3.1. B cell and $CD4^+$ T cell purification 81

6.4. *In vivo* cell adoptive transfers 81

6.5. ELISPOT Assay 82

6.6. Serum Immunoglobulin ELISA 82

6.7. Cell labelling and Flow cytometry 82

6.7.1. Surface and intracellular staining 82

6.7.2. Tetramer preparation 85

6.8. Histochemistry 85

6.9. Purification of viral nuclei acids from serum and qPCR analyses 85

6.10. Antibiotic treatment 86

6.11. Faecal microbiota transplant (FMT) 86

6.12. Murine stool collection and stool culture 86

6.13. Biochemical analysis 87

6.14. Statistical analysis 87

7. REFERENCES 89

ACRONYMS AND ABBREVIATIONS

AAV	Adeno-associated Viruses
Ag	Antigen
AHB	Acute Hepatitis B
ALT	Alanine Aminotransferase
APC	Antigen Presenting Cell
atMBC	Atypical Memory B Cells
AxFl	Alexa Fluor
BCR	B Cell Receptor
BM	Bone Marrow
cccDNA	Covalently Closed Circular DNA
CD	Cluster Differentiation antigen
CFU	Colony-forming Units
CHB	Chronic Hepatitis B
DC	Dendritic Cell
DNA	Deoxyribonucleic Acid
EDTA	EthylenDiaminoTetracetyc Acid
ER	Endoplasmic Reticulum
FACS	Fluorescent Activated Cell Sorter
FBS	Foetal Bovine Serum
FMT	Faecal Microbiota Transplantation
GC	Germinal Centre
H&E	Haematoxylin and Eosin
HBcAg	HBV-core Antigen
HBeAg	HBV "e" Antigen
HBsAb	anti-HBV-surface antigen Antibody
HBsAg	HBV-surface Antigen
HBSS	Hanks' Balanced Salt Solution
HBV	Hepatitis B Virus
HCC	Hepatocellular Carcinoma
HCV	Hepatitis C Virus

HNF1α	Hepatocyte nuclear factor 1 alpha
HSC	Hepatic Stellate Cell
HSPG	Heparan Sulphate Proteoglycans
i.v.	Intravenously
IFN	Interferon
Ig	Immunoglobulin
IHL	Intrahepatic Leukocytes
IL	Interleukin
ILC1	Innate Lymphoid Cells Type 1
KC	Kupffer Cell
LCMV	Lymphocytic Choriomeningitis Virus
LSEC	Liver Sinusoidal Endothelial Cell
MAMP	Microbial-associated Molecular Pattern
MBC	Memory B Cell
MHC	Major Histocompatibility Complex
mLN	Mesenteric Lymph Node
NF-kB	Nuclear Factor Kappa-light-chain-enhancer of activated B cells
NK	Natural Killer
NTCP	Na+-Taurocholate Co-transporting Polypeptide
ORF	Open Reading Frames
PBS	Phosphate Buffered Saline
PC	Plasma Cell
PCK	Protein Kinase C
pgRNA	Pre-Genomic RNA
PMA	Phorbol 12-myristate 13-acetate
Rag	Recombination-Activating Gene
rcDNA	Relaxed Circular DNA
SCA	Short-chain Fatty Acids
SLO	Secondary Lymphoid Organ
SVP	Subviral Particles
TCR	T-cell Receptor
Tet	Tetramer

Tfh	T Follicular Helper
Tfr	T Follicular Regulatory
Tg	Transgenic
TLS	Tertiary Lymphoid Structure
TNF	Tumour Necrosis Factor
Treg	Regulatory T
WT	Wild Type

1. LIST OF FIGURES AND TABLE

Figure 1. Liver anatomy 11
Figure 2. Liver parenchyma and liver cell subsets 13
Figure 3. The Gut-Liver axis 15
Figure 4. HBV viral particle and genomic structure 16
Figure 5. HBV life cycle 18
Figure 6 . Course of acute and chronic infection with HBV 20
Figure 7. Antiviral function of anti-HBs antibodies in HBV infection 23
Figure 8. Crosstalk between B cells and $CD4^+$ T 27
Figure 9. HBV replication-competent transgenic mice spontaneously undergo HBs-seroconversion 30
Figure 10. Female HBV replication-competent transgenic mice spontaneously undergo HBs-seroconversion 36
Figure 11. HBsAg-Specific B cells localise to the spleen, liver, bone marrow, and colon following seroconversion in HBV transgenic mice 37
Figure 12. Detection of HBs-specific B cells by HBsAg-tetramers 38
Figure 13. Anti-HBs highly restricted to IgG1 and IgG3 in $HBsAg^-$ HBV transgenic mice 39
Figure 14. Characterisation of global B cell populations in $HBsAg^+$ and $HBsAg^-$ HBV transgenic mice 42
Figure 15. CD40-CD40L engagement has a role in the antibody-mediated clearance of the surface antigen and the generation of HBsAg-specific B cells in HBV transgenic mice 46
Figure 16. Antigen presentation has a role in the antibody-mediated clearance of the surface antigen in HBV transgenic mice 48
Figure 17. Characterisation of global $CD4^+$ T cell populations in $HBsAg^+$ and $HBsAg^-$ HBV transgenic mice 50
Figure 18. Splenocyte transfer of $CD4^+$ T cells from $HBsAg^-$ mice resolves HBsAg persistence 53
Figure 19. Cage-mates exhibit similar trends in serum HBsAg and HBsAb levels 56

Figure 20. Faecal microbiota transplant in young HBV Tg mice from HBsAg^{+} and HBsAg^{-} donor mice 58
Figure 21. Faecal microbiota transplant from HBsAg^{-} mice leads to seroconversion 59
Figure 22. Faecal Microbiota Transplantation fails to induce HBsAg clearance in HBV Tg x CD40L$^{-/-}$ mice 61
Figure 23. Impact of antibiotic treatment and microbiome reconstitution on HBsAg clearance, antibody production in HBV Tg mice 63
Figure 24. Co-housing with seroconverted mice promotes HBsAg clearance in antigen-persistent HBV transgenic mice 65

Table 1. List of Antibodies 85

INTRODUCTION

2. INTRODUCTION

2.1. The Liver

2.1.1. Overview

One of the leading causes of death globally is liver disease. In fact, the combined fatalities from Hepatitis B (HBV), Hepatitis C (HCV), malaria, and complications arising from alcohol-related diseases, amount to nearly 3 million per year (Ficht & Iannacone, 2020). In particular, Hepatitis B virus infection is a major contributor to liver diseases, triggering complications like cirrhosis and hepatocellular carcinoma, which claim around 1 million lives per year (www.who.int/news-room/fact-sheets).

The high mortality rate associated with liver disease is a direct result of the liver's critical functional, metabolic, and physiological roles. Indeed, the liver is responsible for many vital functions including i) energy storage, ii) maintaining blood homeostasis, iii) extracting and metabolising a wide array of nutrients, foreign substances, and damaged molecules and cells, and iv) neutralising microbes and microbial products coming from the gut (Arias *et al*, 2009; Ben-Moshe & Itzkovitz, 2019).

Beyond its vital physiological importance, the liver is also an immunologically complex organ due to its unique architecture and specialised immune cell populations (Robinson *et al*, 2016). It serves as a critical interface between the systemic circulation and the gut microbiome, enabling the liver to process antigens and manage immune responses to prevent excessive inflammation. Indeed, the progression of HBV-related liver disease hinges on the balance between immune control and immune tolerance. In particular, adaptive immune responses are crucial in resolving viral infections or promoting inflammation, depending on the liver's microenvironment. The presence of various immune cell types, such as Kupffer cells, dendritic cells, and regulatory T cells, contributes to this complexity by modulating the immune response and maintaining homeostasis. Therefore, understanding the functional biology of immune cells within the liver's unique environment, especially in the context of hepatotropic virus infections, is essential.

2.1.2. Liver anatomy

The unique structure of the liver has a profound impact on how the immune system functions within this organ. The liver is a multicellular tissue characterised by a unique angioarchitecture. The parenchyma is primarily composed of hepatocytes, organised into functional units called lobules; they have a hexagonal shape where blood enters at the corners, known as portal tracts (made up by lymphatics, a branch of the portal vein, a branch of hepatic artery, and a tributary of the bile duct), and flows radially inward through sinusoidal blood vessels towards a draining central vein (**Figure 1 B**). Nutrient-rich blood arrives to the liver from the gastrointestinal tract through the portal vein, while oxygen-rich blood enters through the hepatic artery (**Figure 1 A**) (Jenne & Kubes, 2013; Ben-Moshe & Itzkovitz, 2019). The incoming blood mixes in the sinusoids, liver-specific capillaries. These are composed of liver sinusoidal endothelial cells (LSECs) which lack in organised basement membrane and contain numerous fenestrae. These fenestrae facilitate the exchange of small molecules between the blood and the hepatocytes, aiding essential liver functions. Furthermore, the absence of a basal membrane creates a gap known as the space of Disse, limiting direct contact between the liver parenchyma and the sinusoidal lumen (Wisse *et al*, 1996; Zheng *et al*, 2013).

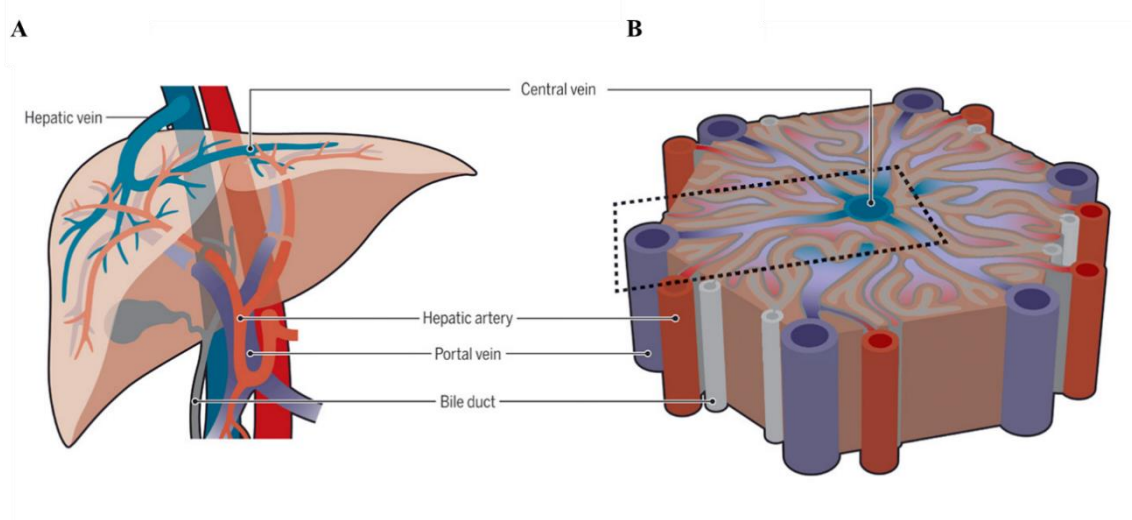


Figure 1. Liver anatomy

(A) *Representation of the macro-anatomy of the human liver: Nutrient-rich blood arrives through the portal vein, while oxygen-rich blood enters through the hepatic artery. The blood then flows out through the hepatic vein.* ***(B)*** *Schematic representation of the liver lobule: hexagonal shaped*

columns delimited by portal tracts. Here the blood flows towards the central veins by which it exits the organ. (Adapted from Ficht X and Iannacone M., 2020)

2.1.3. Immunological features of the liver

As mentioned before, its intricate structure and its heterogeneous immune cell composition define the liver as an immunologically complex organ (**Figure 2**) (Racanelli & Rehermann, 2006). The slow blood flow within the microcirculatory system (Sironi *et al*, 2014), the presence of fenestrae (Warren *et al*, 2006), and the absence of a basement membrane, allows facilitated contact between circulating pathogens and the endothelium, leading to the detection and capture by liver resident antigen presenting cells (APCs) and the arrival of lymphocytes. The liver contains several types of antigen-presenting cells, including Kupffer cells (KCs), dendritic cells (DCs), and LSECs. Among them, KCs are the most abundant; they act as immune sentinels by protruding portions of their cell bodies into the space of Disse, where they interact with hepatic stellate cells (HSCs) and hepatocytes. Furthermore, KCs support T cell responses in the presence of inflammatory cytokines (Ficht & Iannacone, 2020).

The liver houses many other immune cells. For example, group 1 ILCs, (including both innate lymphoid cells type 1 (ILC1) and natural killer (NK) cells) and NKT cells are more prevalent in the liver compared to other tissues. These cells are able to kill target cells through the release of cytotoxic molecules and can also shape the immune responses by producing inflammatory cytokines to recruit circulating lymphocytes. In addition, the liver contains a diverse array of lymphocytes distributed throughout the liver parenchyma and within the portal tracts (**Figure 2**). Among these, $CD8^+$ T cells are particularly abundant, outnumbering $CD4^+$ T cells, along with other adaptive immune system cells such as B cells (Crispe, 2003; Racanelli & Rehermann, 2006; Ficht & Iannacone, 2020).

This coordination between liver-resident immune cells and circulating leukocytes allows to have a balance between immunity and tolerance. Under physiological conditions, liver resident cells express low levels of major histocompatibility complex (MHC), both class I and class II, and costimulatory molecules, crucial for limiting immune responses thereby avoiding severe immune-mediated damage (Knolle *et al*, 2015). The liver's immunosuppressive environment partly explains why certain

hepatotropic viruses, such as HBV, can exploit it to establish persistent infections (Guidotti & Chisari, 2006). However, despite this tendency towards immune tolerance, the liver can mount a robust immune response, as seen in HBV-infected patients who can clear the virus during the acute phase of the infection (Iannacone & Guidotti, 2022).

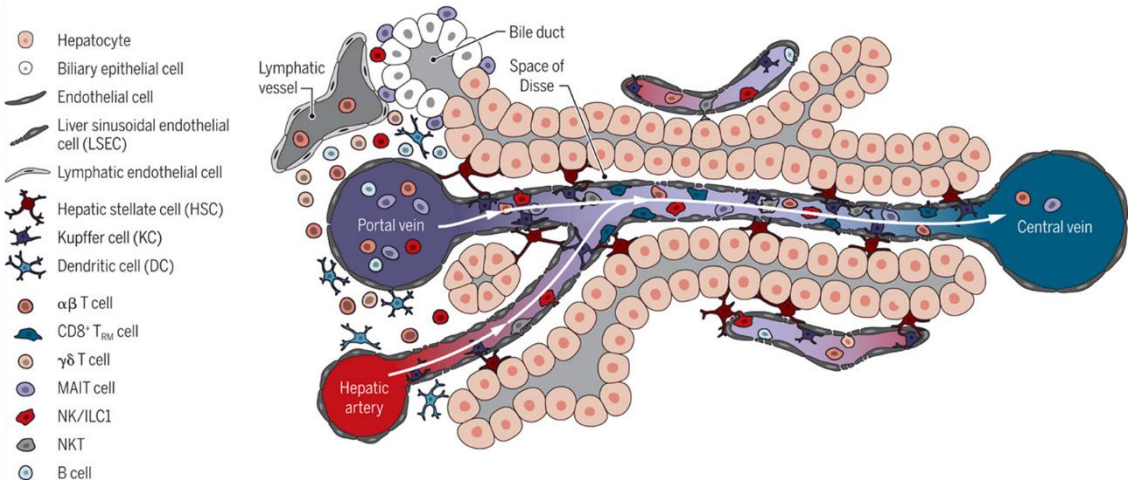


Figure 2. Liver parenchyma and liver cell subsets

Schematic representation of the cell subtest within the liver. Hepatocytes are arranged in chords and are surrounded by bile ducts where bile is collected and then released in the portal tracts. Fenestrated LSECs constitute the specialized liver endothelium, sinusoids. HSCs are located within the space of Disse. KCs are found in the vasculature. DCs are mainly found near the portal tract. Other immune cell subsets include Mucosal Associated Invariant T (MAIT) cells, NK cells, NK-T, γδ T cells, and B cells. The direction of the blood flow is indicated by arrows. (Adapted from Ficht X and Iannacone M., 2020)

2.1.4. Gut-Liver axis

The liver extensively interacts with the gut via several pathways. Blood from the small and the large intestine drains into the portal vein, carrying gut-derived products, such as nutrients, metabolites and microbial-derived products, to the liver. The liver, in turn, communicates with the gut through the biliary duct; bile, containing bile acids and antimicrobial molecules, is secreted into the intestine, modulating gut mobility, permeability, as well as regulating the gut microbiota. This bidirectional crosstalk is known as the gut–liver axis (**Figure 3**) (Hartmann *et al*, 2015; Tripathi *et al*, 2018; Milosevic *et al*, 2019; Albillos *et al*, 2020). The gut microbiota constitutes a central

element of the gut-liver axis, shaping the physiology and pathophysiology of both the gut and the liver (Tripathi *et al*, 2018; Hsu & Schnabl, 2023). Comprising of more than 100 trillion microorganisms including bacteria, fungi, viruses and archaea, the gut microbiota significantly impacts health. Additionally, the gut microbiome encompasses these microorganisms, their genes, and the environmental factors that influence them (Huttenhower *et al*, 2012). Liver immunology is deeply intertwined with the gut microbiota. In fact, immune cells in the liver, such as KCs and hepatic DCs are strategically located in the sinusoids to clear the portal blood from gut-derived microorganisms and microbial-associated molecular patterns (MAMPs). For example, KCs detect microbial products and metabolites that enter the liver, leading to the production of pro-inflammatory cytokines and chemokines, while DCs in the liver present antigens from gut-derived microbes to T cells, thereby coordinating adaptive immune responses (Kazankov *et al*, 2018; De Muynck *et al*, 2021).

A balanced gut microbiota supports liver health by enhancing the metabolism of dietary compounds, reducing inflammation, and protecting against liver diseases. Disruption of this balance, known as dysbiosis, can impair the gut barrier, promote systemic inflammation, and lead to metabolic and liver-related disorders (Albillos *et al*, 2020; Wang *et al*, 2020b).

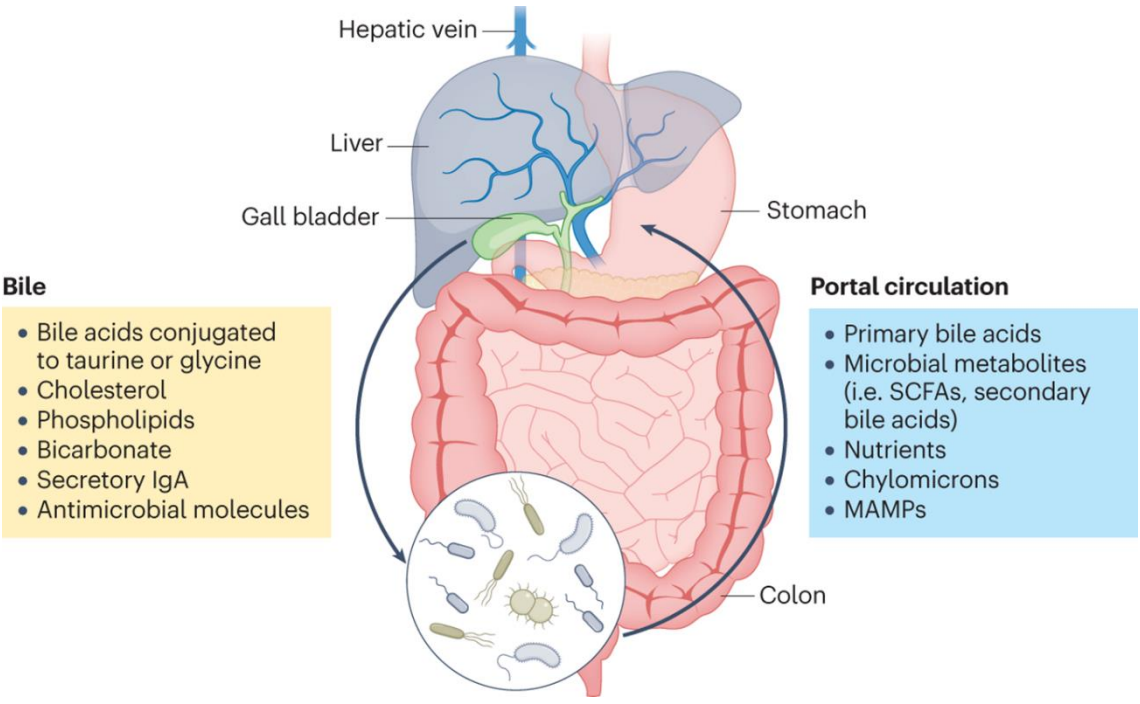


Figure 3. The Gut-Liver axis

Schematic representation of the bidirectional crosstalk between the liver and the gut. The liver produces bile, composed of cholesterol, phospholipids, proteins, bicarbonate, antimicrobial molecules, and bile acids, which is directed to the gut via the bile duct. It modulates gut mobility, permeability, and regulates the gut microbiota. Conversely, the gut's nutrients, lipids, microbial products, and microbial metabolites are brought to the liver through the portal vein and influence liver function. SCFAs, short-chain fatty acids; MAMP, microorganism-associated molecular pattern. (Adapted from Hsu C.L. & Schnabl B., 2023) (License Number 5896021240285)

2.2. Hepatitis B Virus (HBV)

2.2.1. HBV infection: generalities

Hepatitis B is an infection of the liver caused by Hepatitis B virus (HBV) and can lead to both acute and chronic disease. The severity and the duration of the disease hinges on the host's immune system's ability to clear the virus. In most immunocompetent adults, the infection is controlled, and the virus is cleared within a few months, resulting in acute hepatitis B. However, in some cases, for example in case of vertical transmission of the virus from mother to newborn, chronic hepatitis B can develop. This chronic infection triggers an inadequate immune response that cannot clear the virus, posing a long-term risk of complications like cirrhosis and hepatocellular carcinoma (HCC) (10 to 30% of chronic patients) (Guidotti & Chisari, 2006; Iannacone & Guidotti, 2022).

According to the World Health Organization (WHO), approximately 1.2 million people are infected with HBV annually. In 2022, around 254 million people were living with chronic HBV infection, and in the same year 1.1 million people died due to complications (liver cirrhosis and HCC). While highly effective preventive vaccines exist, offering nearly 98% protection against chronic infection, therapeutic options for persistent HBV infection remain limited (www.who.int/news-room/fact-sheets). This limitation is mainly due to the incomplete understanding of the immune mechanisms involved in HBV pathogenesis.

2.2.2. Hepatitis B virus: virological features

Hepatitis B virus is a member of the hepadnaviridae family, and is a non-cytopathic, hepatotropic DNA virus. It has a partially double stranded circular DNA of approximately 3.2 kb in size, packaged in an icosahedral nucleocapsid surrounded by a viral envelope. The mature HBV infectious virion is ≈ 42nm in diameter (**Figure 4 A**)(Guidotti & Chisari, 2006). The HBV genome contains four overlapping open reading frames (ORFs) that translate into vital viral proteins: the longest ORF encodes for a translating polymerase; the PreS1/PreS2/S-ORF encode for the three different components of the viral envelope: large (L), medium (M), and small (S) surface antigens (HBsAg); the PreC/C ORF which encodes for both the secretory protein of HBV called HBeAg and the core protein HBcAg. HBcAg assembles to form the viral nucleocapsid; the X ORF encodes for the 'X' protein (HBx), required for viral replication (**Figure 4 B**) (Tu *et al*, 2017).

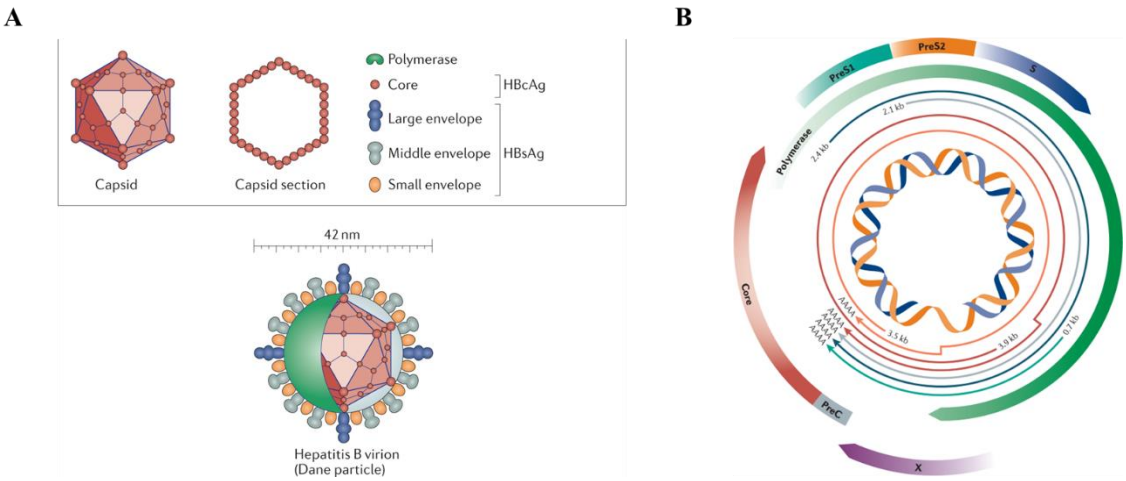


Figure 4. HBV viral particle and genomic structure

(A) *Representation of the HBV viral particle. The HBV virion is ~42 nm in diameter, consisting of an envelope made up by three different viral gene products termed large (L), middle (M), and small (S) envelope proteins, all expressing the determinant of HBsAg. Within this envelope is enclosed the nucleocapsid made up of HBsAg homodimers arranged in an icosahedral structure.* **(B)** *The coloured blocks represent the four main open reading frames (ORFs) that translate into vital viral proteins. At the centre, the helixes represent the partially double-stranded, relaxed circular DNA of HBV. The thin lines depict the overlapping RNAs produced by HBV genome translation. (Adapted from Iannacone M and Guidotti L, 2022) (License Number 5896030036389)*

The HBV replication cycle (**Figure 5**) commences with the attachment of the virus to its specific target, the hepatocyte. Initiation of infection is a multistep process that begins with the binding of highly conformational determinant region of the HBsAg to heparan sulphate proteoglycans (HSPGs) on the cell surface (Sureau & Salisse, 2013). HBV then forms a high specificity interaction between the N-terminal domain of the large HBsAg and the receptor sodium taurocholate co-transporting polypeptide (NTCP) found on the hepatocyte surface (Ni *et al*, 2014; Herrscher *et al*, 2020). Following the receptor-mediated internalization of the virion, the relaxed circular DNA (rcDNA) is eventually transported to the nucleus. Here the rcDNA is converted into covalently closed circular DNA (cccDNA) which serves as a transcriptional template. HBV transcripts are then transported to the cytoplasm for translation into viral proteins (Seeger & Mason, 2015). A crucial transcript is the pre-genomic RNA (pgRNA) that, together with the viral polymerase, is encapsidated into viral capsids. Within these capsids, pgRNA undergoes reverse transcription, generating single-stranded viral DNA, which then serves as a template for generating a second DNA strand, forming rcDNA. Some of these viral capsids are transported back to the nucleus to amplify the cccDNA pool, while others bud into the endoplasmic reticulum (ER), acquiring an envelope composed of the three forms of HBsAg. Finally, these mature virions are released into the bloodstream (Ganem & Prince, 2004; Tu *et al*, 2017; Iannacone & Guidotti, 2022). Notably, alongside infectious virions, the blood also contains non-infectious subviral particles (SVPs). The SVPs outnumber the virions by $\approx 10^6$ folds and are thought to act as a decoy for neutralising humoral responses which would otherwise limit the spread and replication of the virus (Kim & Tilles, 1973; Chai *et al*, 2008)

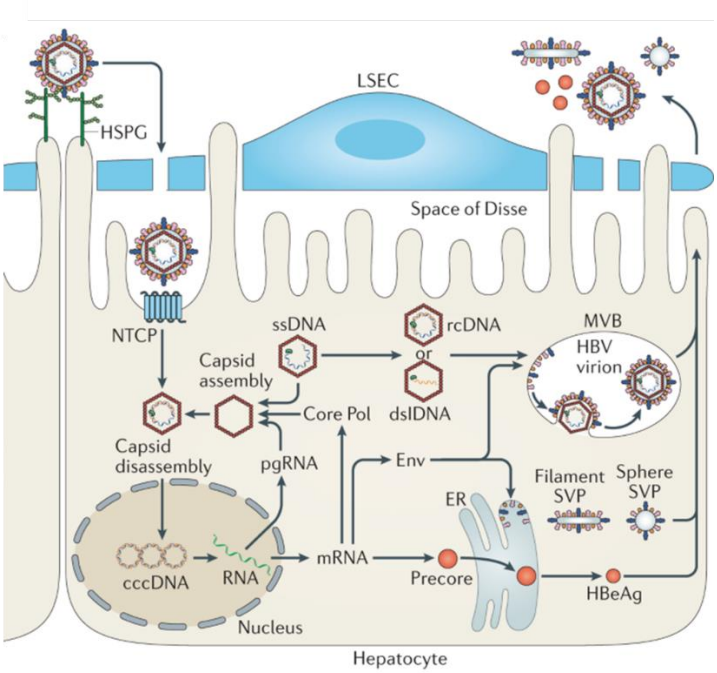


Figure 5. HBV life cycle

Upon entering the cell through the engagement of the NTCP, HBV's relaxed circular DNA reaches the nucleus and converts into cccDNA. This function as a template producing all the transcripts necessary for viral replication and virion assembly. The longest transcript, the pgRNA, serves for replication within nucleocapsids. These nucleocapsids acquire an envelope in the ER, forming mature virions released from the cell into the bloodstream. (Adapted from Iannacone M and Guidotti L, 2022) (License Number 5896030433334)

2.2.3. HBV pathogenesis: acute and chronic infection

HBV can be transmitted through horizontal and vertical transmission. Horizontal transmission encompasses diverse scenarios involving exposure to infected blood and bodily fluids (e.g. sexual contact with HBV-positive individuals, use of contaminated needles). In regions with high HBV prevalence, however, vertical transmission remains the most prevalent mode. Vertical transmission occurs from an infected mother to the child during birth (Yuen *et al*, 2018; www.who.int/news-room/fact-sheets). Under most circumstances, HBV is noncytopathic. Hepatocellular injury is, in fact, mediated by the host immune response.

During the initial phase of infection, there is a period (incubation period) of 4-7 weeks where the HBV DNA and HBsAg are undetectable. HBV is in fact a “stealth” virus, capable of evading initial innate immune responses (Wieland *et al*, 2004). In acute

infections in immunocompetent adults, once viremia becomes detectable, the HBV DNA level reach 10^8-10^9 viral copies per ml in the serum, correlated with the appearance of liver injury symptoms. A robust and coordinated adaptive immune response then leads to an increase in serum alanine aminotransferase (ALT), indicative of T-cell mediated liver injury, and a decrease in viral titres in the blood and liver (**Figure 6 A**) (Shin *et al*, 2016). Nearly 90% of acutely infected adults develop anti-HBeAg and anti-HBsAg specific antibodies after clearing the infectious virions. Consequently, the presence of HBV-specific T cells and specific antibodies provides lifelong protective immunity.

Acute hepatitis B (AHB) with complete clinical recovery is uncommon when the infection occurs perinatally and in very early childhood due to the immaturity of the immune system, which can lead to chronic infection. Chronic hepatitis B (CHB) infection can be divided into distinct phases (**Figure 6 B**). In the initial phase, termed the immune tolerance phase, is characterised by high viral load, high levels of circulating HBeAg and HBV DNA, near normal liver histology, and normal levels of ALT. This phase, which can persist for years, transitions to an immune active phase of the infection, where the activation of T-cell mediated immune response leads to an increase in ALT levels and a reduction of HBV DNA (McMahon, 2008; Shi & Shi, 2009). However, the intensity of the immune response varies over time, resulting in fluctuating levels of ALT, HBeAg, and HBV DNA. These fluctuations, also known as hepatitis flares, can cause liver damage and may lead to different degrees of fibrosis and cirrhosis. Most subjects spontaneously develop anti-HBeAg antibodies with a reduction of HBV DNA concentrations and transit to a low replicative phase (Seto *et al*, 2018; Yuen *et al*, 2018).

The diagnosis of HBV infection and determination of the disease phase primarily rely on serological analysis for the detection of specific HBV antigens and anti-HBV antibodies. In fact, while an assessment of the fibrosis and cirrhosis status through clinical, histological, and biochemical evaluations may contribute to the diagnosis workup, serological markers remain the cornerstone of HBV diagnosis (Lampertico *et al*, 2017). Detection of HBsAg in the serum serves as the standard serological test to confirm HBV infection for both acute and chronic disease. Chronic HBV infection is diagnosed by a repeat positive test 6 months after the initial positive test. On the other hand, in individuals who successfully recover from acute infection, HBsAg levels become undetectable. Importantly, HBsAg persists as a detectable marker even when HBV DNA

falls to undetectable levels. The detection of antibodies against HBsAg serves as a clinical marker. The presence of these antibodies signifies a favourable outcome, indicating both infection resolution and protection against future re-infection (Botha *et al*, 1984; Seto *et al*, 2014). Levels of HBeAg help distinguish two stages of infection: HBsAg-positive and HBeAg-negative chronic infection. The presence of anti-HBeAg antibodies marks the transition from the immune clearance phase to the immune control phase. Finally, total anti-HBc, measurable by immunoassay, is a marker of acute, chronic and resolved infection (Yuen *et al*, 2018).

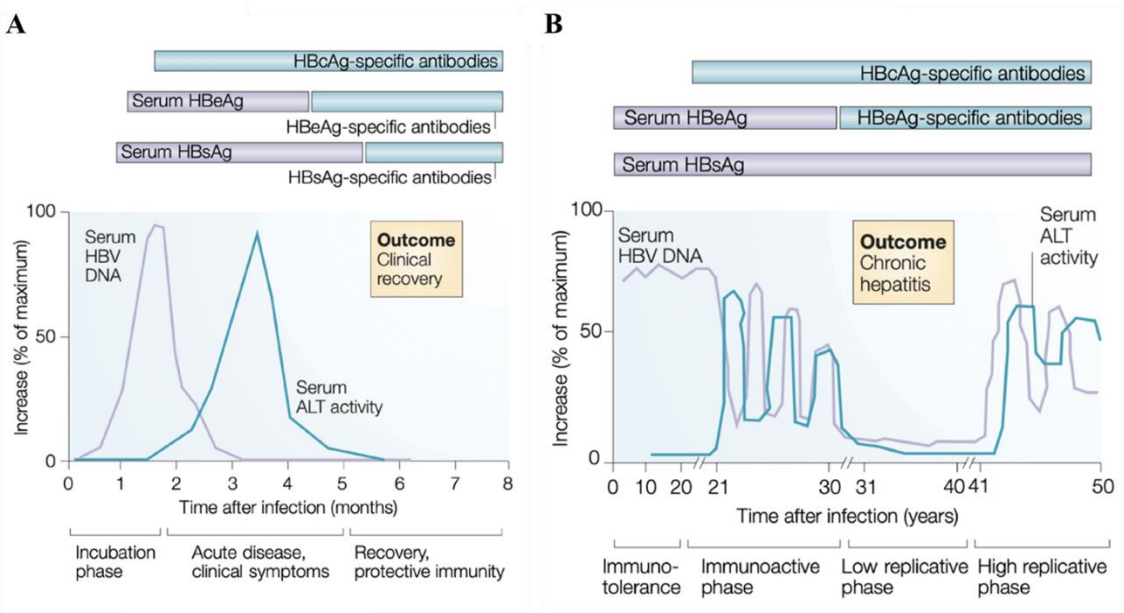


Figure 6 . Course of acute and chronic infection with HBV

Representation of the serological features that characterise HBV infection. Violet lines indicate serum HBV DNA levels, blue lines indicate serum ALT levels. Specific antibodies indicated with blue bars and HBV proteins in violet bars. **(A)** *Schematic representation of the serological features self-limited acute HBV infection* **(B)** *Schematic representation of the serological features of chronic HBV infection***.** *(Adapted from Rehermann, B. et al., 2005) (License Number 5896030795478)*

2.3. Liver immune response in HBV infection

As previously mentioned, the liver microenvironment harbours a diverse population of immune cells that play a crucial role during hepatotropic infections, especially in the case of HBV infection. The role of the innate immune cells in controlling HBV is still

debated but it is known that this virus triggers a weak innate response (Hildreth & O'sullivan, 2019). In fact, a coordinated activation of both the cellular and humoral arms of the adaptive immune response is responsible for determining the disease outcome. Within the adaptive immune system, $CD8^+$ T cells are the main cellular subset involved in mediating viral clearance. However, for a complete immunological control, the presence of HBV-specific antibody producing B cells is essential (Chisari & Ferrari, 1995; Bertoletti & Ferrari, 2016). The following sections will provide specifics of the contribution of the humoral immune response during HBV infection.

2.3.1. B cell-mediated immunity in HBV infection

While vigorous HBV-specific $CD8^+$ T cell responses are a well-established hallmark of acute HBV clearance, the contribution of humoral immune response, mediated by B cells and antibodies, has been less thoroughly investigated. B cell immunity was initially thought to be limited to preventing reinfection, but recent findings have highlighted its broader significance in controlling persistent infections through memory B cells. This was indirectly demonstrated in studies where researchers showed a viral reactivation in patients that were previously infected with HBV and treated with B-cell depleting agents, such as Retuximab (anti-CD20) (Voican *et al*, 2016; Loomba & Liang, 2017). Similarly, recipients of liver transplants from HBV-vaccinated donors were shown to be protected from infection thanks to HBV-specific humoral and cellular immunity acquired from the donor's liver (Schumann *et al*, 2009). Additionally, the detection of HBV-specific antibodies in the serum serves as a well-established tool for defining different stages of infection. In particular, anti-HBsAg antibodies are considered a hallmark of acute HBV resolution and provide protective immunity after vaccination. Furthermore, recent studies have shown that HBsAg-specific B cells are present in acute, chronic, and resolved HBV infections at similar frequencies. However, in chronic HBV infection, these specific B cells exhibit an impaired antiviral capacity and are unable to differentiate into anti-HBsAg antibodies producing cells (Burton *et al*, 2018; Salimzadeh *et al*, 2018; Le Bert *et al*, 2020).

These observations shifted the attention of researchers towards the comprehensive characterisation of HBV-specific B cells, their response to antigen, and their role in pathogenesis of chronic HBV infection.

2.3.1.1. HBV-specific antibodies

The antibody response delineates the various clinical stages of HBV infection: HBsAg specific antibodies (anti-HBsAg Abs) are protective and indicative of viral control and resolved infection; anti-HBcAg specific antibodies (anti-HBcAg Abs) can be present even during active viral replication and have been linked to HBV-acute liver failure (Hoofnagle *et al*, 1973; Farci *et al*, 2010). While HBc-specific B cells in CHB patients are able to mature into anti-HBcAg Abs producing cells when stimulated *in vitro*, HBs-specific B cells present a maturation defect, corresponding to low or null levels of anti-HBs Abs. The discrepancy in the maturation of HBc- and HBs-specific B cells in chronic patients could be eventually explained by the different level in antigen exposure. In fact, core antigen resides primarily within infected hepatocytes and naked core particles released by infected hepatocytes are a minimal fraction of viral particles; on the other hand, envelope protein can be present on the surface of hepatocytes and are highly abundant in the periphery (as whole virions or empty subviral particles). Consequently, HBs-specific B cells might become dysfunctional and, while anti-HBs Abs are produced, they become trapped by the abundance of circulating antigen (Bohne *et al*, 2008; Le Bert *et al*, 2020; Kawashima *et al*, 2024).

Anti-HBsAg Abs production is thought to be T cell dependent, and the dysfunction of HBs-specific B cells during chronic HBV infection may be linked to impaired T cell responses. Anti-HBsAg Abs have the peculiarity of being the only antibodies with neutralising activity due to their ability to block HBV viral entry into the hepatocytes (Corti *et al*, 2018). They prevent infection by binding to the antigenic loop region, the “a-determinant” (interacts with HSPGs on cell surface) and the preS1 domain (binds directly NTCP) of HBsAg. Beside their neutralising capacity, anti-HBsAg Abs can mediate antibody-dependent cellular toxicity by binding directly to HBsAg on the surface of

infected hepatocytes or by inducing direct lysis via complement activation (Bertoletti & Ferrari, 2016; Maini & Burton, 2019) (**Figure 7**).

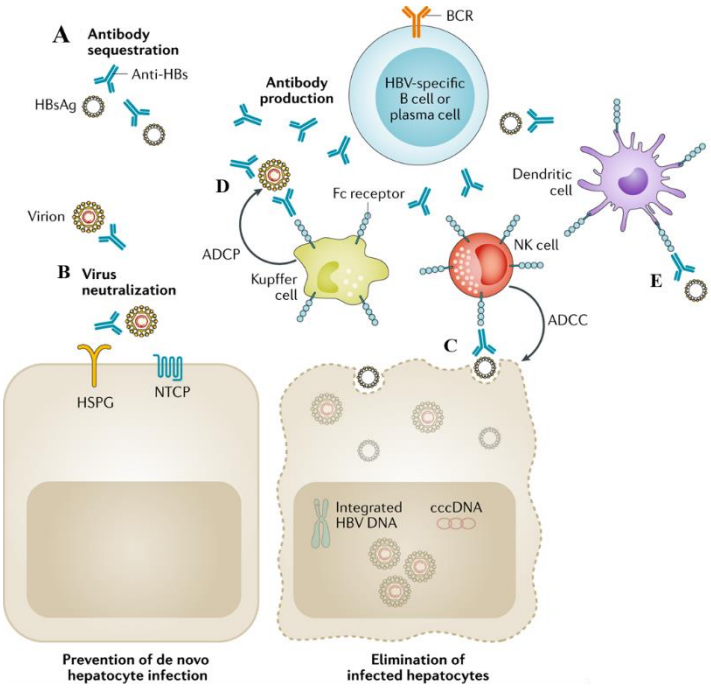


Figure 7. Antiviral function of anti-HBs antibodies in HBV infection

(A) *HBs-specific antibodies (anti-HBs Abs) are sequestered by circulating HBsAg.* **(B)** *Anti-HBs Abs bind to HBsAg on virions thus preventing attachment to HSPG or entry via NTCPs.* **(C)** *Anti-HBs Abs bind to HBsAg found on the surface of hepatocytes and favours Fc-dependent elimination via antibody-dependent cell-mediated cytotoxicity (ADCC).* **(D)** *Anti-HBs Abs bind to HBsAg on the surface of virions to induce antibody-dependent cellular phagocytosis (ADCP).* **(E)** *Anti-HBs Abs form immune complexes with HBsAg and are then bound by DCs to induce vaccinal effects (Adapted from Maini M.K. & Burton A.R., 2019) (License Number 5896031007262)*

2.3.1.2. HBV surface antigen (HBsAg) seroconversion

Hepatitis B surface antigen seroconversion, marked by the loss of HBsAg and the emergence of anti-HBs antibodies, is a critical marker in the natural history and treatment of HBV infection and is generally considered a hallmark of therapeutic success (Papatheodoridis *et al*, 2012; Iannacone & Guidotti, 2022). It signifies the transition from an active replicative phase to a non-replicative or low-replicative state of HBV and it is often associated with the clearance of viral particles and a reduction in liver disease and damage. In fact, patients who experience seroconversion from HBsAg-positive/anti-HBs Ab-negative to HBsAg-negative/anti-HBs Ab-positive show a gradual reduction in liver

inflammation and fibrosis (McMahon *et al*, 2001; Chu & Liaw, 2007b). Additionally, serum HBV DNA levels in these seroconverted individuals decrease until reaching undetectable levels, indicating a strong correlation between loss of circulating HBsAg and effective HBV control (McMahon, 2009). Furthermore, clinical studies emphasise that spontaneous HBsAg seroconversion is often correlated with a good prognosis and a reduced risk of developing cirrhosis and HCC. Unfortunately, HBsAg loss and seroconversion in HBV patients is rare as it occurs in 1-3% of cases per year, depending on the age and status of liver disease (Liaw *et al*, 1991; McMahon *et al*, 2001; Chu & Liaw, 2007a; Simonetti *et al*, 2010; Liu *et al*, 2010).

2.3.1.3. B cells and their immune response in HBV infection

While the formation of lasting memory B cells (MBCs) and long-lived plasma cells is essential for protective immunity following viral infection, chronic infections exhibit a distinct phenomenon. These chronic infections are often associated with the development of a unique population of memory B cells with altered characteristics, function, and tissue distribution known as exhausted or atypical memory B cells (atMBCs) (Portugal *et al*, 2017). Generally speaking, the differentiation of B cells into MBCs typically happens in secondary lymphoid organs (SLOs) such as the spleen and lymph nodes. Here naïve B cells encounter and engage with antigens on the surface of dendritic cells through their B cell receptors (BCRs), thus leading to their activation. The BCR-bound antigen is then internalised, processed, and presented on MHC class II molecules on the B cell surface. B cells then engage with antigen activated $CD4^+$ T cells, which will further differentiate into T follicular helper (Tfh) cells. Tfh cells provide survival signals to B cells and favour their proliferation, clonal expansion, affinity maturation and class switching within the dark zone of the germinal centre (GC). In the light zone of GCs, high affinity B cells further differentiate into lasting MBCs and long-lived plasma cells. However, if the T-B cell interaction is inadequate, or if the architecture of the follicles is disrupted, B cells fail to enter the GCs and differentiate into short-lived antibody secreting plasma cells (PCs) (Kurosaki *et al*, 2015; De Silva & Klein, 2015).

As previously mentioned, chronic infections are often associated with the generation of atypical memory B cells. These atMBCs do not undergo GC selection and instead differentiate into low-affinity, short-lived plasma cells (Portugal *et al*, 2017). In chronic HBV infection, HBs-specific B cells, as well as global B cells, exhibit atypical memory characteristics, with low expression of CD21 and CD27, high expression of PD-1 and T-bet, and defective antibody production. They also show a lower calcium flux upon BCR engagement and exhibit a lower production of antiviral cytokines such as IL-6 and TNF-α (Burton *et al*, 2018), which have non-cytolytic antiviral activity during HBV infection. In particular, the diminished production of IL-6 can adversely affect HBV control, as it downregulates the expression of NTCP by HBV-infected hepatocytes (Bouezzedine *et al*, 2015), inhibits cccDNA transcription (Palumbo *et al*, 2015), and promotes Tfh cell responses (Harker *et al*, 2011).

Of note, the function of atMBCs obtained from CHB patients can be partially restored *in vitro* through IL-2, IL-21, and CD40L-expressing feeder cells and the addition of PD-1 blockade (Burton *et al*, 2018; Salimzadeh *et al*, 2018). These findings suggest that atMBCs could be viable therapeutic targets, offering new avenues for the development of treatments aimed at enhancing immune responses in chronic hepatitis B patients.

2.3.1.4. $CD4^+$ T cell responses in HBV infection

$CD4^+$ T cells are known to be essential for the development, maintenance, and control of the adaptive immune system during viral infections, including HBV. One of the most well-documented roles of $CD4^+$ T cells is the promotion of antibody production by B cells. However, they can exert many other critical functions during viral infection, such as the recruitment of innate immune cells and the sustainment of the antiviral $CD8^+$ T cell response (Luckheeram *et al*, 2012; Swain *et al*, 2012; Kawashima *et al*, 2024).

In the context of HBV pathogenesis, $CD4^+$ T cells play a fundamental role in shaping the immune response. They are thought to have a crucial role in determining the clinical outcome during the initial priming phase of the infection. Despite their significance, their role has not been as extensively studied as $CD8^+$ T cells. Work has begun to address this gap. For instance, studies in chimpanzees have shown that the depletion of $CD4^+$ T cell

prior to HBV inoculation results in persistent infection (Asabe *et al*, 2009). Similarly, in murine studies, depletion of $CD4^+$ T cells led to an impaired $CD8^+$ T cell response eventually causing chronic liver infection (Yang *et al*, 2010; Trautmann *et al*, 2014).

Clinically, in the natural course of infection, $CD4^+$ T cells appear in the blood, together with $CD8^+$ T cells, between 7 to 10 weeks after infection, even before symptoms develop (Webster *et al*, 2000; Ferrari, 2015). Patients with acute, self-limiting infection show strong, polyfunctional $CD4^+$ T cell responses that contribute to viral clearance. In contrast, patients with chronic HBV exhibit a reduced – or, according to some studies, nearly undetectable – frequency of circulating HBV-specific $CD4^+$ T cells (Jung *et al*, 1995; Penna *et al*, 1996; Boni *et al*, 2007a). These observations underscore the essential role of $CD4^+$ T cells in determining whether HBV infection resolves or progresses to chronicity. Moreover, $CD4^+$ T cells are critical in co-infections, such as in patients co-infected with HBV and hepatitis C virus, where the absence of HBV-specific $CD4^+$ T cells correlates with persistent HBV infection, despite the presence of HBV-specific $CD8^+$ T cells(Urbani *et al*, 2005).

Despite significant advances, understanding the precise molecular mechanisms governing $CD4^+$ T cell function in HBV infection remains an active area of research.

2.3.1.5. Crosstalk between B cells and $CD4^+$ T cells

As previously mentioned, B cells and T cells are closely interconnected and must cooperate to maximise the efficiency of the immune response. B cells, through BCR-mediated antigen endocytosis, process and present antigen on major histocompatibility complex (MHC) class II to $CD4^+$ T cells. This interaction promotes the differentiation of $CD4^+$ T cells into T follicular helper cells, via IL-6, IL-21 and inducible T cell co-stimulator (ICOS)–ICOS ligand (ICOS-L) engagement. Tfh cells, in turn, provide survival signals via IL-4 and IL-21 to GC B cells and facilitate their proliferation through CD40-CD40L engagement. Furthermore, IL-4 and IL-21 secreted by Tfh cells induce B cell differentiation into highly antigen-specific plasma cells and memory B cells. This cooperation of $CD4^+$ T cells and B cells is important for the generation of potent high-affinity anti-HBsAg specific antibodies (**Figure 8**) (Crotty, 2015; Bertoletti & Ferrari,

2016; Maini & Burton, 2019). However, their production can be hindered by the low frequency of functional HBV-specific $CD4^+$ T cells during CHB infection (Boni *et al*, 2007b; Raziorrouh *et al*, 2014). Additionally, it has been shown that anti-HBs B cell responses may also be impaired by T follicular regulatory (Tfr) cells, which express the regulatory transcription factor FOXP3, by suppressing conventional Tfh activity within the GC, thus inhibiting their maturation (Linterman *et al*, 2011; Wu *et al*, 2018).

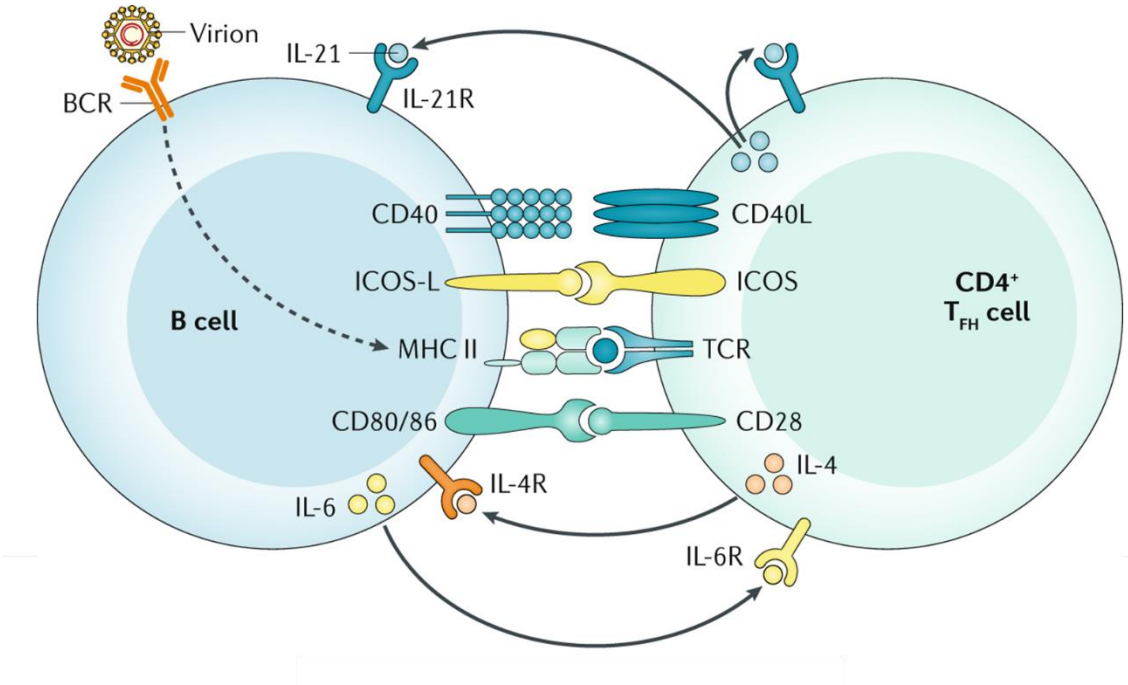


Figure 8. Crosstalk between B cells and $CD4^+$ T

Schematic representation of the key interactions between B cells and $CD4^+$ T cells. B cells activate T follicular helper (T_{FH}) cells through B cell receptor (BCR)-mediated antigen endocytosis followed by processing and presentation on major histocompatibility complex (MHC) class II molecules; they regulate $CD4^+$ T cell differentiation into T_{FH} cells via IL-6, IL-21, or inducible T cell co-stimulator (ICOS)–ICOS ligand (ICOS-L) engagement. T_{FH} promote B cell survival via IL-4 and proliferation through CD40–CD40L engagement; they induce B cell differentiation into plasma cells and promote antibody mutation and class-switching via IL-4 or IL-21 (Adapted from Maini M.K. & Burton A.R., 2019) (License Number 5896031007262)

2.4. The role of gut microbiota in HBV infection

The gut microbiota constitutes a symbiotic ecosystem that maintains homeostasis within the human body, playing a crucial role in the regulation of health (Bäckhed *et al*,

2005). The dysregulation and the disruption of the intestinal microbiota can lead, in fact, to disease. As previously mentioned, the gut microbiota and the liver communicate through the gut-liver axis where microbial products and metabolites can directly impact liver health via the portal vein (Tripathi *et al*, 2018; Albillos *et al*, 2020). Indeed, recent studies suggest that the gut microbiota is involved in several liver diseases (Chassaing *et al*, 2014; Albillos *et al*, 2020), including chronic HBV. In recent years, some preliminary studies have analysed the gut microbiota composition of HBV-infected patients, including patients with HBV-induced liver cirrhosis, and HBV-related HCC, revealing gut microbiota dysbiosis (Schwabe & Greten, 2020; Li *et al*, 2022b). They showed that certain bacterial taxa, including the phyla *Firmicutes* and *Proteobacteria*, and the genera *Streptococcus* and *Prevotella*, could exacerbate inflammation and liver injury, promoting HBV replication and persistence (Chen *et al*, 2011; Wang *et al*, 2017, 2020c). The importance of the gut microbiota in HBV was also demonstrated following faecal microbiota transplantation (FMT) in patients who remained HBeAg positive despite long-term antiviral treatment. In fact, FMT was shown to be effective in HBeAg clearance (Ren *et al*, 2017). Preclinical studies additionally showed that HBV infection alone can alter the composition of the gut microbiota (Zhu *et al*, 2019), and that entecavir (ETV) treatment effectively corrected gut microbiota dysbiosis developed in HBV-infected mice (Li *et al*, 2020).

Therapeutic strategies targeting gut microbiota, such as probiotics, prebiotics, and faecal microbiota transplantation, are being explored as potential adjunct treatments for HBV infection, aiming to restore microbial balance and enhance antiviral immunity.

2.5. Experimental models to study HBV pathogenesis and HBsAg-seroconversion

Hepatitis B virus infects only human and chimpanzees, historically limiting the study of HBV infection. The fact that chimpanzees have the genetic background and immune system that are closest to humans makes them the host of choice for studying the innate and adaptive immune response to HBV infection. However, given the prohibitive costs

and ethical concerns associated with the use of these animals, mice have become the focal point of research due to their ease of manipulation and well-defined immune system.

Nearly 30 years ago, an HBV-replication-competent transgenic mouse model, named 1.3.32 (or HBV Tg), was generated. These mice were created by microinjection of a terminally redundant viral DNA construct 1.3 HBV genomes in length, containing only HBV promoters and enhancers. In this mouse model, hepatocytes replicate the complete virus genome and its structural proteins at high levels without any evidence of cytopathology. HBV replication occurs in viral nucleocapsids within the cytoplasm, predominantly in centrilobular hepatocytes surrounding the central vein of the liver. Trace amounts of the viral genome can also be detected in other tissues, such as the kidney. However, high-level viral gene expression and replication were observed mainly in the liver (Guidotti *et al*, 1995). This is likely due to the presence of appropriate host transcription factors. For instance, hepatocyte nuclear factor 1 alpha (HNF1α), predominantly expressed in hepatocytes, might play a critical role in enabling the liver-specific activity of the viral genome (Raney et al, 2001).

Thanks to the efficient viral replication, infectious viral particles, indistinguishable from human virions, are found in the serum of these mice at levels up to 10^7-10^8 viral particles per ml. Interestingly, cccDNA, the template for viral transcription, is not detectable in the hepatocytes of these transgenic mice (Guidotti *et al*, 1995; Iannacone & Guidotti, 2015). Furthermore, mouse NTCP cannot function as an HBV receptor (Yan *et al*, 2013). As a result, viral replication is restricted to hepatocytes already containing the integrated viral genome, and the infection does not propagate to new cells.

Furthermore, HBV Tg mice exhibit immune tolerance to all HBV antigens due to the early and sustained expression of viral proteins as self-antigens, providing an excellent platform to evaluate immunotherapeutic strategies aimed at breaking tolerance and eradicating persistent HBV infection (Guidotti *et al*, 1995; Iannacone & Guidotti, 2015).

Findings revealed that approximately 60% of these 1.3.32 HBV transgenic mice spontaneously cleared serum HBsAg, and that this spontaneous loss is due to anti-HBsAg antibodies production which clear the circulating antigen (*i.e.* seroconversion) (**Figure 9 A, B**). Furthermore, it was shown that HBV Tg mice that lack the expression of antibodies could not clear HBsAg during their life (**Figure 9 C, D**), confirming the critical role of B

cells and antibodies in HBs seroconversion (Fumagalli *et al*, 2020). As previously mentioned, HBsAg seroclearance and seroconversion (development of antibodies against HBsAg) can increase the survival of CHB patients. Therefore, these recent findings place the 1.3.32 transgenic mice as an invaluable model for investigating seroconversion, a phenomenon that has been inadequately explored but holds the key to developing more effective therapies for chronic hepatitis B infection.

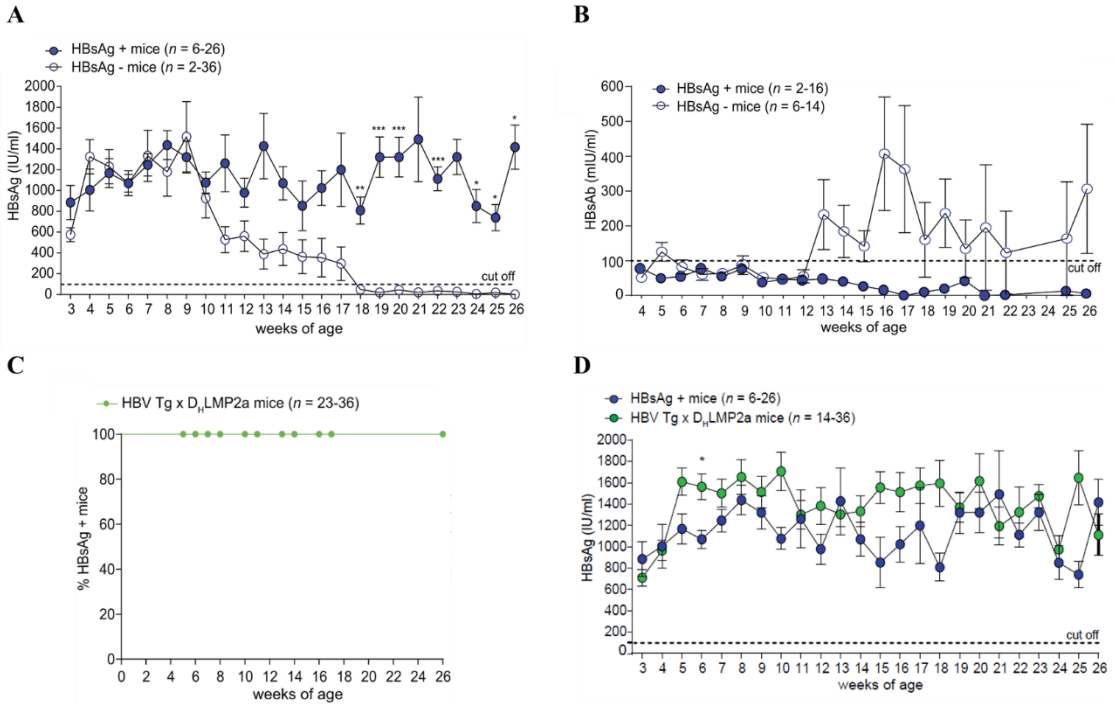


Figure 9. HBV replication-competent transgenic mice spontaneously undergo HBs-seroconversion

(A) *Approximately 60% of 1.3.32 transgenic mice spontaneously lose circulating HBsAg (HBsAg- mice, empty blue dots), while around 40% maintains high levels of circulating HBsAg (HBsAg+ mice, blue dots).* **(B)** *The same mice that lost the circulating HBsAg (HBsAg- mice, empty blue dots), show increased levels of circulating HBsAb (anti-HBsAg antibodies).* **(C, D)** *100% of antibody-deficient HBV Tg mice (HBV Tg x DHLMP2a, green dots) showed detectable circulating HBsAg similarly to HBsAg^{+} mice. (Adapted from Fumagalli V. et al, 2020)* (*Order number: 1539801)*

AIM OF THE WORK

3. AIM OF THE WORK

The rationale of this project is aimed at characterising the endogenous B cell response in Hepatitis B Virus (HBV) pathogenesis and at investigating the molecular mechanisms underlying the phenomenon of Hepatitis B Surface Antigen (HBsAg) seroconversion in HBV-replication competent 1.3.32 transgenic mice.

Given that HBV infection remains a global health challenge, understanding the immune mechanisms involved in its resolution is crucial. HBs seroconversion, the development of antibodies against HBsAg, represents a critical milestone in the resolution of HBV infection, as it is associated with improved clinical outcomes and reduced risk of liver-related complications. Recent findings have identified the importance of HBsAg seroclearance and seroconversion in improving the survival of chronic HBV (CHB) patients. However, the mechanisms driving seroconversion, including the contributions of $CD4^+$ T cells and the potential influence of the microbiome on B cell responses, are still not well understood. Using the 1.3.32 transgenic mouse model, which has been shown to be an ideal model for studying seroconversion, this research focuses on three specific objectives:

Aim I: Localisation and characterisation of endogenous HBsAg-specific B cells
Aim II: Study the role of $CD4^+$ T cells in promoting HBs seroconversion
Aim III: Investigating the role of the microbiome in promoting HBs seroconversion

Collectively, the ultimate goal of the project is to gather information which will advance our understanding of the immune mechanisms involved in HBV seroconversion, potentially providing new therapeutic strategies for enhancing HBV clearance in patients.

RESULTS

4. RESULTS

4.1. Aim I: Localisation and characterisation of endogenous HBsAg-Specific B cells in HBV-replication competent transgenic mice

4.1.1. Spontaneous HBsAg seroconversion in female HBV-replication competent transgenic mice

As previously mentioned, in the study involving 1.3.32 HBV transgenic mice, it was observed that 60% of these mice spontaneously cleared serum HBsAg. This spontaneous loss of HBsAg is attributed to the production of anti-HBsAg antibodies, which effectively clear the circulating antigen, leading to seroconversion (Fumagalli *et al*, 2020). Notably, this phenomenon was documented only in male mice. Given that sex differences in immune responses are well-documented, with females generally exhibiting stronger B cell immunity due to hormonal factors (Klein & Flanagan, 2016; Taneja, 2018), the first aim of this research was to determine if this phenomenon also occurs in female HBV-replication competent transgenic (HBV Tg) mice, expanding the understanding of seroconversion dynamics across sexes.

We began the study by conducting longitudinal measurements HBsAg concentrations, as was previously described (Fumagalli *et al*, 2020), in the serum of female HBV Tg mice. Consistent with the findings in male mice, we observed that, although the initial HBsAg concentrations were similar (**Figure 10 A**), from 7 weeks of age, serum HBsAg levels gradually decreased overtime in ≈ 60% of female mice until reaching undetectable levels ($HBsAg^-$) (**Figure 10 B**). This spontaneous loss coincided with the presence of anti-HBsAg antibodies (HBsAb) (**Figure 10 C**). We speculate that the reason not all the $HBsAg^-$ mice show high levels of HBsAb (**Figure 10 D**) may be due to the ELISA-based detection assay's inability to detect HBsAg-HBsAb complexes. The absence of serum HBsAg levels did not affect serum HBeAg levels (an indirect marker of hepatic HBV gene expression) which stayed the same throughout the observation period (up to 22 weeks) (**Figure 10 E**). Serum HBsAg clearance associated with a significant reduction in viremia (**Figure 10 F**). Finally, we saw no evidence of spontaneous immunopathology in

HBsAg$^-$ mice, as assessed by serum transaminases and intrahepatic leukocyte absolute number (**Figure 10 G, H**). These results demonstrate that the spontaneous seroconversion seen in HBV Tg mice previously documented in male mice, also occurs in female mice, demonstrating that seroconversion due to anti-HBsAg antibody production is not gender-specific in this transgenic model. Interestingly, seroconversion appeared to occur more rapidly in female mice compared to males. Based on the obtained results, both genders were included in subsequent research work to ensure comprehensive analysis.

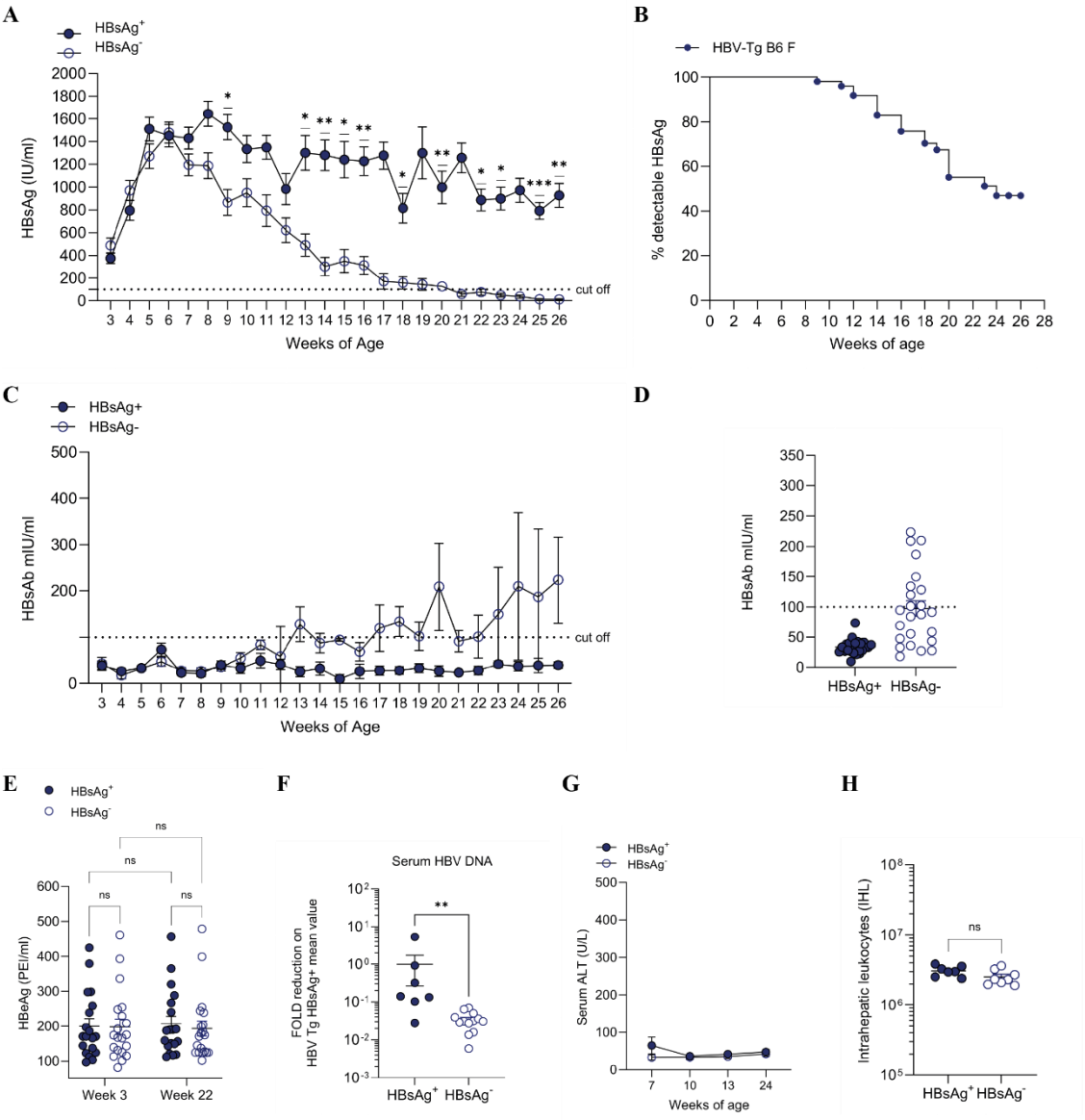


Figure 10. Female HBV replication-competent transgenic mice spontaneously undergo HBs-seroconversion

(A) *Serum HBsAg levels (IU/ml) of female HBV Tg mice monitored from 3 weeks to 26 weeks of age by ELISA assay (cut off = 100 IU/ml). Solid blue symbols: HBsAg$^+$ mice (n=18); empty blue symbols: HBsAg$^-$ mice (n=20).* **(B)** *Percentage of female HBV Tg mice with detectable serum HBsAg.* **(C-D)** *Serum anti-HBsAg (HBsAb) levels (mIU/ml) of female HBV Tg mice monitored from 3 weeks to 26 weeks of age by ELISA assay (cut off = 100 IU/ml). Solid blue symbols: HBsAg$^+$ mice (n=13); empty blue symbols: HBsAg$^-$ mice (n=15).* **(E)** *Serum HBeAg levels (PEI/ml) of HBsAg$^+$ (solid blue symbols, n=19) and HBsAg$^-$ (empty blue symbols, n=20) measured at 3 weeks and 22 weeks of age by ELISA assay.* **(F)** *Quantification of HBV DNA in the sera of HBsAg$^+$ (solid blue symbols, n=7) and HBsAg$^-$ (empty blue symbols, n=13) at 22 weeks of age. Values are expressed as FOLD reduction on HBV Tg HBsAg$^+$ mean value. Values were measured with reference to standard curves* **(G)** *Transaminase (ALT, U/L) 8activity in the sera of HBsAg$^+$ (solid blue symbols, n=8) and HBsAg$^-$ (empty blue symbols, n=8) measured at 7, 10, 13, and 24 weeks of age.* **(H)** *Intrahepatic leukocytes in HBsAg$^+$ (solid blue symbols, n=7) and HBsAg$^-$ (empty blue symbols, n=8) mice at 22 weeks of age.*
*Data are expressed as mean ± SEM and are representative of at least 2 independent experiments. * p value < 0.05, ** p value < 0.01, *** p value < 0.001; two-way ANOVA followed by Sidak's multiple comparison test (**B, E**), or Mann-Whitney U-test (**F, H**).*

4.1.2. HBsAg-Specific B cells localise to the spleen, liver, bone marrow, and colon following seroconversion in HBV transgenic mice

Our results indicated that the spontaneous HBsAg loss observed in both male and female HBV Tg mice is due to Ab-mediated clearance, highlighting the crucial role for B cells in HBs seroconversion. Consequently, the next objective of our work was to locate and characterise HBsAg-specific B cells in these HBV Tg mice.

To enumerate and phenotype HBsAg-specific B cells in HBV Tg mice that had undergone seroconversion, we performed ELISpot assays. Specifically, we sacrificed HBV Tg mice at 22 weeks of age and mesenteric lymph nodes (mLN), Payer's patches, colon, liver, spleen and bone marrow (BM) were surgically collected and processed (**Figure 11 A**). Serum HBsAg (**Figure 11 B**) and HBsAb (**Figure 11 C**) concentrations were measured to stratify the HBV Tg mice in HBsAg$^+$ and HBsAg$^-$ mice. We demonstrated our ability to detect HBsAg-specific B cells in mice that underwent HBs seroconversion. Indeed, we could detect HBsAg-specific B cells in the spleen, liver, BM and colon of HBsAg- HBV Tg mice, but not in the mesenteric lymph nodes or Payer's patches (**Figure 11 D, E**).

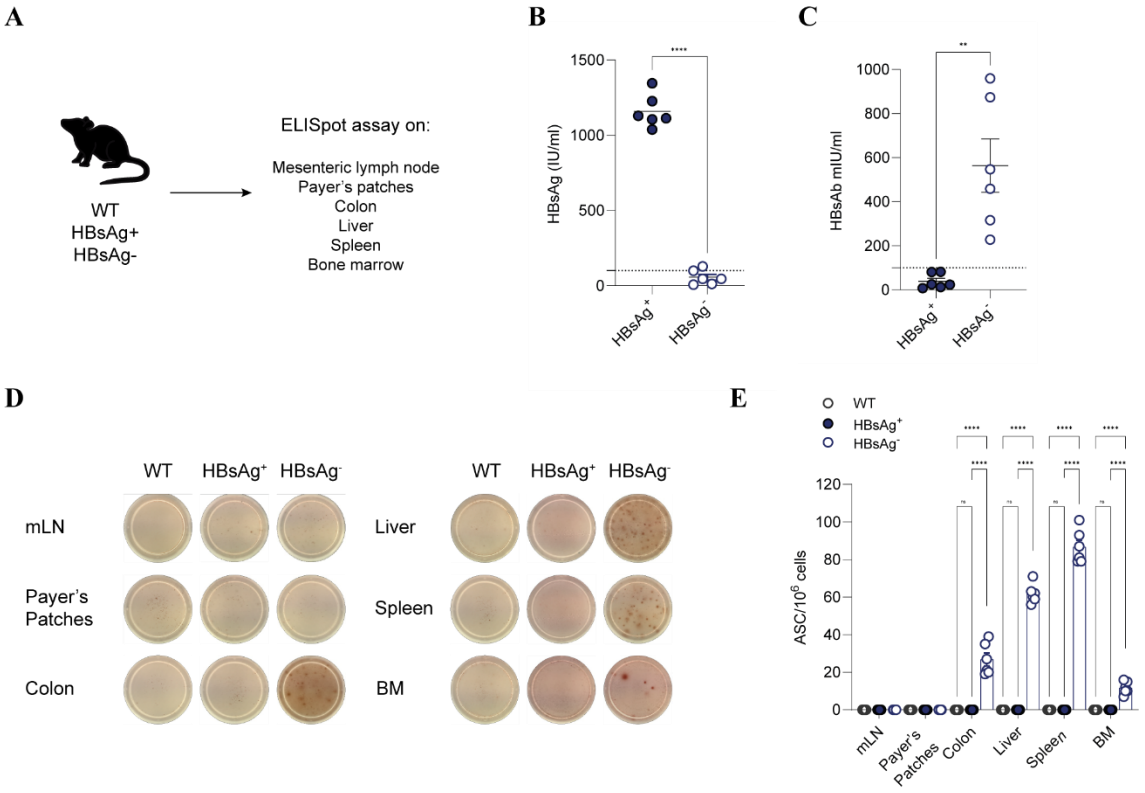


Figure 11. HBsAg-Specific B cells localise to the spleen, liver, bone marrow, and colon following seroconversion in HBV transgenic mice

(A) *Schematic representation of the experimental setup. HBsAg$^+$ and HBsAg$^-$ HBV Tg mice were sacrificed at 22 weeks of age. WT B6 mice were used as control. Various organs were collected and analysed by ELISpot.* **(B)** *Serum HBsAg levels (IU/ml) of HBV Tg mice at 22 weeks of age by ELISA assay (cut off = 100 IU/ml). Solid blue symbols: HBsAg$^+$ mice (n=6); empty blue symbols: HBsAg$^-$ mice (n=6).* **(C)** *Serum anti-HBsAg (HBsAb) levels (mIU/ml) of HBV Tg mice at 22 weeks of age by ELISA assay (cut off = 100 IU/ml). Solid blue symbols: HBsAg$^+$ mice (n=6); empty blue symbols: HBsAg$^-$ mice (n=6).* **(D)** *Representative ELISpot scans of anti-HBsAg-secreting B cells in the liver, spleen, bone marrow (BM), mesenteric lymph nodes (mLN), Payer's patches, and colon of HBsAg$^+$ and HBsAg$^-$ HBV Tg mice.* **(E)** *Total number of antibody secreting cells (ASC) per 10^6 of cells in various organs of control mice (WT C57BL/6; grey dots, n=6), HBsAg$^+$ HBV Tg mice (solid blue symbols, n=6), and HBsAg$^-$ HBV Tg mice (empty blue symbols, n=6).*
Data are expressed as mean ± SEM and representative of at least 3 independent experiments.
*ns p-value > 0.05, ** p value < 0.01, *** p value < 0.001, **** p value < 0.0001; unpaired t-test (**B, C**); two-way ANOVA followed by Tukey multiple comparison test (**E**).*

We then developed a novel multimer-based technique that couples biotinylated HBsAg with two different fluorochrome-labelled streptavidins (AxFl-488 and AxFl-647) to precisely detect HBs-specific B cells. After stratifying the HBV Tg mice into two distinct groups, HBsAg$^+$ and HBsAg$^-$, we performed flow cytometry analysis on organs showing the highest number of detectable HBsAg-specific B cells (liver and spleen) (**Figure 12 A**). Although this method is highly sensitive and specific (HBs-specific BCR heavy and

light chain knock in mice were used as positive control), we were unable to detect HBsAg-specific B cells in our seroconverted HVB Tg mice (**Figure 12 B**). Several factors could potentially hinder the detection of these cells: first, the low sensitivity of the detection system in identifying low-affinity clones; second, the low frequency of HBsAg-specific B cells in HBV Tg mice; third, the complete downregulation of the BCR in antibody-secreting cells, preventing antigen binding and therefore detection; and fourth, the generation of HBsAg-specific clones that are unable to recognise the recombinant protein used in the assay.

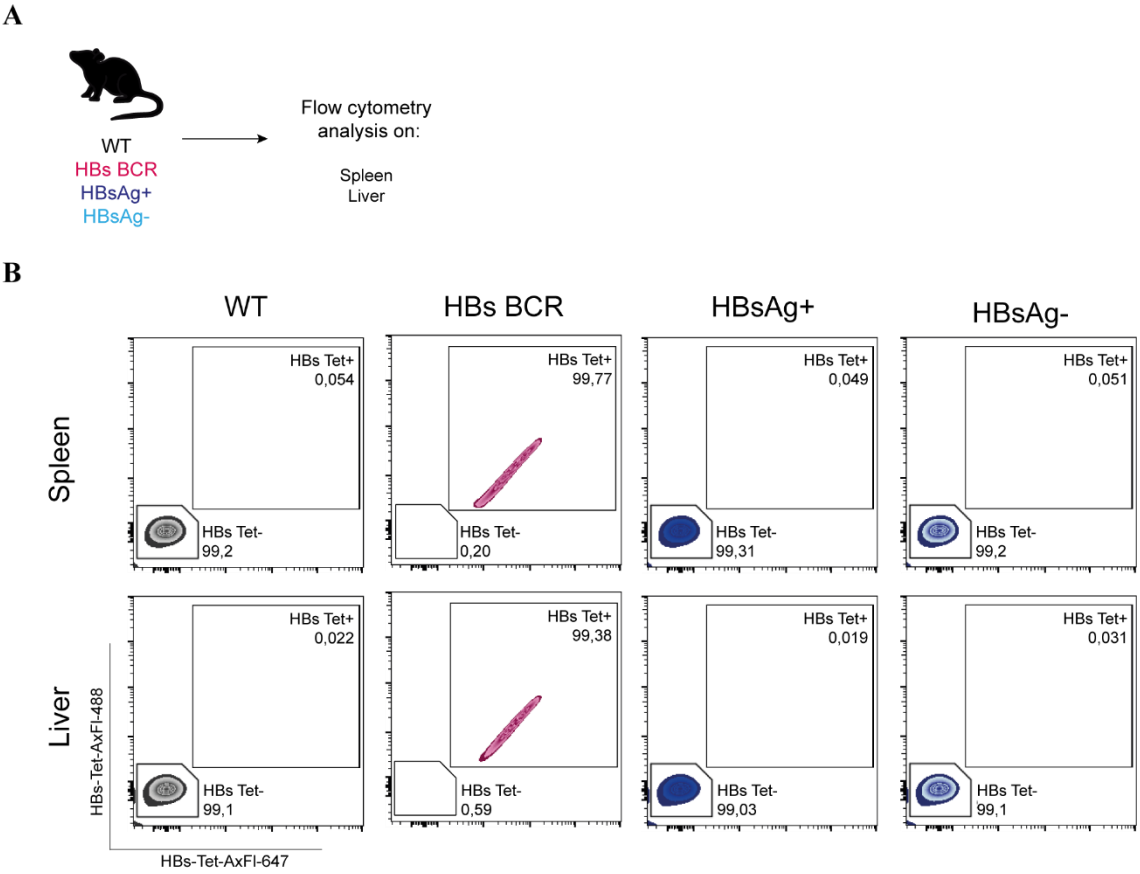


Figure 12. Detection of HBs-specific B cells by HBsAg-tetramers

(A) *Schematic representation of the experimental setup. HBsAg$^+$ and HBsAg$^-$ HBV Tg mice were sacrificed at 22 weeks of age. WT B6 mice and HBs-specific BCR knock-in mice were used as controls. Livers and spleens were collected and analysed by flow cytometry.* **(B)** *Representative flow cytometry plots of HBs-tetramer positive cells found in the liver and spleen of control mice (WT C57BL/6; grey plots; HBs BCR; pink plots), HBsAg$^+$ HBV Tg mice (dark blue plots), and HBsAg$^-$ HBV Tg mice (empty blue plots). HBs-Tetramer positive cells are identified as Live, CD45$^+$B220$^+$CD19$^+$.*
Data are representative of at least 3 independent experiments.

Finally, we characterised the isotypes of the antibodies produced by HBsAg-specific B cells upon seroconversion. After monitoring the HBsAg (**Figure 13 A**) and the anti-HBsAg antibody (**Figure 13 B**) levels in the sera by ELISA assay for ≥ 20 weeks in HBV Tg mice, we identified the isotypes of the antibodies produced in HBsAg$^-$ mice at three distinct time points post seroconversion. These specific time points were selected as they mark the onset of seroconversion, the decline of HBsAg to levels below the detection threshold, and the complete establishment of seroconversion. Consistently across all time points, we observed a predominant production of IgG1 and IgG3 (**Figure 13 C**), indicating isotype switching.

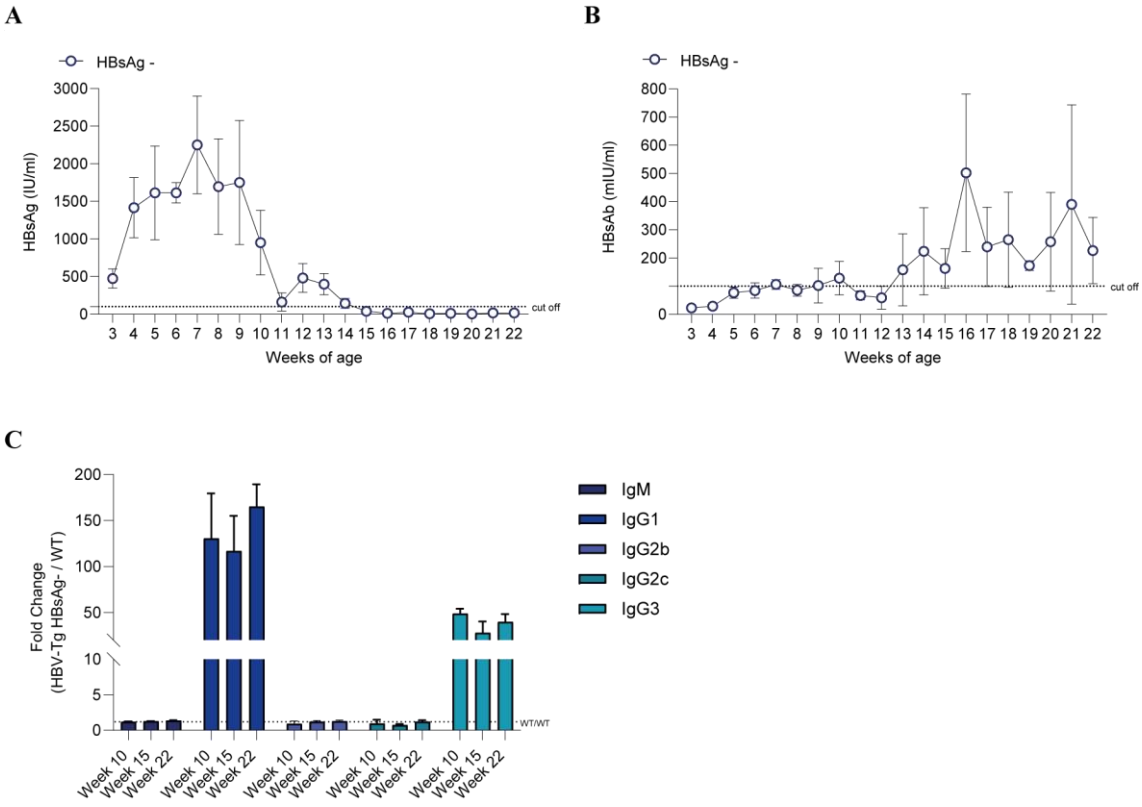


Figure 13. Anti-HBs highly restricted to IgG1 and IgG3 in HBsAg$^-$ HBV transgenic mice

(A) *Serum HBsAg levels (IU/ml) and* **(B)** *Serum anti-HBsAg (HBsAb) levels (mIU/ml) of HBsAg$^-$ HBV Tg mice monitored from 3 weeks to 22 weeks of age by ELISA assay (cut off = 100 IU/ml) (n=5).* **(C)** *Contributions of IgM and IgG subclasses in anti-HBsAg response in the sera of HBsAg$^-$ HBV Tg mice analysed at 10, 15, and 22 weeks of age. Values are expressed as FOLD change on WT mean value.*
Data are expressed as mean ± SEM and representative of at least 2 independent experiments.

4.1.3. Characterisation of global B cell populations in HBsAg$^+$ and HBsAg$^-$ HBV transgenic mice reveals no significant differences

Considering the inability to detect and therefore characterise HBsAg-specific B cells by flow cytometry, we redirected our focus to the analysis of the global B cell populations in HBsAg$^+$ and HBsAg$^-$ HBV Tg mice. With this purpose, major primary and secondary lymphoid organs were surgically collected and processed. The resulting cell suspensions were subsequently analysed by flow cytometry (**Figure 14 A**).

The total number of B cells obtained from the various organs was comparable between the two experimental groups (**Figure 14 B**). Phenotypic analysis revealed no significant differences in the overall B cell populations between HBsAg$^+$ and HBsAg$^-$ HBV Tg mice. Specifically, the frequencies of innate-like B cells (B1-a and B1-b) and conventional B cells (B2) (**Figure 14 C, D, E, F**), transitional B cells (T1and T2), and mature B cells (**Figure 14 G, H, I, J**) (Loder *et al*, 1999; Hardy & Hayakawa, 2001; Berland & Wortis, 2002) recovered from the different organs of HBsAg$^+$ HBV Tg mice were similar to the ones obtained from HBsAg$^-$ HBV Tg mice. Additionally, there were no significant differences in the percentage of neither germinal centre B cells (GC) or plasma cells (PC) B cells between the groups (**Figure 14 K, L**).

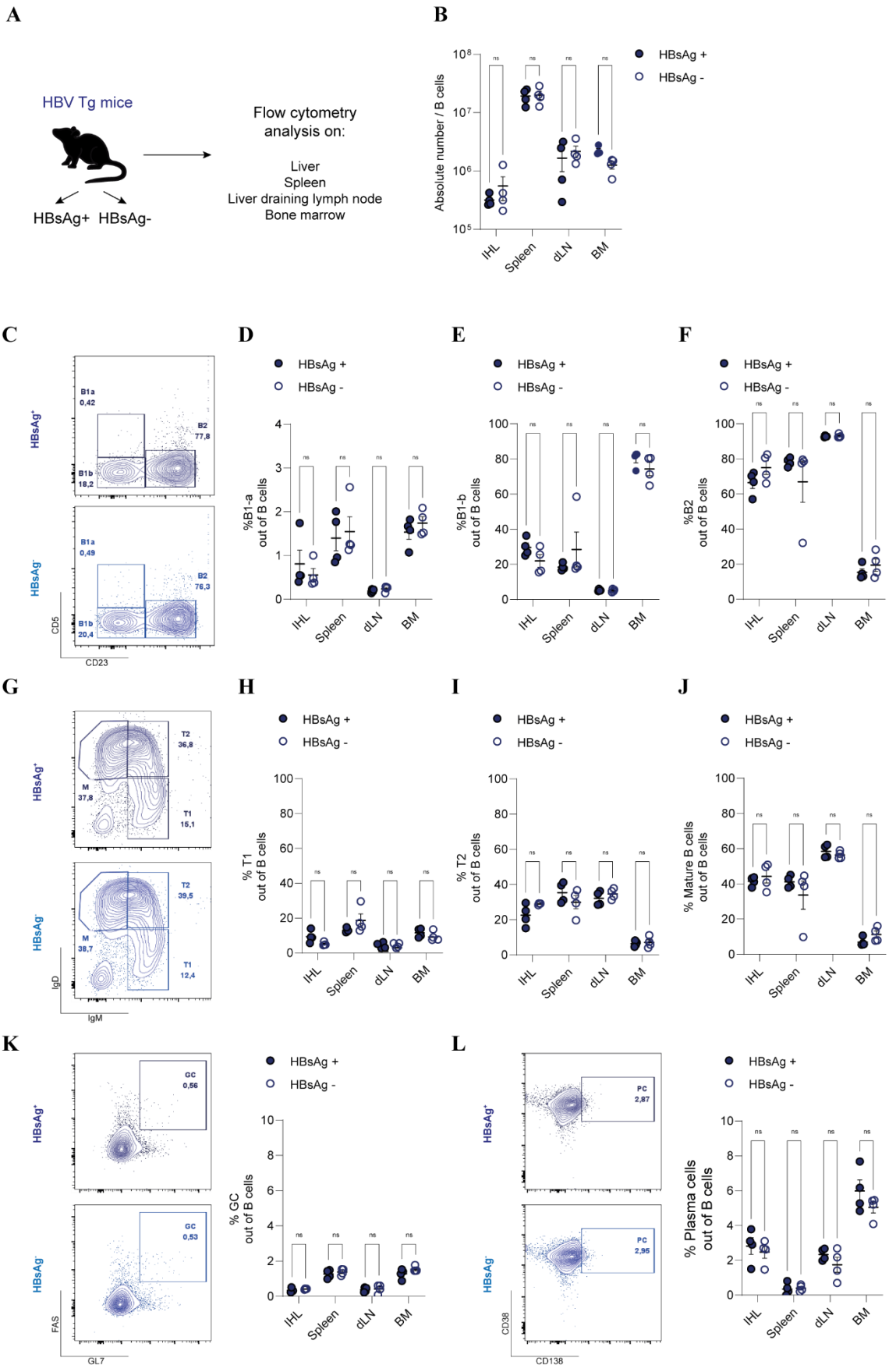

A
HBV Tg mice
HBsAg+ HBsAg-
Flow cytometry analysis on:
Liver
Spleen
Liver draining lymph node
Bone marrow
B
Absolute number / B cells
HBsAg +
HBsAg -
IHL
Spleen
dLN
BM
C
HBsAg+
HBsAg-
B1a 0,42
B2 77,8
B1b 18,2
B1a 0,49
B2 76,3
B1b 20,4
CD5
CD23
D
%B1-a out of B cells
E
%B1-b out of B cells
F
%B2 out of B cells
G
T2 36,8
M 37,8
T1 15,1
T2 39,5
M 38,7
T1 12,4
IgD
IgM
H
% T1 out of B cells
I
% T2 out of B cells
J
% Mature B cells out of B cells
K
GC 0,56
GC 0,53
FAS
GL7
% GC out of B cells
L
PC 2,87
PC 2,95
CD38
CD138
% Plasma cells out of B cells

Figure 14. Characterisation of global B cell populations in HBsAg$^+$ and HBsAg$^-$ HBV transgenic mice

(A) *Schematic representation of the experimental setup. HBsAg$^+$ and HBsAg$^-$ HBV Tg mice were sacrificed at 22 weeks of age. Various organs were collected and analysed by flow cytometry.* ***(B)*** *Absolute number quantification of total B cells in the liver, spleen, liver draining lymph nodes (dLN), and bone marrow (BM) of HBsAg$^+$ (solid blue symbols, n=4) and HBsAg$^-$ (empty blue dots, n=4) HBV Tg mice.* **(C)** *Representative flow cytometry plots of innate-like B cells (B1-a and B1-b) and conventional B cells (B2) obtained from the liver of HBsAg$^+$ (top) and HBsAg$^-$ (bottom) HBV Tg mice. Percentage of B1-a* **(D)**, *B1-b* **(E)**, *and B2* **(F)** *B cells in various organs of HBsAg$^+$ (solid blue symbols, n=4) and HBsAg$^-$ (empty blue dots, n=4) HBV Tg mice. Populations were defined as: B1-a (Live,CD8$^-$CD4$^-$,B220^{low},IgD$^-$,IgM^{hi}, CD11b$^+$,CD23$^-$,CD5$^+$), B1-b (Live,CD8$^-$CD4$^-$,B220$^+$,IgD$^-$,IgM^{hi}, CD11b$^+$,CD23$^-$,CD5$^-$), B2 (Live,CD8$^-$CD4$^-$,B220$^+$,IgD$^+$,IgM^{low}, CD11b$^-$,CD23$^+$,CD5$^-$).* **(G)** *Representative flow cytometry plots of transitional B cells (T1and T2), and mature B cells (M) obtained from the spleen of HBsAg$^+$ (top) and HBsAg$^-$ (bottom) HBV Tg mice. Percentage of T1* **(H)**, *T2* **(I)**, *and Mature* **(J)** *B cells in various organs of HBsAg$^+$ (solid blue symbols, n=4) and HBsAg$^-$ (empty blue dots, n=4) HBV Tg mice. Populations were identified as: T1 (Live,CD8$^-$CD4$^-$,B220$^+$,IgD$^-$,IgM^{hi}, CD23$^-$), T2 (Live,CD8$^-$CD4$^-$,B220$^+$,IgD^{hi},IgM^{hi}, CD23^{low}), Mature (Live,CD8$^-$CD4$^-$,B220$^+$,IgD$^+$,IgM^{low}, CD23$^+$).* **(K)** *Representative flow cytometry plots (left) of germinal centre (GC) B cells obtained from the liver of HBsAg$^+$ (top) and HBsAg$^-$ (bottom) HBV Tg mice. Percentage (right) of GC B cells in various organs of HBsAg$^+$ (solid blue symbols, n=4) and HBsAg$^-$ (empty blue dots, n=4) HBV Tg mice. Populations were identified as: GC (Live,CD8$^-$CD4$^-$,B220$^+$,IgD$^-$,IgM$^-$,CD38$^-$,CD95$^+$,GL7$^+$).* **(L)** *Representative flow cytometry plots (left) of plasma cell (PC) B cells obtained from the liver of HBsAg$^+$ (top) and HBsAg$^-$ (bottom) HBV Tg mice. Percentage (right) of PC B cells in various organs of HBsAg$^+$ (solid blue symbols, n=4) and HBsAg$^-$ (empty blue dots, n=4) HBV Tg mice. Populations were identified as: PC (Live,CD8$^-$CD4$^-$,B220$^+$,IgD$^-$,CD38$^+$,CD138$^+$, CD80$^-$).*
*Data are expressed as mean ± SEM and are representative of at least 2 independent experiments. ns p-value > 0.05; two-way ANOVA followed by Sidak's multiple comparison test (**B, D, E, F, H, I, J, K, L**).*

We hypothesise that the lack of detectable differences in the B cell population is likely due to the very low frequency of HBs-specific B cells. Therefore, alternative methods for the detection and characterisation of HBsAg-specific B cells should be explored to overcome these limitations and enhance detection sensitivity.

4.1.4. Summary Aim I

In conclusion of **AIM I**, we expanded on the previous observation of spontaneous HBsAg seroconversion in male HBV Tg mice (Fumagalli *et al*, 2020) by demonstrating that also female HBV Tg mice clear serum HBsAg spontaneously due to the production of anti-HBs antibodies. Taking into consideration the importance of B cells in the context of seroconversion, we revealed that HBs-specific B cells were localised primarily in the

spleen, liver, bone marrow, and colon of seroconverted mice, predominantly producing IgG1 and IgG3 antibodies. The low frequency of HBs-specific B cells precluded detection by flow cytometry; however, analysis of global B cell populations in $HBsAg^+$ and $HBsAg^-$ mice showed no significant differences, suggesting that seroconversion does not significantly alter the overall B cell composition.

4.2. Aim II: Study the role of $CD4^+$ T cell in promoting HBsAg seroconversion

$CD4^+$ T cells play a vital role in enhancing the quality of B cell responses by providing crucial support through cytokine secretion and direct cell-to-cell interactions, facilitating the generation of high-affinity antibodies. This collaboration not only promotes affinity maturation within germinal centres but also influences B cell differentiation into long-lived plasma cells, ultimately shaping the effectiveness of the adaptive immune response. Through their ability to process and present antigens via major histocompatibility complex (MHC) class II molecules, B cells play a crucial role in engaging $CD4^+$ T cells, which subsequently leads to the differentiation of T follicular helper (Tfh) cells (Lanzavecchia, 1990). Tfh cells are essential for germinal centre formation, where B cells undergo somatic hypermutation and class-switch recombination to produce high affinity Abs. Through the CD40-CD40L engagement and various other co-stimulatory molecules, Tfh cells provide critical survival signals to B cells, promoting their proliferation and differentiation into plasma cells and memory B cells (Mitchison, 2004; Vinuesa *et al*, 2010). The coordinated interaction between $CD4^+$ T cells and B cells is necessary to ensure effective humoral immunity, and disruptions in this collaboration can result in impaired antibody production or autoimmune conditions (Lund & Randall, 2010).

Recognising the importance of these interactions in regulating B cell responses and antibody maturation, a necessary step which leads to seroconversion, we aimed to elucidate the cellular and molecular mechanisms by which HBs-specific B cells are being activated in HBV Tg mice. Consequently, we decided to evaluate whether HBsAg seroconversion relies on the help of $CD4^+$ T cells.

4.2.1. CD40-CD40L and MHC-II pathways are essential for the anti-HBsAg antibody response in HBV transgenic mice

To understand the contribution of $CD4^+$ T cells in HBsAg clearance in HBV Tg mice, we examined the necessity of CD40 signalling for the anti-HBs antibody response. As previously described, CD40 is a co-stimulatory molecule mainly found on antigen-

presenting cells, including B cells, and its ligation ultimately results in supporting cell activation and survival. CD40L, primarily expressed by $CD4^+$ T cells, binds to CD40 on B cells promoting germinal centre formation, leading to class-switching and affinity maturation (Kooten & Banchereau, 1997a; Elgueta *et al*, 2009). To determine the specific role of CD40-CD40L engagement in the development of the anti-HBs antibody response, we generated HBV Tg mice deficient in CD40L expression (HBV Tg x $CD40L^{-/-}$), thereby preventing $CD4^+$ T cells from providing help to B cells (Xu *et al*, 1994; Renshaw *et al*, 1994). HBV Tg x $CD40L^{-/-}$ mice showed serum HBeAg concentrations, as well as serum HBV DNA levels at weaning and at the end of the observation period, comparable to those of HBV Tg mice (**Figure 15 B, C**). Furthermore, HBV Tg x $CD40L^{-/-}$ mice showed no evidence of liver immunopathology (**Figure 15 D, E**) and had hepatic HBcAg amount and staining pattern that are comparable to those of HBV Tg mice (Fumagalli *et al*, 2020) (**Figure 15 F**). We then monitored the HBsAg levels in the sera HBV Tg x $CD40L^{-/-}$. Specifically, starting from 3 weeks of age, mice were bled weekly for 20 weeks and the HBsAg levels in the sera were quantified by ELISA assay (**Figure 15 A, G**). HBV Tg x $CD40L^{-/-}$ mice failed to clear HBsAg after 7 weeks of age and did not become HBsAg-negative for the entire duration of the study (**Figure 15 G**). In contrast, antibodies specific for HBsAg were undetectable in HBV Tg x $CD40L^{-/-}$ mice throughout the observation period (**Figure 15 H**). Given that spontaneous HBsAg clearance is HBsAb-dependent, we next examined components of the humoral immune response. After isolating lymphocytes from the liver, spleen, bone marrow and colon of HBV Tg x $CD40L^{-/-}$ mice, we performed an ELISpot assay to detect HBsAg-specific B cells (**Figure 15 A**). While we were able to enumerate HBsAg-specific B cells in the control group ($HBsAg^-$ HBV Tg mice) across all organs, no detectable spots were observed for the HBV Tg x $CD40L^{-/-}$ mice (**Figure 15 I, J**).

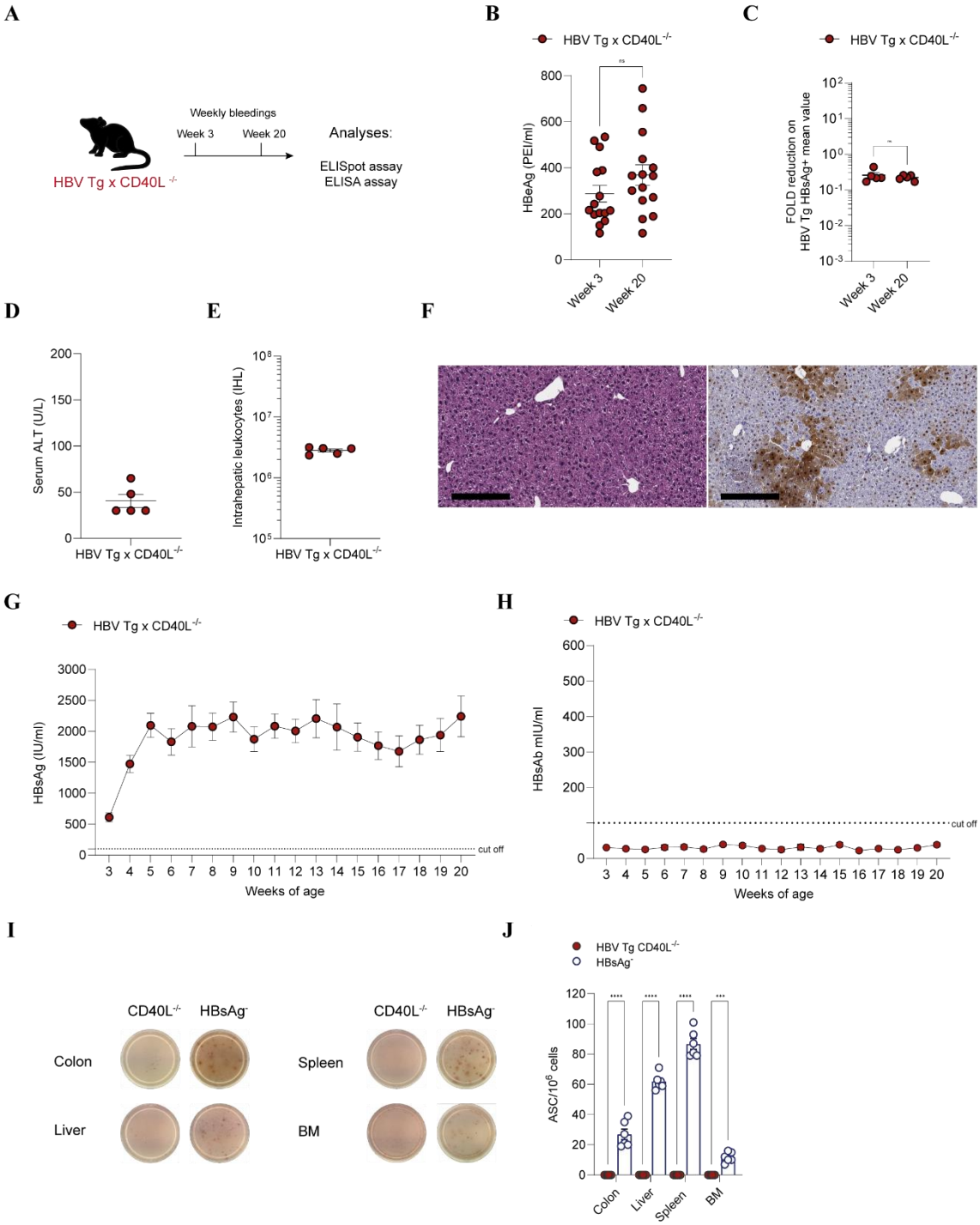


Figure 15. CD40-CD40L engagement has a role in the antibody-mediated clearance of the surface antigen and the generation of HBsAg-specific B cells in HBV transgenic mice

(A) *Schematic representation of the experimental setup. HBV Tg x CD40L$^{-/-}$ mice (n=22) were bled weekly from 3 to 20 weeks of age. HBsAg and HBsAb serum levels were analysed by ELISA assay. At 20 weeks of age the mice were sacrificed, and various organs were collected and analysed by ELISpot.* **(B)** *Serum HBeAg levels (PEI/ml) of HBV Tg x CD40L$^{-/-}$ mice (n=15) measured at 3 weeks and 20 weeks of age by ELISA assay.* **(C)** *Quantification of HBV DNA in the sera of HBV Tg x CD40L$^{-/-}$ mice (n=5). Values are expressed as FOLD reduction on HBV Tg*

$HBsAg^+$ mean value. Values were measured with reference to standard curve. **(D-E)** *Serum transaminase activity (ALT, U/L)* **(D)** *and absolute number of intrahepatic leukocytes* (**E**) *in HBV Tg x $CD40L^{-/-}$ mice (n = 5) at 20 weeks of age.* **(F)** *Representative immunohistochemical micrographs of liver sections from HBV Tg x $CD40L^{-/-}$ mice showing H&E staining (right) and HBV core antigen (HBcAg) staining (left, expression is shown in brown). Scale bars represent 200 µm.* (**G**) *Serum HBsAg levels (IU/ml) of HBV Tg x $CD40L^{-/-}$ mice monitored from 3 weeks to 20 weeks of age by ELISA assay (cut off = 100 IU/ml) (dark orange symbols, n=22).* **(H)** *Serum anti-HBsAg (HBsAb) levels (mIU/ml) of HBV Tg x $CD40L^{-/-}$ mice monitored from 3 weeks to 20 weeks of age by ELISA assay (cut off = 100 IU/ml) (dark orange symbols, n=22).* **(I)** *Representative ELISpot scans of anti-HBsAg-secreting B cells in the colon, liver, spleen, and bone marrow (BM) of $HBsAg^-$ (control) and HBV Tg x $CD40L^{-/-}$ mice.* **(J)** *Total number of antibody secreting cells per 10^6 of cells in various organs of control mice $HBsAg^-$ HBV Tg mice (empty blue symbols, n=6) and HBV Tg x $CD40L^{-/-}$ mice (dark orange symbols, n=6).*
*Data are expressed as mean ± SEM and are representative of at least 2 independent experiments. ns p-value > 0.05, *** p value < 0.001, **** p value < 0.0001; unpaired t-test (**B, C**); two-way ANOVA followed by Sidak's multiple comparison test (**J**)*

Similar results were also observed in major histocompatibility complex class II (MHC-II)- deficient HBV Tg mice. We generated HBV Tg mice lacking the expression of MHC-II molecules (HBV Tg x MHC-$II^{-/-}$), which exhibited a near-complete absence of mature $CD4^+$ T cell (data not shown). Moreover, B cells from MHC-$II^{-/-}$ mice are unable to be activated by antigen-specific T cells in cognate manner (Madsen *et al*, 1999). HBV Tg x MHC-$II^{-/-}$ mice showed serum HBeAg concentrations as well as serum HBV DNA levels at weaning and at the end of the observation period comparable to those of HBV Tg mice (**Figure 16 B, C**). Furthermore, HBV Tg x MHC-$II^{-/-}$ mice showed no evidence of liver immunopathology (**Figure 16 D, E**) and had hepatic HBcAg amount and staining pattern that are comparable to those of HBV Tg mice (Fumagalli *et al*, 2020) (**Figure 16 F**). We monitored the HBsAg levels in the sera HBV Tg x MHC-$II^{-/-}$. Specifically, starting from 3 weeks of age, mice were bled weekly for 20 weeks and the HBsAg levels in the sera were quantified by ELISA assay (**Figure 16 A**). Similar to HBV Tg x $CD40L^{-/-}$ mice, HBV Tg x MHC-$II^{-/-}$ mice did not undergo seroconversion; serum levels of HBsAg remained persistently high (**Figure 16 G**) and HBsAb remained undetectable throughout the study (**Figure 16 H**).

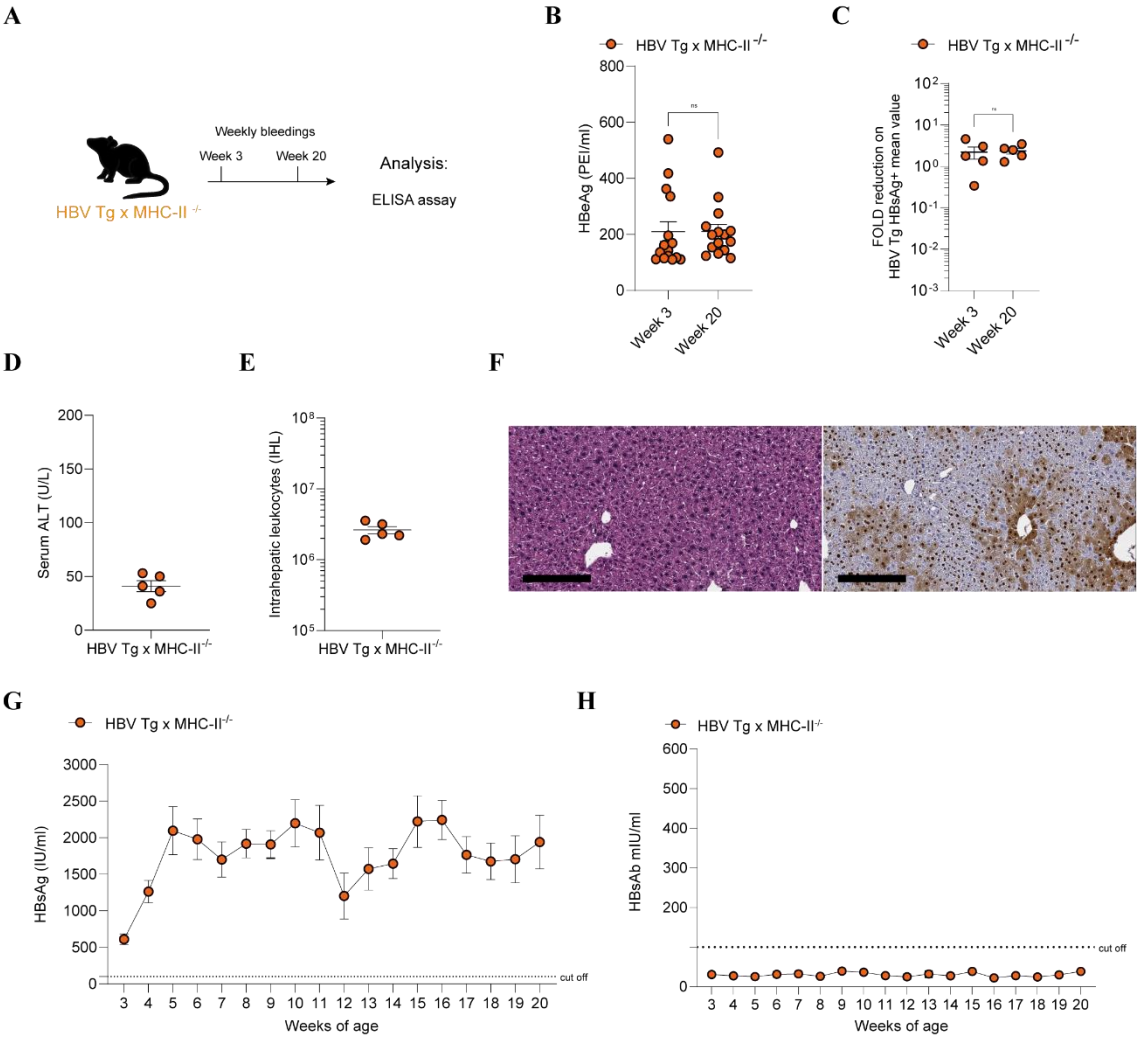


Figure 16. Antigen presentation has a role in the antibody-mediated clearance of the surface antigen in HBV transgenic mice

(A) *Schematic representation of the experimental setup. HBV Tg x MHC-II$^{-/-}$ mice (n=22) were bled weekly from 3 to 20 weeks of age. HBsAg and HBsAb serum levels were analysed by ELISA assay.* **(B)** *Serum HBeAg levels (PEI/ml) of HBV Tg x MHC-II$^{-/-}$ (n=15) measured at 3 weeks and 20 weeks of age by ELISA assay.* **(C)** *Quantification of HBV DNA in the sera of HBV Tg x MHC-II$^{-/-}$ mice (n=5). Values are expressed as FOLD reduction on HBV Tg HBsAg^{+} mean value. Values were measured with reference to standard curve.* **(D-E)** *Serum transaminase activity (ALT, U/L)* **(D)** *and absolute number of intrahepatic leukocytes* **(E)** *in HBV Tg x MHC-II$^{-/-}$ mice (n = 5) at 20 weeks of age.* **(F)** *Representative immunohistochemical micrographs of liver sections from HBV Tg x MHC-II$^{-/-}$ mice showing H&E staining (right) and HBV core antigen (HBcAg) staining (left, expression is shown in brown). Scale bars represent 200 µm.* **(G)** *Serum HBsAg levels (IU/ml) of HBV Tg x MHC-II$^{-/-}$ mice monitored from 3 weeks to 20 weeks of age by ELISA assay (cut off = 100 IU/ml) (orange symbols, n=22).* **(H)** *Serum anti-HBsAg (HBsAb) levels (mIU/ml) of HBV Tg x MHC-II$^{-/-}$ mice monitored from 3 weeks to 20 weeks of age by ELISA assay (cut off = 100 IU/ml) (orange symbols, n=22).*
*Data are expressed as mean ± SEM and are representative of at least 2 independent experiments. ns p-value > 0.05; unpaired t-test (**B, C**).*

These findings indicate the essential role of $CD4^+$ T cells in enhancing B cell function and promoting T-B cell interactions through CD40-CD40L engagement. This collaboration is vital for generating a robust functional neutralising anti-HBsAg antibody response, which is crucial for achieving HBsAg seroconversion in HBV Tg mice.

4.2.2. Enhanced Tfh cell frequency and IFNɣ production characterise $CD4^+$ T cell responses in $HBsAg^-$ HBV transgenic mice

Given the fundamental role of $CD4^+$ T cells in generating a functional anti-HBsAg antibody response, we next sought to characterise the $CD4^+$ T cell population in $HBsAg^+$ and $HBsAg^-$ HBV Tg mice. To this end, we monitored HBsAg and HBsAb levels in the sera by ELISA assay and sacrificed the mice at 22 weeks of age. The liver and the spleen of the mice were surgically collected and processed for further analysis (**Figure 17 A**). We initially attempted to detect HBsAg-specific $CD4^+$ T cells by taking advantage of class II fluorescent tetramers loaded with the immunodominant HBsAg peptide (HBs-Tet) (I-A(b) RGLYFPAGGSSSG) obtained from NIH Tetramer Facility Core. However, although this method is highly sensitive and specific (HBV-specific $CD4^+$ TCR transgenic mice in which $CD4^+$ T cells carry a reactive T-cell receptor that is specific for the HBsAg were used as positive control), these cells were not detectable (**Figure 17 B**). Consequently, we focused on characterising the global $CD4^+$ T cell population in $HBsAg^+$ and $HBsAg^-$ HBV Tg mice.

Despite comparable total $CD4^+$ cell counts in the spleen and liver of both $HBsAg^+$ and $HBsAg^-$ mice (**Figure 17 C**), we observed a significant difference in the percentage of follicular helper CD4 T cells in the spleen, and Tfh-like cells in the liver, in $HBsAg^-$ mice compared to $HBsAg^+$ HBV Tg mice (**Figure 17 D, E**). Additionally, $HBsAg^-$ $CD4^+$ T cells presented an increased expression of Ki-67 (**Figure 17 F**), suggesting enhanced proliferative capacity. Furthermore, these $CD4^+$ T cells demonstrated a greater production of IFNɣ, as evidenced by the increased percentage of IFNɣ-producing $CD4^+$ T cells after *in vitro* stimulation with PMA/Ionomycin in $HBsAg^-$ HBV Tg mice (**Figure 17 G**). Of note, it is known that *in vitro* stimulation of T cells using PMA/Ionomycin activates protein kinase C (PKC) and triggers $Ca2^+$ mobilization independently of T-cell receptor

(TCR) signalling, resulting in IFNγ production through the NF-kB pathway (Ai *et al*, 2013).

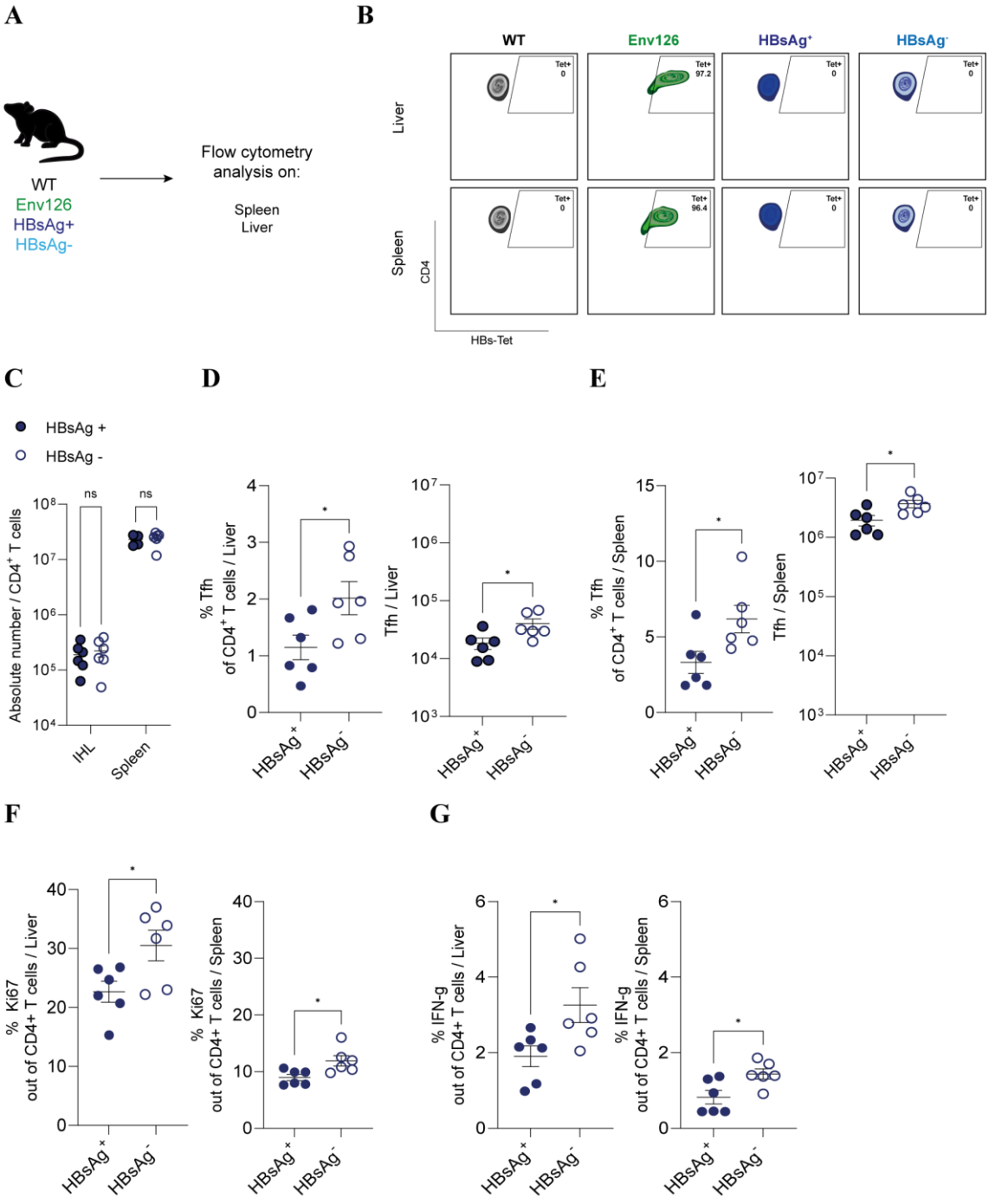


Figure 17. Characterisation of global CD4⁺ T cell populations in HBsAg⁺ and HBsAg⁻ HBV transgenic mice

(A) *Schematic representation of the experimental setup. HBsAg⁺ and HBsAg⁻ HBV Tg mice were sacrificed at 22 weeks of age. Various organs were collected and analysed by flow cytometry.* ***(B)***

Representative flow cytometry plots of HBs-tetramer positive cells found in the liver, and spleen of control mice (WT C57BL/6, grey plots; Env126 Rag1$^{-/-}$ mice, green plots), HBsAg^{+} HBV Tg mice (dark blue plots), and HBsAg^{-} HBV Tg mice (empty blue plots). Cell suspensions were stained with HBs126-138 peptide loaded tetramer (I-Ab HBsAg). HBs-Tetramer positive CD4^{+} T cells are identified as Live, CD45^{+}B220^{-}CD19^{-}CD8^{-}CD4^{+}Tet^{+}. **(C)** *Absolute number quantification of total CD4^{+} T cells in the liver (IHL) and spleen of HBsAg^{+} (solid blue symbols, n=6) and HBsAg^{-} (empty blue dots, n=6) HBV Tg mice.* **(D)** *Follicular helper CD4 T cells (Tfh) frequency out of total CD4^{+} T cell population in the liver (IHL) of indicated group of mice (left graph); absolute Tfh cells numbers in the liver of indicated groups (right graph). Tfh cells were defined as Live, CD45^{+}B220^{-}CD19^{-}CD4^{+}Bcl6^{+}ICOS^{+}PD1^{+}.* **(E)** *Follicular helper CD4 T cells (Tfh) frequency out of total CD4^{+} T cell population in the spleen of indicated group of mice (left graph); absolute Tfh cells numbers in the liver of indicated groups (right graph). Tfh cells were defined as Live, CD45^{+}B220^{-}CD19^{-}CD4^{+}Bcl6^{+}ICOS^{+}PD1^{+}.* **(F)** *Ki-67-expressing CD4^{+} T cells frequency out of total CD4^{+} T cell population in the liver (IHL) (left graph) and spleen (right graph) of indicated group of mice; CD4^{+} T cells are identified as Live, CD45^{+}B220^{-}CD19^{-}CD8^{-}CD4^{+}Ki67^{+}.* **(G)** *IFNɣ-expressing CD4 T cells frequency out of total CD4^{+} T cell population in the liver (IHL) (left graph) and spleen (right graph) of indicated group of mice; CD4^{+} T cells are identified as Live, CD45^{+}B220^{-}CD19^{-}CD8^{-}CD4^{+} IFNɣ$^{+}$.*
*Data are expressed as mean ± SEM and are representative of at least 2 independent experiments. ns p-value > 0.05, * p value < 0.05; two-way ANOVA followed by Sidak's multiple comparison test (**C**); unpaired t-test (**D, E, F, G**).*

These results indicate that HBsAg^{-} HBV Tg mice exhibit a higher proportion of follicular helper CD4^{+} T cells, enhanced CD4^{+} T cell proliferation, and increased IFNγ production compared to HBsAg^{+} mice, highlighting a more robust and active CD4^{+} T cell response associated with effective HBsAg clearance.

4.2.3. Adoptive transfer of CD4^{+} T cells from HBsAg^{-} mice resolves HBsAg persistence

Building on these observations, we sought to determine whether activated CD4^{+} T cells from HBV Tg seroconverted mice could modulate antigen persistence. Thus, we investigated whether an adoptive transfer of CD4^{+} T cells isolated from HBsAg^{-} mice could promote HBsAg clearance in recipient HBV Tg mice. Briefly, B cells and CD4^{+}T cells were isolated from the spleen of HBsAg^{+} and HBsAg^{-} HBV Tg mice and then transferred via intravenous injection (i.v.) into HBsAg persistent mice lacking immunoglobulin expression (HBV Tg x CD40L$^{-/-}$ and HBV Tg x DHLP2a (Fumagalli *et al*, 2020)) (**Figure 18 A**). Fractions of CD4^{+} T cells and B cells were both ~95% pure as determined by flow cytometry (**Figure 18 B**). As anticipated, recipients of B cells and/or

CD4$^+$ T cells isolated from HBsAg$^+$ mice maintained persistently high levels of serum HBsAg. In contrast, recipients of B cells and/or CD4$^+$ T cells isolated from HBsAg$^-$ mice experienced a significant HBsAg reduction by week 2 post- transfer. Notably, while recipients of HBsAg$^-$ B cells alone were initially able to reduce HBsAg levels, they failed to sustain this control beyond day 14 post-transfer. HBsAg levels eventually rose to pre-transfer levels or even higher, suggesting that B cells derived from seroconverted mice alone are insufficient to maintain a lasting antibody response. On the other hand, recipients that received CD4$^+$ T cells, either alone or in combination with B cells, could sustain HBsAg loss over time, until reaching levels below detection limits (**Figure 18 C**).

Interestingly, anti-HBsAg antibodies were detectable only in the sera of recipients that received CD4$^+$ T cells, either alone or with B cells (**Figure 18 D**), emphasising the critical and indispensable role of these cells in triggering the activation and differentiation of HBsAg-specific B cells. However, the levels of these antibodies were variable, likely due to the formation of HBsAg/HBsAb immune complexes which are not detectable by available ELISA assays.

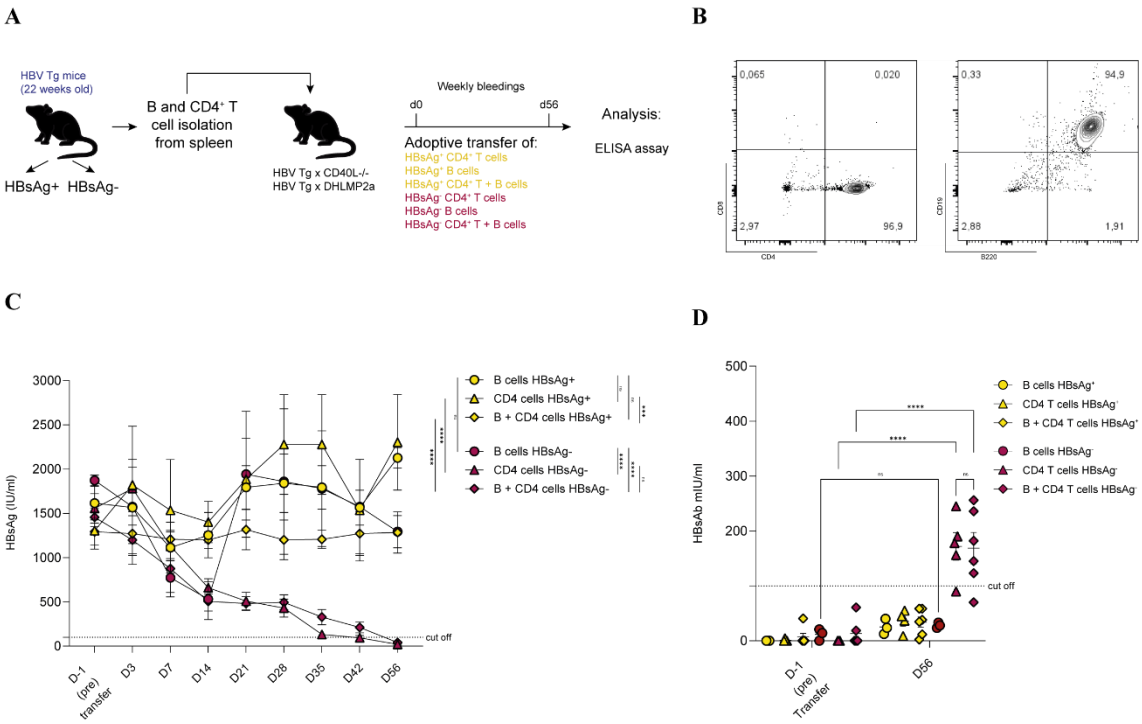


Figure 18. Splenocyte transfer of CD4$^+$ T cells from HBsAg$^-$ mice resolves HBsAg persistence

(A) *Schematic representation of the experimental setup. B and CD4$^+$ T cells were isolated from the spleen of HBsAg$^+$ and HBsAg$^-$ HBV Tg mice (22 weeks of age). The isolated cells were then adoptively transferred by intravenous injection in HBV Tg x CD40L$^{-/-}$ and HBV Tg x DHLP2a mice (5 weeks of age). The recipient mice received either B and/or CD4$^+$ T cells isolated from HBsAg$^+$ or B and/or CD4$^+$ T cells isolated from HBsAg$^-$. The mice were then bled at day 3, 7, 14, 21, 28, 35, and 56 post-transfer and the serum levels of HBsAg and HBsAb were measured by ELISA assay. 0.8x10^6 B cells and 0.8x10^6 CD4$^+$T cells were transferred in each condition.* **(B)** *B cell (left) and CD4$^+$ T cell (right) purity following magnetic column separation was determined by flow cytometry* ***(C)*** *Serum HBsAg levels (IU/ml) of recipient HBV Tg x CD40L$^{-/-}$ (n=15) and HBV Tg x DHLP2a mice (n=15) monitored from D-1 (day before transfer) to D56 post-transfer by ELISA assay (cut off = 100 IU/ml)* **(D)** *Serum anti-HBsAg (HBsAb) levels (mIU/ml)) of recipient HBV Tg x CD40L$^{-/-}$ (n=15) and HBV Tg x DHLP2a mice (n=15) at D-1 (day before transfer) and at D56 post-transfer by ELISA assay (cut off = 100 IU/ml); (yellow circle = mice recipient of HBsAg$^+$ B cells, yellow triangle = mice recipient of HBsAg$^+$ CD4 T cells, yellow diamond = mice recipient of HBsAg$^+$ B cells + CD4 T cells; dark red circle = mice recipient of HBsAg$^-$ B cells, dark red triangle = mice recipient of HBsAg$^-$ CD4 T cells, dark red diamond = mice recipient of HBsAg$^-$ B cells + CD4 T cells).*
Data are expressed as mean ± SEM and are representative of 1 experiment.
*ns p-value > 0.05, *** p value < 0.001, **** p value < 0.0001; two-way ANOVA followed by Tukey's multiple comparison test (**C, D**).*

These findings demonstrate that CD4$^+$ T cells from HBsAg$^-$ HBV Tg mice can effectively induce HBsAg clearance when transferred to antigen-persistent mice. These findings further support the pivotal role of CD4$^+$ T cell in driving HBs seroconversion in HBV Tg mice.

4.2.4. Summary of Aim II

This study reveals that the presence of CD4$^+$ T cells and CD40-CD40L pathway are essential for a functional anti-HBsAg antibody response in HBV Tg mice, as mice deficient in CD40L or MHC-II expression, and consequently lacking mature CD4$^+$ T cells, failed to clear HBsAg and did not develop HBsAg-specific antibodies. Further analysis demonstrated that HBsAg$^-$ HBV Tg mice exhibit a higher frequency of follicular helper CD4$^+$ T cells, increased CD4$^+$ T cell proliferation, and enhanced IFNγ production compared to HBsAg$^+$ mice, indicating a more robust CD4$^+$ T cell response associated with effective HBsAg clearance. Building on these findings, adoptive transfer of CD4$^+$ T cells from HBsAg$^-$ mice to antigen-persistent HBV Tg mice resulted in sustained HBsAg

reduction and the induction of anti-HBsAg antibodies. These results underscore the importance of $CD4^+$ T cells in mediating HBsAg seroconversion by providing T cell help to B cells and highlight the possibility of leveraging these immune mechanisms in future therapeutic strategies.

4.3. Aim III: Investigating the role of the microbiome in promoting the HBsAg seroconversion

Emerging evidence suggest that the gut microbiome significantly influences host immune responses, with alterations in the gut microbiota being associated with chronic liver diseases, including HBV-related liver pathologies. The gut-liver axis plays, in fact, a crucial role in immune regulation, and disruptions in the intestinal microbiome have been shown to affect the immune response. Studies have demonstrated that specific microbial communities can modulate the activity and differentiation of key immune cells, such as $CD4^+$ T cells and B cells, which are central to adaptive immunity. In the context of HBV pathogenesis, these microbial-induced changes in immune cell function could potentially impact the course of HBV infection and resolution (Tripathi *et al*, 2018; Zheng *et al*, 2020; Albillos *et al*, 2020). Moreover, altered and flexible profile of gut microbiota has been observed in HBV-infected individuals (Schwabe & Greten, 2020; Li *et al*, 2022b), further supporting the link between gut microbial composition and HBV pathophysiology.

Given these findings, we hypothesized that the gut microbiome might impact HBsAg clearance and seroconversion by modulating the immune landscape. We are particularly interested in this area of research because HBs seroconversion occurs only in a fraction of HBV Tg mice, and it is unclear why some mice successfully clear HBsAg while others do not. Investigating the interplay between the gut microbiome and seroconversion could provide novel insights into why this variability occurs and could identify microbiome-targeted therapies that enhance seroconversion rates and improve clinical outcomes in chronic HBV infection.

4.3.1. Faecal microbiota transplant from HBsAg$^-$ mice leads to seroconversion

Because we observed that seroconversion often occurred among animals housed in the same cage (**Figure 19 A, B, C**), we reasoned that the composition of the intestinal microbiome composition influences this process.

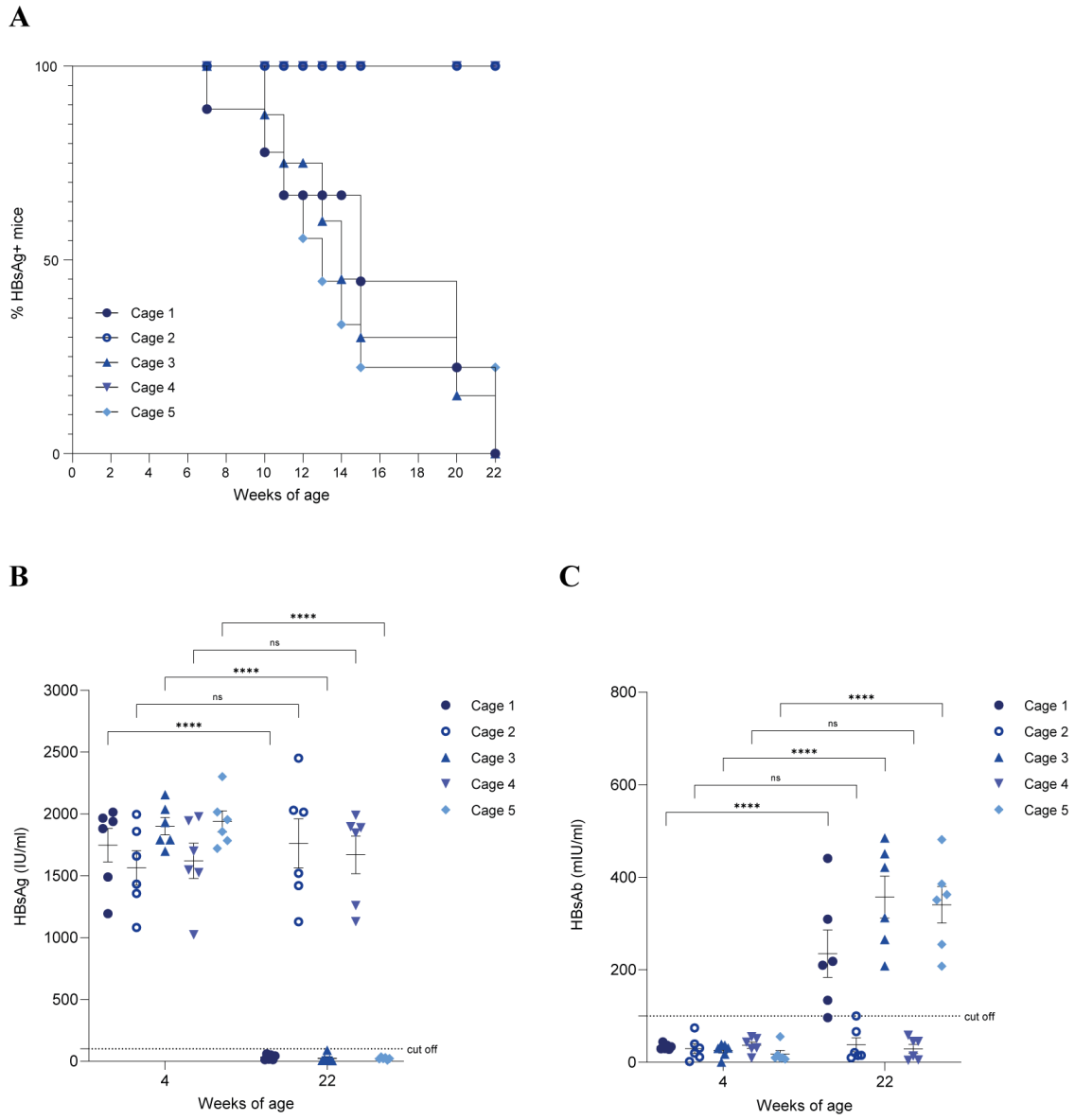


Figure 19. Cage-mates exhibit similar trends in serum HBsAg and HBsAb levels

(A) *Percentage of HBV Tg mice with detectable serum HBsAg across five different cages (Cage 1 solid blue circles, n=6; Cage 2 empty blue circles, n=6; Cage 3 blue triangles (up), n=6; Cage 4 blue triangles (down), n=6; Cage 5 blue diamonds, n=6).* **(B)** *Serum HBsAg levels (IU/ml) of HBV Tg mice across five different cages (Cage 1 solid blue circles, n=6; Cage 2 empty blue circles, n=6; Cage 3 blue triangles (up), n=6; Cage 4 blue triangles (down), n=6; Cage 5 blue diamonds, n=6) measured at 4 and 22 weeks of age by ELISA assay (cut off = 100 IU/ml).* **(C)** *Serum anti-HBsAg (HBsAb) levels (mIU/ml) of of HBV Tg mice across five different cages (Cage 1 solid blue circles, n=6; Cage 2 empty blue circles, n=6; Cage 3 blue triangles (up), n=6; Cage 4 blue triangles (down), n=6; Cage 5 blue diamonds, n=6) measured at 4 and 22 weeks of age by ELISA assay (cut off = 100 IU/ml).*
*Data are expressed as mean ± SEM and are representative of at least 6 independent experiments. ns p-value > 0.05, **** p value < 0.0001; two-way ANOVA followed by Sidak's multiple comparison test (**B, C**).*

To test this hypothesis, we treated 4-week-old (pre-seroconversion) HBV Tg mice with a broad-spectrum antibiotic regimen (neomycin, metronidazole, vancomycin, and clindamycin) before performing a faecal microbiota transplant (FMT) with faeces derived from $HBsAg^+$ or $HBsAg^-$ HBV Tg mice (**Figure 20 A**). Specifically, all mice received antibiotic treatment for 4 days, followed by a 1-day rest period, and were then randomised to receive FMT. Mice were administered either $HBsAg^+$ FMT or $HBsAg^-$ FMT by oral gavage for three consecutive days. No adverse effects or deaths were observed during the antibiotic treatment, and the animals maintained good health, as confirmed by continuous weight gain throughout the study period (**Figure 20 B**). To evaluate the efficacy of the broad-spectrum antibiotics, we performed bacterial culture assays. At day 0, prior to antibiotic treatment, high bacterial loads were detected. After 3 days of antibiotic treatment, a significant reduction in colony-forming units (CFUs) was observed, indicating effective gut decontamination (**Figure 20 C**). Furthermore, an increase in cecum weight was observed in mice that received the antibiotic cocktail (**Figure 20 D**), consistent with previous studies showing that antibiotic administration can significantly increase cecum size and weight due to alterations in gut microbiota composition and subsequent changes in the digestive and absorptive processes within the gut (Reikvam *et al*, 2011; Ge *et al*, 2017; Kim *et al*, 2017).

Following FMT, serum HBsAg and HBsAb levels in the recipient mice were monitored by ELISA. Notably, 10 days post-transplant, mice that received FMT from $HBsAg^-$ donors already showed lower serum HBsAg levels compared to those that received FMT from $HBsAg^+$ donors. By day 100 post-FMT, all mice that received faeces from $HBsAg^-$ donors had seroconverted, with HBsAg levels dropping below the detection limit (**Figure 20 E**). Moreover, HBV Tg mice that received FMT from $HBsAg^-$ donors showed detectable anti-HBsAg antibodies as early as 3 days post-FMT (**Figure 20 F**), in contrast to those that received FMT from $HBsAg^+$ donors which showed no detectable antibodies. Significantly, mice that received FMT from $HBsAg^+$ donors lost the ability to undergo spontaneous seroconversion (**Figure 20 E, F**).

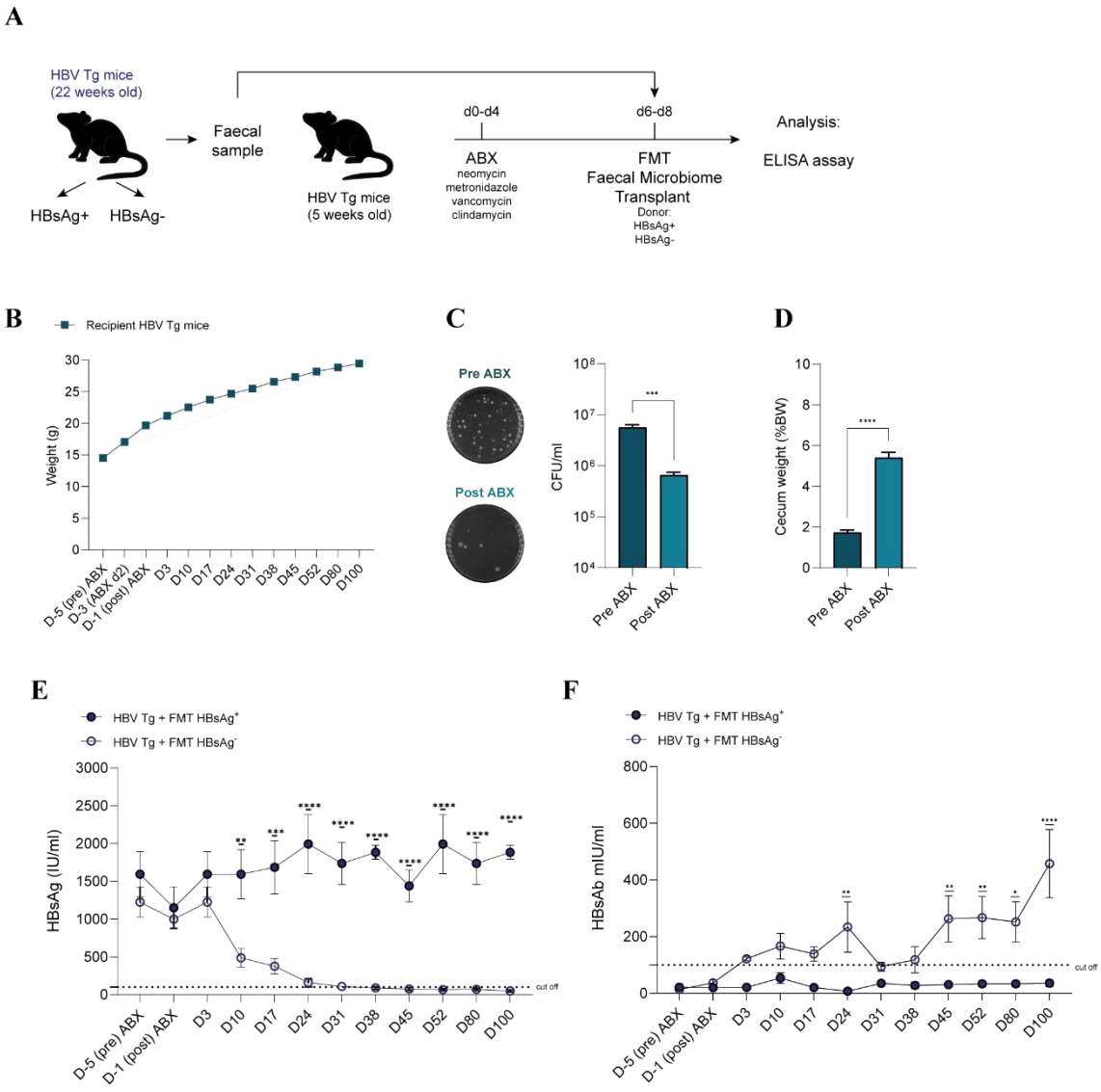


Figure 20. Faecal microbiota transplant in young HBV Tg mice from HBsAg$^+$ and HBsAg$^-$ donor mice

(A) *Schematic representation of the experimental setup. 5 weeks old HBV Tg mice were treated with a cocktail of broad-spectrum antibiotics (ABX) (neomycin, metronidazole, vancomycin, and clindamycin) before receiving a faecal microbiota transplant (FMT) with faeces derived from HBsAg$^+$ or HBsAg$^-$ HBV Tg mice. The recipient mice were repeatedly bled up to 100 days post FMT in order to perform ELISA assays.* **(B)** *Mouse body weight over the course of the experiment, from D-5 (pre-FMT) to D100 (post-FMT).* **(C)** *On the left, bacterial culture of stool samples on Tryptone Soy agar plates pre-antibiotic (pre-ABX) treatment (top) and post-antibiotic (post-ABX) treatment; on the right, quantification of the colony formations obtained from bacterial culture of stool samples of the indicated groups.* **(D)** *The weight of cecum pre-antibiotic (pre-ABX) treatment and post-antibiotic (post-ABX) treatment adjusted by weight of mice.* **(E)** *Serum HBsAg levels (IU/ml) of HBV Tg mice that received FMT from HBsAg$^+$ (solid blue symbols, n=6) and HBsAg$^-$ (empty blue symbols, n=6) donor mice monitored from D-5 (pre-FMT) to D100 (post-FMT) by ELISA assay (cut off = 100 IU/ml).* **(F)** *Serum anti-HBsAg (HBsAb) levels (mIU/ml) of HBV Tg mice that received FMT from HBsAg$^+$ (solid blue symbols, n=6) and HBsAg$^-$ (empty blue symbols, n=6) donor mice monitored from D-5 (pre-FMT) to D100 (post-FMT) by ELISA assay (cut off =*

100 IU/ml).
*Data are expressed as mean ± SEM and are representative of at least 3 independent experiments. ** p value < 0.01, *** p value < 0.001, **** p value < 0.0001; unpaired t-test (**C, D**), two-way ANOVA followed by Sidak's multiple comparison test (**E, F**).*

To further investigate whether the microbiome alone could drive seroconversion in HBsAg$^+$ mice, which showed antigen persistence, we repeated the same experimental setup above shown with 22-week-old HBsAg$^+$ mice (**Figure 21 A**). Remarkably, starting around day 17 post-FMT, serum HBsAg levels began to decline in mice that received FMT from HBsAg$^-$ donors, reaching undetectable levels by day 45 post-transfer (**Figure 21 B**). Additionally, HBV Tg mice that received FMT from HBsAg- donors displayed detectable anti-HBsAg antibodies as early as 3 days post-FMT (**Figure 21 C**).

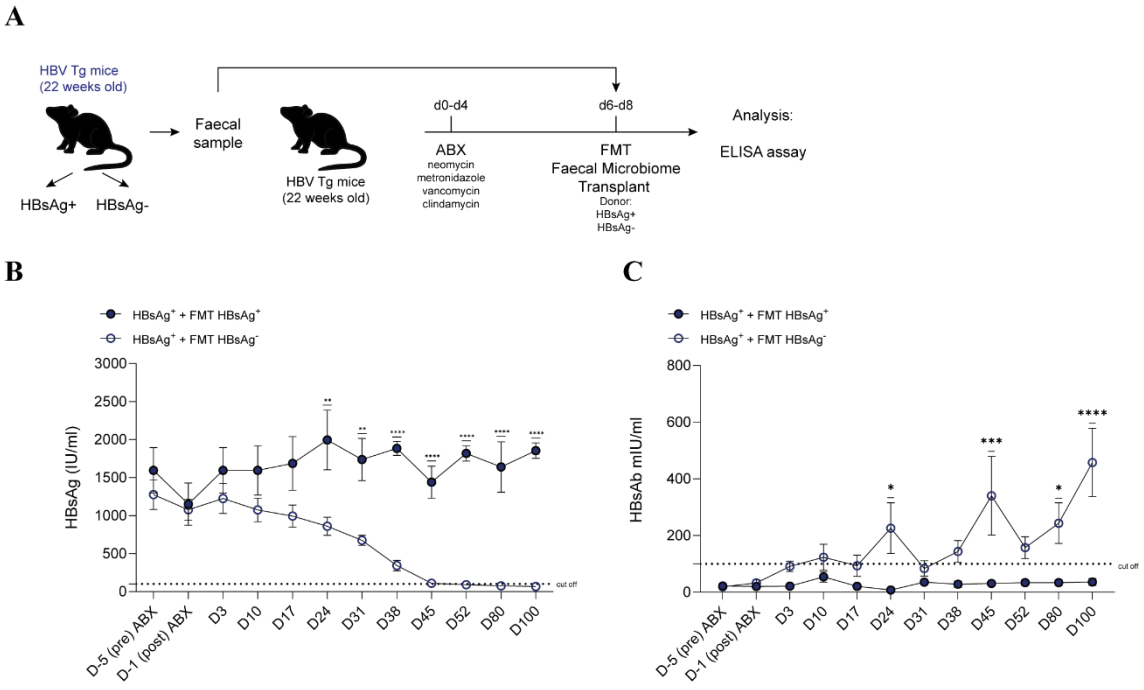


Figure 21. Faecal microbiota transplant from HBsAg$^-$ mice leads to seroconversion

(A) *Schematic representation of the experimental setup. 22 weeks old HBsAg$^+$ HBV Tg mice were treated with a cocktail of broad-spectrum antibiotics (ABX) (neomycin, metronidazole, vancomycin, and clindamycin) before receiving a faecal microbiota transplant (FMT) with faeces derived from HBsAg$^+$ or HBsAg$^-$ HBV Tg mice. The recipient mice were repeatedly bled up to 100 days post FMT in order to perform ELISA assays.* **(B)** *Serum HBsAg levels (IU/ml) of HBsAg$^+$ mice that received FMT from HBsAg$^+$ (solid blue symbols, n=6) and HBsAg$^-$ (empty blue symbols, n=6) donor mice monitored from D-5 (pre-FMT) to D100 (post-FMT) by ELISA assay (cut off = 100 IU/ml).* **(C)** *Serum anti-HBsAg (HBsAb) levels (mIU/ml) of HBsAg$^+$ mice that received FMT*

*from HBsAg$^+$ (solid blue symbols, n=6) and HBsAg$^-$ (empty blue symbols, n=6) donor mice monitored from D-5 (pre-FMT) to D100 (post-FMT) by ELISA assay (cut off = 100 IU/ml). Data are expressed as mean ± SEM and are representative of at least 2 independent experiments. ** p value < 0.01, *** p value < 0.001, **** p value < 0.0001; two-way ANOVA followed by Sidak's multiple comparison test (**B, C**).*

Taken together these results suggest that the gut microbiome can modulate HBsAg clearance and seroconversion in HBV Tg mice.

4.3.2. Faecal Microbiota Transplantation fails to induce HBsAg clearance in HBV Tg x CD40L$^{-/-}$ mice

We have previously shown (**Figure 15**) that HBV Tg x CD40L$^{-/-}$ mice, which lack CD40L expression, do not undergo seroconversion under normal conditions. In the following part of the study, we aimed to determine whether FMT from HBsAg$^-$ mice could overcome the antigen persistence observed in HBV Tg x CD40L$^{-/-}$ mice. To explore this, we treated 4-week-old HBV Tg x CD40L$^{-/-}$ mice with broad-spectrum antibiotics (neomycin, metronidazole, vancomycin, and clindamycin) to deplete their gut microbiota. Following antibiotic treatment, the mice received FMT via oral gavage with faeces derived from HBsAg$^+$ or HBsAg$^-$ HBV Tg mice. Serum HBsAg levels were then monitored for 100 days post-transplant to assess any potential changes in antigen persistence (**Figure 22 A**). Notably, regardless of whether the transplanted faeces originated from HBsAg$^+$ or HBsAg$^-$ mice, recipient HBV Tg x CD40L$^{-/-}$ mice maintained persistently high levels of serum HBsAg throughout the entire observation period (**Figure 22 B**). Furthermore, no HBsAb were detectable in the sera of the recipient mice, indicating lack of seroconversion (**Figure 22 C**).

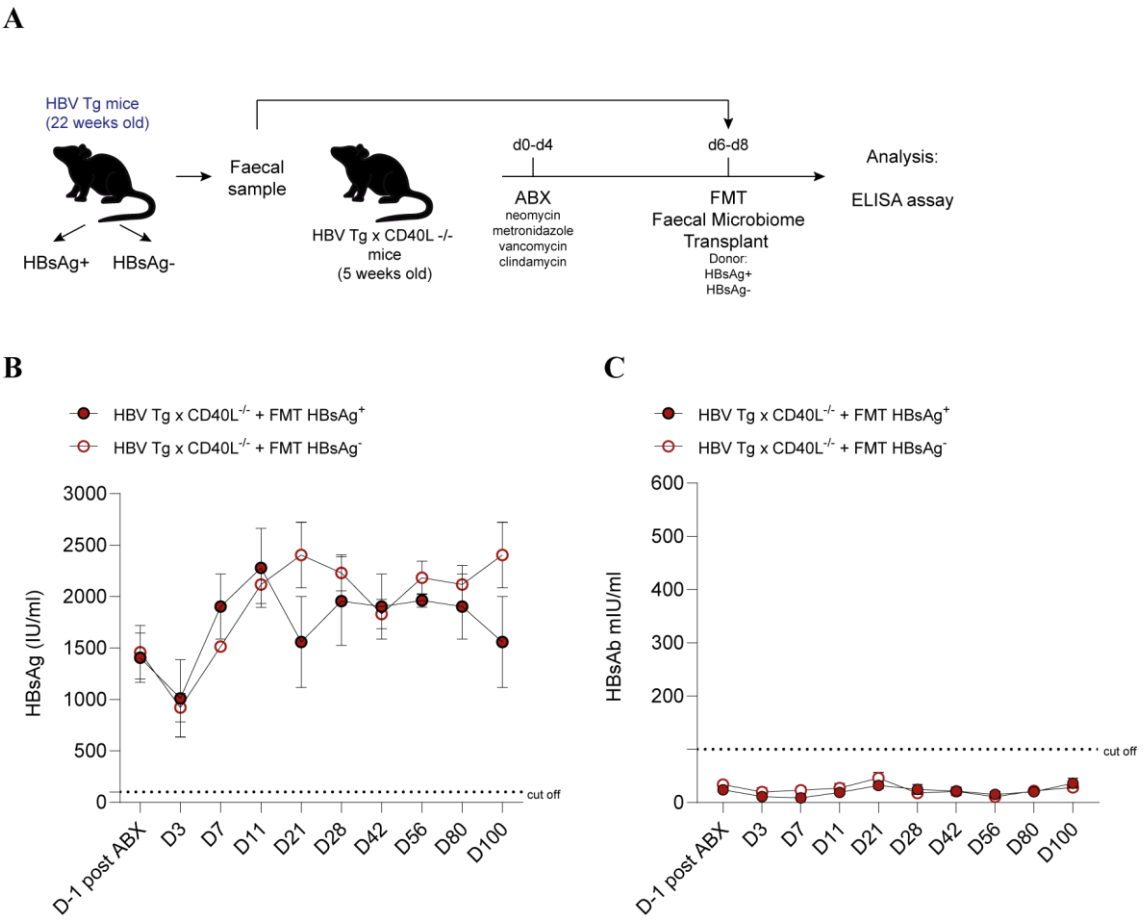


Figure 22. Faecal Microbiota Transplantation fails to induce HBsAg clearance in HBV Tg x CD40L$^{-/-}$ mice

(A) *Schematic representation of the experimental setup. 5 weeks old HBV Tg x CD40L$^{-/-}$ mice were treated with a cocktail of broad-spectrum antibiotics (ABX) (neomycin, metronidazole, vancomycin, and clindamycin) before receiving a faecal microbiota transplant (FMT) with faeces derived from HBsAg^{+} or HBsAg^{-} HBV Tg mice. The recipient mice were repeatedly bled up to 100 days post FMT in order to perform ELISA assays.* **(B)** *Serum HBsAg levels (IU/ml) of HBV Tg x CD40L$^{-/-}$ mice that received FMT from HBsAg^{+} (solid dark orange symbols, n=6) and HBsAg^{-} (empty dark orange symbols, n=6) donor mice monitored from D-5 (pre-FMT) to D100 (post-FMT) by ELISA assay (cut off = 100 IU/ml).* **(C)** *Serum anti-HBsAg (HBsAb) levels (mIU/ml) of HBV Tg x CD40L$^{-/-}$ mice that received FMT from HBsAg^{+} (solid dark orange symbols, n=6) and HBsAg^{-} (empty dark orange symbols, n=6) donor mice monitored from D-5 (pre-FMT) to D100 (post-FMT) by ELISA assay (cut off = 100 IU/ml).*
*Data are expressed as mean ± SEM and are representative of at least 2 independent experiments. Comparisons are not statistically significant; two-way ANOVA followed by Sidak's multiple comparison test (**B, C**).*

These results suggest that, in the absence of CD40L-mediated signalling, altering the gut microbiome alone is insufficient to induce seroconversion or reduce antigen levels in HBV Tg x CD40L$^{-/-}$ mice. This underscores the critical importance of CD40-CD40L

interactions in driving effective immune responses necessary for HBsAg clearance and seroconversion in HBV Tg mice.

4.3.3. Antibiotic treatment alone fails to induce HBsAg clearance without microbiome reconstitution

Next, we sought to determine whether antibiotic treatment alone, without subsequent microbiome reconstitution via faecal microbiota transplant (FMT), could impact HBsAg seroconversion. To address this, three experimental groups were established: an antibiotic-only treated group, a group of mice treated with antibiotics followed by FMT from $HBsAg^+$ mice, and a group of mice treated with antibiotics followed by FMT from $HBsAg^-$ mice (**Figure 23 A**). HBV Tg mice were therefore administered a broad-spectrum antibiotic regimen (neomycin, metronidazole, vancomycin, and clindamycin) for 4 days to deplete the gut microbiota. Mice that received only antibiotics treatment showed no reduction in serum HBsAg levels over the course of the study (**Figure 23 B**). Furthermore, these mice failed to produce any detectable anti-HBsAg antibodies (**Figure 23 C**). In contrast, mice treated with antibiotics followed by FMT from $HBsAg^-$ donors exhibited a marked reduction in serum HBsAg levels (**Figure 23 B**), coupled with the emergence of detectable anti-HBsAg antibodies (**Figure 23 C**), consistent with findings from previous experiments (**Figure 20 E, F**).

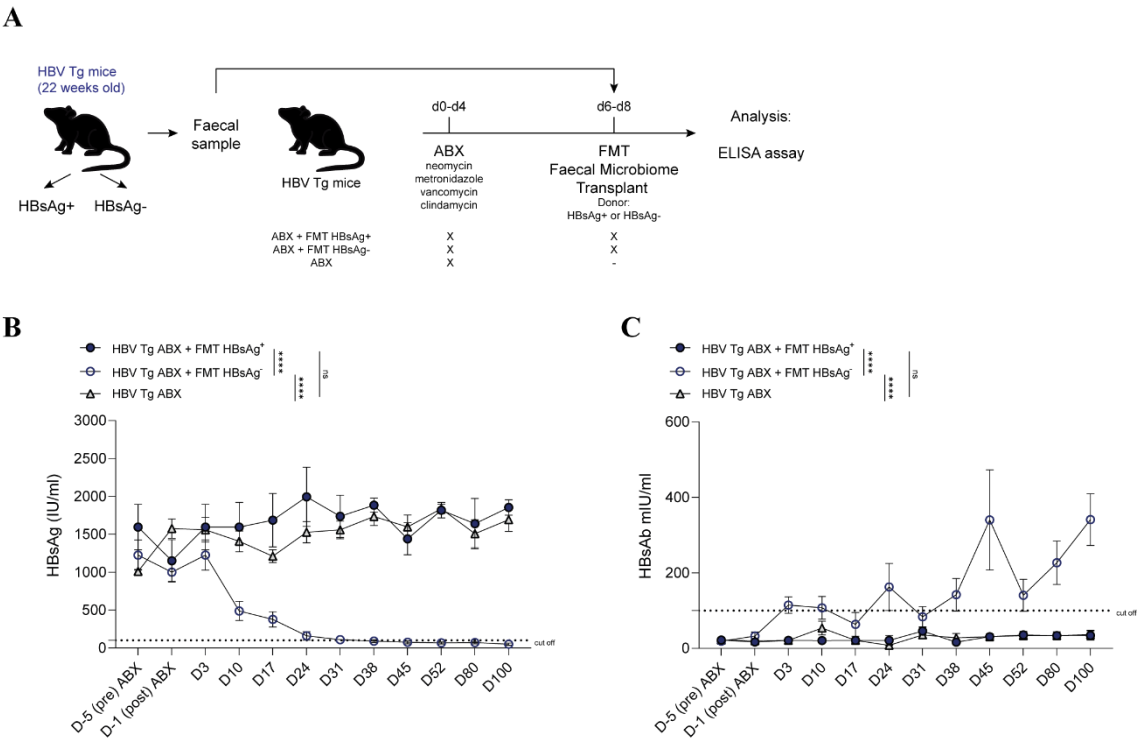


Figure 23. Impact of antibiotic treatment and microbiome reconstitution on HBsAg clearance, antibody production in HBV Tg mice

(A) *Schematic representation of the experimental setup. HBV Tg mice were treated with a cocktail of broad-spectrum antibiotics (ABX) (neomycin, metronidazole, vancomycin, and clindamycin). Some mice also received a faecal microbiota transplant (FMT) with faeces derived from HBsAg$^+$ or HBsAg$^-$ HBV Tg mice. The mice were repeatedly bled up to 100 days post FMT in order to perform ELISA assays.* **(B)** *Serum HBsAg levels (IU/ml) of HBV Tg mice that received ABX only (grey triangle, n=6), ABX + FMT from HBsAg$^+$ (solid blue symbols, n=6) and ABX + FMT HBsAg$^-$ (empty blue symbols, n=6) donor mice monitored from D-5 (pre-FMT) to D100 (post-FMT) by ELISA assay (cut off = 100 IU/ml).* **(C)** *Serum anti-HBsAg (HBsAb) levels (mIU/ml) of HBV Tg mice that received ABX only (grey triangle, n=6), ABX + FMT from HBsAg$^+$ (solid blue symbols, n=6) and ABX + FMT HBsAg$^-$ (empty blue symbols, n=6) donor mice monitored from D-5 (pre-FMT) to D100 (post-FMT) by ELISA assay (cut off = 100 IU/ml).*
Data are expressed as mean ± SEM and are representative of 1 independent experiment.
*ns p-value > 0.05, **** p value < 0.0001; two-way ANOVA followed by Tukey's multiple comparison test (**B, C**).*

Collectively, these findings demonstrate that microbiome reconstitution through FMT is essential for promoting HBsAg clearance and antibody production following antibiotic-induced microbiome depletion.

4.3.4. Co-housing with seroconverted mice promotes HBsAg clearance in antigen-persistent HBV transgenic mice

Next, we investigated whether co-housing HBV Tg mice with female HBV Tg mice that had already undergone seroconversion could promote HBsAg loss in antigen-persistent mice. Co-housing allows the transfer of gut microbiota between animals through shared living environments, including bedding and grooming behaviours. This natural exchange could potentially alter the microbiome composition of the antigen-persistent mice, thereby modulating their immune response. By performing co-housing experiments, we aimed to determine whether exposure to a microbiome from seroconverted mice would influence the ability of $HBsAg^+$ HBV Tg mice to clear HBsAg. In fact, it has been demonstrated that co-housing can alter disease outcomes by transferring gut microbiota between mice (Caruso *et al*, 2019).

To explore this, we first conducted longitudinal measurements HBsAg concentrations in HBV Tg mice over a 20-week period to stratify the experimental mice in two groups: $HBsAg^+$ and $HBsAg^-$ mice (**Figure 24 A**). Anti-HBsAg (HBsAb) serum levels were also assessed (**Figure 24 B**). Mice were then co-housed in mixed groups, with $HBsAg^+$ and $HBsAg^-$ mice placed together. Serum HBsAg and HBsAb levels were then monitored following co-housing (**Figure 24 C**). Remarkably, as early as one week after initiating co-housing, $HBsAg^+$ mice in both setups began to exhibit a progressive decline in serum levels of HBsAg, reaching undetectable levels by 7 weeks post co-housing. Furthermore, by this time, all mice displayed detectable anti-HBsAg antibodies (**Figure 24 D**).

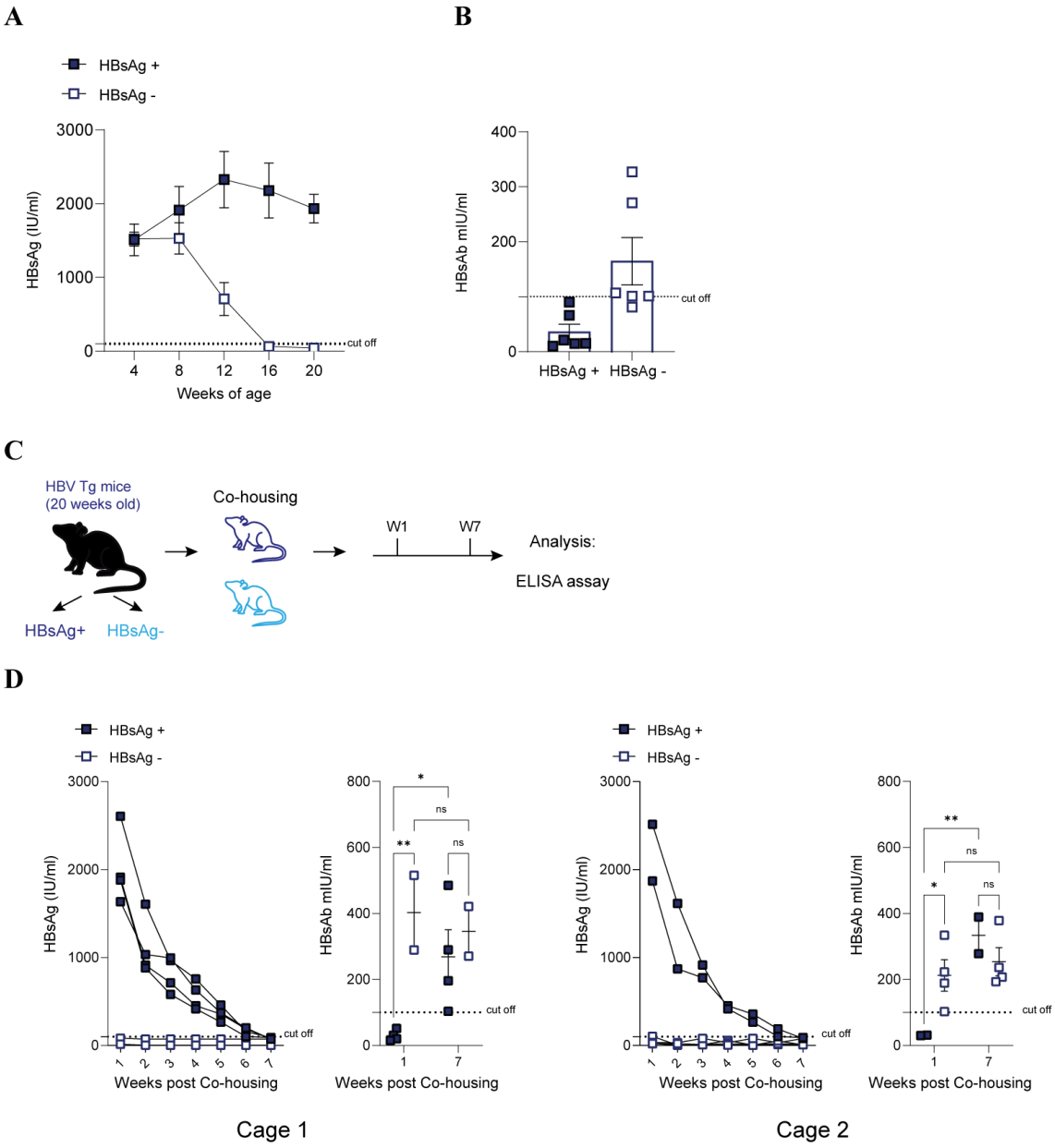


Figure 24. Co-housing with seroconverted mice promotes HBsAg clearance in antigen-persistent HBV transgenic mice

(A) *Serum HBsAg levels (IU/ml) of HBV Tg HBsAg$^+$ (full blue square, n=6) and HBsAg$^-$ (empty blue square, n=6) mice monitored from 4 weeks to 20 weeks of age by ELISA assay (cut off = 100 IU/ml).* **(B)** *Serum anti-HBsAg (HBsAb) levels (mIU/ml) of HBV Tg HBsAg$^+$ (full blue square, n=6) and HBsAg$^-$ (empty blue square, n=6) mice at 20 weeks of age by ELISA assay (cut off = 100 IU/ml).* **(C)** *Schematic representation of the experimental setup. HBV Tg HBsAg$^+$ mice were mixed together with HBsAg$^-$ mice to perform co-housing experiments. They were left in co-housing conditions for 7 weeks, during which the mice were bled weekly to perform ELISA assays.* **(D)** *Serum HBsAg levels (IU/ml) and anti-HBsAg (HBsAb) levels (mIU/ml) of HBV Tg HBsAg$^+$ (full blue square) and HBsAg$^-$ (empty blue square) mice monitored from 1 weeks to 7 weeks post co-housing by ELISA assay (cut off = 100 IU/ml). Each graph is representative of one cage containing either four HBsAg$^+$ mice together with two HBsAg$^-$ mice (left) or two HBsAg$^+$ mice together with four HBsAg$^-$ mice (right).*

*Data are expressed as mean ± SEM and are representative of at least 2 independent experiments. ns p-value > 0.05, * p value < 0.05, ** p value < 0.01; two-way ANOVA followed by Sidak's multiple comparison test (**D**).*

These findings suggest that exposure to a microbiome from seroconverted mice can indeed promote HBsAg loss in antigen-persistent HBV Tg mice, likely through microbiota-mediated immune modulation.

4.3.5. Summary of Aim III

The results of this study highlight the significant role of the gut microbiome in modulating HBsAg clearance and promoting seroconversion in HBV Tg mice. Faecal microbiota transplantation (FMT) from $HBsAg^-$ mice effectively induces seroconversion in HBV Tg mice. When 4-week-old or 22-week-old HBV Tg mice received FMT from $HBsAg^-$ donors following broad-spectrum antibiotic treatment, a significant reduction in serum HBsAg levels was observed, with complete seroconversion achieved in most mice within 45 to 100 days post-transplant. In contrast, in HBV Tg x $CD40L^{-/-}$ mice, which lack CD40L expression critical for B-T cell interactions (Xu *et al*, 1994; Renshaw *et al*, 1994), FMT from $HBsAg^-$ mice failed to clear circulating HBsAg, indicating that CD40L-mediated signalling is essential for effective immune responses in this model. Additionally, antibiotic treatment alone was insufficient to induce HBsAg clearance without microbiome reconstitution. Co-housing experiments further revealed that antigen-persistent HBV Tg mice exposed to the microbiome of seroconverted mice experienced a rapid decline in HBsAg levels, with most achieving undetectable levels by 7 weeks. These findings suggest that while the gut microbiome can significantly modulate HBs seroconversion, its effectiveness is contingent upon intact immune signalling pathways, particularly those involving CD40-CD40L interactions.

DISCUSSION

5. DISCUSSION

Hepatitis B virus (HBV) infection causes both acute and chronic necro-inflammatory liver diseases and is the most common severe liver infection worldwide. Its chronic persistence is associated with varying degrees of liver damage that often progresses to liver cirrhosis and, ultimately, hepatocellular carcinoma (Levrero & Zucman-Rossi, 2016; Iannacone & Guidotti, 2022). The global burden of Hepatitis B is staggering, with nearly 300 million people chronically infected. Of these, approximately 1.5 million people succumb to complications of HBV infection annually (www.who.int/news-room/fact-sheets).

Prophylactic vaccination is highly effective in preventing new infections (Chen, 2009). However, there are limited therapeutic options available for the treatment of chronic HBV infections. Current treatments, though capable of suppressing viral replication, often fail to eliminate the virus. This is due to the complex immune mechanisms that underlie HBV pathogenesis and chronicity which are still not completely understood. A more comprehensive understanding of these immune processes is necessary to develop therapeutic strategies capable of reverting viral persistence.

Viral clearance during HBV infection relies heavily on the adaptive immune response. Notably, HBV does not trigger significant intrahepatic innate immune responses; it is primarily the adaptive immune system that mediates both the pathogenesis of the disease and the elimination of the virus (Chisari & Ferrari, 1995; Guidotti & Chisari, 2006; Bertoletti & Ferrari, 2016). A significant gap in HBV research has been the limited understanding of the role of B cells in HBV infection. While $CD8^+$ T cells are well-established mediators of viral clearance, the contribution of B cells, particularly HBsAg-specific B cells, has been less thoroughly investigated. The loss of the Hepatitis B surface antigen (HBsAg) and the development of neutralising antibodies against the HBV-surface antigen are considered hallmark of disease resolution. HBsAg seroconversion is, in fact, a marker associated with improved patient prognosis and a reduced risk of developing hepatocellular carcinoma. Unfortunately, HBsAg loss and seroconversion in HBV patients is rare as it occurs in 1-3% of cases per year, depending on the age and status of liver disease (Liaw *et al*, 1991; McMahon *et al*, 2001; Chu & Liaw, 2007a; Simonetti *et*

al, 2010; Liu *et al*, 2010). Despite the importance of this phenomenon, the precise immune mechanisms driving seroconversion and the role of specific adaptive immune cells, such as B cells and $CD4^+$ T cells, remain poorly understood.

To address these knowledge gaps, we took advantage of the HBV-replication competent transgenic (1.3.32 or HBV Tg) mice, a well-established mouse model in which all HBV genome and proteins are expressed and produced inside the hepatocytes. High levels of viral particles are present in the serum (up to 10^7 to 10^8 viral particles per ml), resulting from efficient hepatic viral replication (Guidotti *et al*, 1995). Recent findings revealed that approximately 60% of these HBV transgenic mice spontaneously cleared serum HBsAg, and that this spontaneous loss is due to anti-HBsAg antibodies production which clear the circulating antigen (i.e. seroconversion) (Fumagalli *et al*, 2020). Thus, this model allows for a comprehensive investigation of the immune mechanisms driving HBsAg seroconversion.

Our study expands on these recent findings, confirming the importance of B cells in mediating the immune response to HBsAg. Approximately 60% of female HBV Tg mice spontaneously seroconverted (**Figure 10 B**), resulting in the presence of anti-HBsAg antibodies (HBsAb) in the plasma (**Figure 10 C, D**). HBsAg clearance was not caused by a reduction in circulating HBV "e" antigen (HBeAg) levels (**Figure 10 E**), an indirect marker of hepatic HBV replication. Moreover, transaminase activity and the number of intrahepatic leukocytes were comparable between non-seroconverted ($HBsAg^+$) and seroconverted ($HBsAg^-$) female HBV Tg mice (**Figure 10 G, H**). The lack of alterations in HBeAg and ALT levels despite HBsAg clearance indicates that seroconversion occurred in the absence of notable hepatic inflammation or liver damage. These findings suggest that the immune mechanisms driving HBsAg clearance may differ from those typically associated with viral-induced liver injury. However, serum HBsAg clearance was associated with a significant reduction in viremia (**Figure 10 F**). These findings, in conjunction with previous evidence demonstrating that HBV transgenic mice deficient in antibody production were unable to clear HBsAg throughout their lifespan (**Figure 9 C, D**) (Fumagalli *et al*, 2020), underscore the essential role of B cells and antibodies in HBs seroconversion. Consequently, we focused on locating and characterising HBsAg-specific B cells in these HBV Tg mice to further elucidate their role in the seroconversion process. By performing ELISpot assays, our results revealed that, following HBsAg

seroconversion, HBsAg-specific B cells were predominantly localised in the spleen, liver, bone marrow and colon of HBV Tg mice (**Figure 11 D, E**). The unexpected presence of HBsAg-specific B cells in the colon highlights the potential significance of the gut as a key site for initiating immune responses, possibly contributing to HBsAg seroconversion. This observation supports the emerging concept of the gut-liver axis in liver diseases, where the gut plays a crucial role in modulating immune responses related to hepatic conditions. In fact, the liver receives 70% of its blood supply from the gut, and it is constantly exposed to microbial products and metabolites that can shape liver immunity (Tripathi *et al*, 2018; Brandl *et al*, 2017).

This finding raises further questions regarding the origin of HBsAb-producing B cells, particularly whether these cells originate in a single organ and subsequently migrate to other tissues to initiate HBsAb production. To address this, pharmacological inhibitors of cell migration, such as CD62L (L-selectin) (Ivetic *et al*, 2019) blockade, could be employed to assess whether trafficking is essential for the distribution of antibody-secreting cells across multiple organs. Of note, we observed that the spleen harbours the highest number of HBs-specific B cells. Performing a splenectomy shortly after weaning could help elucidate whether this organ is the primary site of origin for these cells. To further clarify the distribution and dynamics of antibody-producing cells, conducting a time-course analysis of HBs-specific antibody-secreting cells (ASCs) across various tissues following seroconversion would provide valuable insights. Our current data, obtained from mice at 22 weeks of age, demonstrate the presence of antibody-producing cells in the spleen, liver, bone marrow, and colon of $HBsAg^-$ mice. However, it remains uncertain whether these cells are present in all organs immediately following seroconversion. Conducting time-course experiments at earlier stages post-seroconversion would help trace the temporal distribution of these cells, providing insights into whether certain tissues play a more prominent role at specific stages of the immune response during HBsAg seroconversion.

In literature, several techniques were reported to be able to detect specific B cells (Moody & Haynes, 2008). Fluorescent-antigen tetramers were developed to increase the BCR labelling avidity and the staining brightness (Franz *et al*, 2011). Nevertheless, we failed to detect a clear HBsAg-specific B cell population in seroconverted mice (**Figure 12 B**) with this technique. Despite the detection by ELISpot of HBs-specific B cells only in the

tissues of HBsAg$^-$ mice, the analysis of the global B cell populations showed no significant differences in the overall B cell composition in HBsAg$^-$ and HBsAg$^+$ HBV Tg mice (**Figure 14 B-M**). This suggests that HBs-Ag specific B cells represent a small subset of the total B cell population, and their relatively low frequency may hinder the detection of significant differences by traditional flow cytometry. In chronic HBV (CHB) patients, which present functionally altered atypical memory B cells, the low frequency of these cells in is well-documented (Portugal *et al*, 2017; Burton *et al*, 2018), aligning with our findings.

Considering these challenges, alternative approaches could provide a more refined analysis of these low-frequency B cells in mice. Single-cell RNA sequencing (scRNA-seq), for example, allows for high-resolution profiling of individual B cells (Papalexi & Satija, 2017; Nguyen *et al*, 2018), making it suitable for identifying activation or differentiation markers relevant to HBV responses. Coupling scRNA-seq with BCR sequencing further allows for tracking clonal diversity and somatic hypermutation within the B cell repertoire (Morgan *et al*, 2024), especially for the most abundant clonotypes that may show enhanced affinity for HBV antigens. Studies in other chronic and autoimmune diseases, such as multiple sclerosis and lupus, show that by using scRNA-seq and BCR sequencing it is possible to capture a complex landscape of immune responses, identifying unique B cell subpopulations linked to disease-specific responses (Liu *et al*, 2017; Bashford-Rogers *et al*, 2019; Rao *et al*, 2019; Ramesh *et al*, 2020; Zhao *et al*, 2021).

While B cells are crucial for antibody production, their activation and function are often dependent on CD4$^+$ T cell help. CD4$^+$ T cells are widely recognised for their pivotal role in helping B cells; through CD40-CD40L interaction, they aid with the formation and maintenance of germinal centres, where B cells undergo class switching and affinity maturation and subsequent antibody production (Crotty, 2015). A critical aspect of our study was the investigation of the involvement of CD4$^+$ T cells in promoting HBsAg clearance. Our findings demonstrated that in HBV Tg mice, the absence of functional CD4$^+$ T cell help, as seen in mice deficient in CD40L, led to a complete failure to produce anti-HBsAg antibodies (**Figure 15 H**) and to generate HBsAg-specific B cells (**Figure 15 I, J**). The absence of anti-HBsAg antibodies resulted in the persistence of HBsAg (**Figure 15 G**). These results highlight the critical nature of T cell-B cell collaboration.

Interestingly, CD40 expression is not restricted to B cells but is also found on professional antigen-presenting cells (APCs) such as dendritic cells and macrophages (Kooten & Banchereau, 1997b) suggesting a potential role for APCs in bridging innate and adaptive immunity in HBsAg clearance. Further studies should investigate the involvement of APCs, such as dendritic cells, by thoroughly characterising their phenotype and assessing the impact of dendritic cell depletion to provide insights into the role of APCs in HBsAg clearance.

Similarly, HBV Tg mice deficient in MHC-II failed to undergo seroconversion (**Figure 16 G, H**). In MHC class II-deficient mice, $CD4^+$ T cells are present at markedly reduced, yet detectable levels (Grusby & Glimcher, 1995), population that could have potentially influenced seroconversion. However, our findings demonstrate that this is not the case, as antigen-presenting capacity remains dampened, impairing crosstalk between $CD4^+$ T cells and B cells. This is consistent with the fact that MHC-II molecules are essential for presenting viral antigens to $CD4^+$ T cells (Unanue *et al*, 2016) to eventually mount effective antiviral immunity.

Recent studies have recently demonstrated that $CD4^+$ T cells are crucial for generating HBsAb in response to therapeutic immunization in the AAV-HBV model (Su *et al*, 2023). Our findings reinforce this observation, further highlighting the role of $CD4^+$ T cells in promoting antibody responses in the context of HBV. Additionally, chronic lymphocytic choriomeningitis virus (LCMV) studies have shown that depleting or impairing $CD4^+$ T cell during the initial antigen encounter prevents the production of antigen-specific antibodies (Ciurea *et al*, 2001).

Despite comparable total $CD4^+$ T cell counts in the liver and the spleen of both $HBsAg^+$ and $HBsAg^-$ HBV Tg mice (**Figure 17 C**), $HBsAg^-$ mice exhibited a marked increase in follicular helper T (Tfh) cells, a subset of $CD4^+$ T cells specialised in providing help to B cells within germinal centres (**Figure 17 D, E**). In secondary lymphoid organs, efficient interaction between Tfh cells and B cells at the border of the T cell zone of the follicle is crucial for the formation of functional germinal centre B cells and antigen-specific long-lived plasma cells (Vinuesa & Cyster, 2011; Crotty, 2015). These well-organised structures have also been observed in various non-lymphoid tissues, such as the liver, kidney, and bladder, where they are referred to as tertiary lymphoid structures (TLSs) (Gago da Graça *et al*, 2021; Sato *et al*, 2023). Notably, the presence of Tfh-like cells in

the liver of HBsAg$^-$ mice suggests the formation of tertiary lymphoid structures in this organ. This observation raises the intriguing possibility that similar Tfh-B cell interactions could occur within the liver in our HBV Tg mice, potentially playing a significant role in influencing the seroconversion process.

Interestingly, we also observed that CD4$^+$ T cells in seroconverted mice displayed increased proliferation capacity (**Figure 17 F**) and heightened IFNγ production (**Figure 17 G**). Unfortunately, we were unable to determine whether these CD4$^+$ T cells were HBs-specific (**Figure 17 B**). Researchers have shown that the presence of HBV-specific IFNγ producing CD4$^+$ T cells is associated with viral clearance in patients with chronic HBV infection. Furthermore, patients with HBeAg/HBsAg loss after flare showed higher frequency and dominance of HBV-specific IFNγ producing CD4$^+$ T cells, compared to patients without HBeAg/HBsAg loss (Wang *et al*, 2020a).

Building on these observations, we sought to determine whether these activated CD4$^+$ T cells could modulate antigen persistence. Thus, we investigated whether an adoptive transfer of CD4$^+$ T cells isolated from HBsAg$^-$ mice could promote HBsAg clearance. Of note, the precise number of HBs-specific CD4$^+$ T cells transferred was not quantified, as we could not identify, and therefore isolate, HBV-specific CD4$^+$ T cells (**Figure 17 B**). We utilised spleen-derived CD4$^+$ T cells due to their ease of isolation and their availability in sufficient numbers, ensuring adequate cell transfer for the experimental design. Despite these limitations, we demonstrated that the transfer of CD4$^+$ T cells from seroconverted mice to HBsAg-persistent HBV Tg mice successfully reversed antigen persistence (**Figure 18 C**) and led to the production of anti-HBsAg antibodies (**Figure 18 D**). Notably, the transfer of B cells alone was insufficient to promote seroconversion, further supporting the pivotal role of CD4$^+$ T cell in driving HBs seroconversion in HBV Tg mice.

While CD4$^+$ T cells are essential for promoting seroconversion, it is noteworthy that this process occurs only in a fraction of the HBV Tg mice, indicating that additional underlying mechanisms may contribute to this phenomenon. The interaction between CD4$^+$ T cells and B cells might extend beyond canonical secondary lymphoid organs, potentially taking place in non-traditional sites such as the liver and colon. This possibility is supported by the presence of HBsAg-specific B cells in these tissues. Furthermore, we observed an overall difference in total CD4$^+$ T cell populations between HBsAg$^+$ and

HBsAg$^-$ mice. This raises the question of whether specific microenvironmental factors or other immune signals present in these sites might influence the efficacy of CD4$^+$ T cells in promoting seroconversion. Therefore, while CD4$^+$ T cells are indispensable for the HBs seroconversion process, the observation that seroconversion occurs only in a subset of mice suggests that other factors may also play a crucial role in determining the overall immune response.

We next focused our research on understanding why HBs seroconversion occurred in only a fraction of HBV Tg mice. Notably, we observed that seroconversion often took place among animals sharing the same cage (**Figure 19 A, B, C**), leading us to hypothesise that the composition of the intestinal microbiome might influence this process. Recent research has identified the gut microbiome as a key modulator of immune responses in liver diseases, including chronic viral infections such as HBV (Chassaing *et al*, 2014; Albillos *et al*, 2020). Gut microbiota alterations were, in fact, observed in HBV-infected patients (Wang & Wan, 2019; Zeng *et al*, 2020), including patients with HBV-induced cirrhosis (Chen *et al*, 2016) and HCC (Schwabe & Greten, 2020). Compositional changes in the gut microbiota were also observed among patients at varied stages of HBV infection (Li *et al*, 2022a).

We first treated HBV Tg mice with broad spectrum antibiotics, and after assessing the efficacy of the treatment (**Figure 20 B, C, D**), we performed faecal microbiota transplantation (FMT). Our results revealed that mice that received FMT from HBsAg$^-$ mice showed significantly lower serum HBsAg compared to mice that received FMT from HBsAg$^+$ animals (**Figure 20 E**), suggesting that intestinal microbiome has an influence on HBs seroconversion. Furthermore, FMT from HBsAg$^-$ mice into HBsAg$^+$ mice successfully induced HBsAg clearance in recipient mice (**Figure 21 B**). In contrast, FMT failed to induce seroconversion in HBV Tg mice that were deficient in CD40L (**Figure 22 B**), emphasising the importance of intact CD40-CD40L signalling in HBs seroconversion. The inability of FMT to promote seroconversion in the absence of CD40L further suggests that while the microbiome may provide the necessary environmental cues for modulating immune responses, the underlying immune machinery must be intact for effective viral clearance to occur. Next, we aimed to determine whether antibiotic treatment alone, without subsequent microbiome reconstitution via faecal microbiota transplant, could have an impact HBsAg seroconversion. Our results showed that

antibiotic-induced depletion of the gut microbiota alone was insufficient to induce HBsAg seroconversion. In fact, the mice treated with broad-spectrum antibiotics without subsequent FMT, showed no reduction in circulating HBsAg levels (**Figure 23 B**), nor increase in anti-HBsAg antibody production (**Figure 23 C**). These results suggest that depletion of the microbiota alone is not capable of inducing seroconversion. Finally, we demonstrated that exposure to a microbiome from seroconverted mice via co-housing can promote HBsAg loss in $HBsAg^+$ HBV Tg mice (**Figure 24 D**). This suggests that certain microbiome profiles in seroconverted mice may possess immunomodulatory properties that promote the generation of an effective immune response capable of clearing HBsAg. To further explore the role of the microbiome, we propose that future studies should focus on characterising the specific bacterial species or microbial metabolites that are associated with successful HBsAg seroconversion. Analysis of the microbiota composition in seroconverted versus non-seroconverted mice is crucial to determine whether specific bacterial profiles correlate with immune responsiveness. If such differences are found, they could be exploited to develop targeted FMT, or microbiome-based therapies aimed at promoting HBsAg clearance. In chronic hepatitis B (CHB), differences in the gut microbiota between patients with negative and positive HBeAg status have been observed. HBeAg-positive CHB patients tend to have an altered gut microbiota characterised by enrichment of *Eubacterium*, *Christensenellaceae*, *Oscillospirales*, and *Haemophilus* compared to HBeAg-negative at the genus level, while *Erysipelatoclostridium* and *Lachnoclostridium* were decreased (Long *et al*, 2023).

Although many data remain to be collected, it is intriguing to hypothesise one of the possible scenarios. The mechanism underlying HBsAg seroconversion in HBV Tg mice likely involves a complex interplay between adaptive immune responses and the gut microbiome. $CD4^+$ T cells are central to promoting B cell activation, possibly through CD40-CD40L interactions, as evidenced by the enhanced $CD4^+$ T cell help observed in seroconverted mice. The localisation of HBs-specific B cells in the liver and gut suggests that these may be key organs providing a supportive microenvironment for antibody responses against HBsAg. Additionally, the observed role of the microbiome in promoting seroconversion, as demonstrated by HBsAg clearance following microbiota transplantation from seroconverted mice, implies that microbial signals contribute to shaping the immune environment. The exact mechanisms through which the microbiome

exerts these effects remain to be fully elucidated. However, one possible mechanism involves the production of microbial metabolites such as short-chain fatty acids (SCFAs). SCFAs, particularly butyrate, propionate, and acetate, have been shown to modulate immune function, including T cell differentiation and cytokine production (Maslowski & MacKay, 2010). For example, they can promote the activity of regulatory T cells (Tregs) (Furusawa *et al*, 2013; Arpaia *et al*, 2013) or modulate the production of interleukin-10 (IL-10) and interferon-gamma (IFNγ) (Smith *et al*, 2013; Kespohl *et al*, 2017). Additionally, certain microbial species may directly influence immune responses through interactions with antigen-presenting cells (APCs) in the gut, leading to improved antigen presentation and subsequent activation of $CD4^+$ T cells (Ivanov *et al*, 2022), which are critical for B cell help and antibody production (Takeuchi *et al*, 2024).

Despite the significant insights provided by this study, there are some limitations that need to be addressed. The use of the 1.3.32 HBV Tg mice, while advantageous for studying HBs seroconversion, may not fully replicate the complexity of human HBV infection. In these mice, in fact, the HBV genome is constitutively expressed in hepatocytes from birth, which does not accurately reflect the natural infection process in humans, where the virus must enter cells and initiate replication. Additionally, the low frequency of HBsAg-specific B cells poses a challenge for their detection and characterisation, limiting our ability to draw detailed conclusions about their phenotypic and functional properties. Future studies should employ more sensitive techniques to better understand their role in HBV seroconversion. The reliance on mouse models also raises questions about the translational relevance of these findings to human patients; differences in microbiome composition between mice and humans (Nagpal *et al*, 2018) underscore the need to confirm whether microbiome-related mechanisms observed in murine models are applicable to human HBV infection. Therefore, future studies in human clinical samples are essential.

Nevertheless, this study makes significant contributions to our understanding of the immune mechanisms underlying HBs seroconversion, shedding light on the pivotal roles of B cells, $CD4^+$ T cells, and the microbiome. Particularly, our findings on the microbiome's influence in facilitating seroconversion add a new layer of complexity to our understanding of the process of HBV clearance, suggesting that interactions within the gut-liver axis could be integral to immune responses. These insights present novel

possibilities for therapeutic approaches. Specifically, targeted microbiome-based therapies or immune interventions designed to enhance HBsAg seroconversion could offer promising strategies to improve outcomes for patients with chronic HBV infection by leveraging both microbial and immune modulatory pathways, with potentially broader implications for other viral infections, especially those that involve chronic infections or immune evasion mechanisms.

MATERIALS AND METHODS

6. MATERIALS AND METHODS

6.1. Mouse models

C57BL/6 mice were purchased from Chrles River. HBV replication-competent transgenic mice (HBV Tg, lineage 1.3.32, inbred C57BL/6, H-2^{b}), that express all of the HBV antigens and replicate HBV in the liver at high levels without any evidence of cytopathology, have been previously described (Guidotti *et al*, 1995). These mice were used as C57BL/6 and/or C57BL/6 x Balb/c (H-2^{bxd}) F1 hybrids. HBV Tg D_HLMP2A (1.3.32 D_HLMP2A lineage, C57BL/6 inbred) were obtained from the crossing between 1.3.32 lineage and D_HLMP2A lineage (Casola *et al*, 2004). D_HLMP2A mice, which are devoid of surface-expressed and secreted antibodies, were originally provided by K. Rajewsky (Harvard Medical School) and bred >10 generations against C57BL/6 mice. HBV Tg MHC-II $^{-/-}$ (1.3.32 MHC-II $^{-/-}$ lineage, C57BL/6 inbred) were obtained from the crossing between 1.3.32 lineage and MHC-$II^{-/-}$ lineage (B6.129S2-$H2^{dlAb1\text{-}Ea}$/J; JAX stock #003584) (Madsen *et al*, 1999). HBV Tg CD40L $^{-/-}$ (1.3.32 CD40-L $^{-/-}$ lineage, C57BL/6 inbred) were obtained from the crossing between 1.3.32 lineage and CD40-$L^{-/-}$ lineage (B6.129S2-*Cd40lg*^{tm1Imx}/J; JAX stock #002770) (Renshaw *et al*, 1994). Knock-in mice expressing the heavy and light chain of a BCR specific for HBV-surface antigen (HBsAg) were generated by the Core Facility for Conditional Mutagenesis (CFCM) (San Raffaele Scientific Institute). In all presented experiments mice were matched for sex, age and for serum HBeAg levels before experimental manipulations. Mice were housed under specific pathogen-free conditions and used at different weeks of age, as indicated in the experimental layouts. All experimental animal procedures were approved by the Institutional Animal Committee at the San Raffaele Scientific Institute.

6.2. Organ processing

6.2.1. Spleen

Spleens of experimental mice were processed using HBSS (Hanks' Balanced Salt Solution). In details, organs were smashed and filtered through a 70 μm nylon strainer.

The obtained cell suspensions were resuspended in ACK to lyse red blood cells, then washes and resuspended for further analysis.

6.2.2. Liver

Single cell suspension of intrahepatic leukocytes (IHL) was prepared from the liver as previously described (Iannacone *et al*, 2005; Bénéchet *et al*, 2019). Briefly, mice were perfused with 10ml of PBS via the inferior vena cava. After surgically removing the liver, the organ was smashed and filtered through a 70 µm nylon strainer. The obtained cell suspension was then digested with 10 ml RPMI 1640 containing 0.02% of collagenase IV (Sigma-Aldrich #C5138)) and 0.002% of DNase I (Sigma-Aldrich #D4263) and incubated for 40' at 37°C. Cells were then washed with RPMI 1640 and resuspended with a 36% Percoll solution (Sigma #P4937) and centrifuged for 20' at 2000rpm (low brake). The obtained IHLs were then resuspended in ACK to lyse red blood cells, then washed and resuspended for further analysis.

6.2.3. Bone marrow

The bone marrow of mice was processed to obtain a cellular suspension by directly flushing the bone with a syringe using PBS or RPMI 1640. The cellular suspension was then centrifuged, and the pellet resuspended in ACK to lyse red blood cells, then washed and resuspended for further analysis.

6.2.4. Lymph node

The lymph nodes of mice were processed by smashing them through a 70 µm nylon strainer. The obtained cellular suspension was centrifuged, and the pellet was washed and resuspended for further analysis. The protocol was already described in literature (De Giovanni *et al*, 2020).

6.2.5. Payer's patches

Payer's patches were harvested removing them from the small intestine and placed in transport solution (RPMI 1640, 2% FBS, 1mM Hepes, Antibiotics). The Payer's patches were then digested in 1 ml of liberase enzymatic solution (RPMI 2% FBS, Sodium pyruvate, 1mM Hepes, Antibiotics, 0.1mg/ml Liberase TM (Roche #5401119001) and DNAse I (Sigma-Aldrich #D4263) for 30' at 37°C on a thermos shaker. After digestion 20% of quenching solution (RPMI 1640, 0.1M EDTA, 50% FBS, 1mM Hepes and

antibiotics) was added. The digested fragments were then filtered through a 70 μm nylon strainer, washed and resuspended for further analysis.

6.2.6. Colon

Colon was harvested paying attention to removing fat, washed with PBS and flushed with the help of a syringe. It was cut in 1 cm-pieces and placed in and incubate for 30' at room temperature with 10 ml HBSS, Antibiotics, and 1mM DTT (Sigma, # 10197777001). The pieces of colon were then transferred in 10ml HBSS, 5% FBS, Hepes, Antibiotics and 2mM EDTA for 15' at 37°C. After that, EDTA buffer was replaced with a fresh one for other 15' at 37°C. The colon was further chopped and minced fragments were digested with 5ml of HBSS, 5% FBS, Hepes, Antibiotics, 5mM $CaCl_2$, 40μg/ml DNAseI (Sigma-Aldrich #D4263) and 1mg/ml Collagenase/Dispase (Roche # 10269638001) for 20' at 37°C. The digested fragments were then filtered through a 100 μm nylon strainer, washed and resuspended for further analysis.

6.3. Cell culture and cell purification

6.3.1. B cell and $CD4^+$ T cell purification

Splenic B cells and $CD4^+$T cells were purified using immunomagnetic negative selection using EasySep Mouse B cell Isolation Kit (Stem Cell, #19854) and EasySep Mouse $CD4^+$ T Cell Isolation Kit (Stem Cell, #19852) respectively. Manufacturer's guidelines were followed, and purity was assessed by flow cytometry evaluating the percentage of $CD19^+B220^+$ cell for B cells and $CD8^-CD4^+$ for $CD4^+$ T cells in the positive and negative fraction.

6.4. *In vivo* cell adoptive transfers

Isolation of B cells and $CD4^+$T cells from spleens of HBV Tg mice have been performed as described above. Recipient mice were injected intravenously with isolated HBV Tg ($HBsAg^+$ or $HBsAg^-$) B cells and/or HBV Tg ($HBsAg^+$ or $HBsAg^-$) $CD4^+$T cells (0.8×10^6 cells/mouse).

6.5. ELISPOT Assay

For analysis of the production of antibody secreting cells (ASCs), MultiScreen-HA 96-well filter plates (Merk # MAHAS4510) were coated with 50 μg per well of HBs Ag (ayw) (Gilead) in PBS and then blocked with RPMI 2% BSA. Cells from different organs were plated at a concentration of 5 x 10^5 cells per well and then incubated overnight at 37°C. After five washes with PBS-T (PBS + 0.05% Tween20), HRP-conjugated anti-mouse IgG (goat polyclonal Southern) diluted in PBS-T 1% FBS was added. AEC (3-amino-9-ethyl-carbazole) tablet (Sigma #A6926) was used as substrate to develop spots representing individual antibody secreting cells. Spots were scanned and counted using an automated ELISpot reader and the results were expressed as ASCs per 10^6 cells.

6.6. Serum Immunoglobulin ELISA

Total serum IgM and IgG isotype levels were determined by ELISA using SBA Clonotyping System (Southern Biotech #5300-05B) according to manufacturer's specifications. Briefly, 96-well ELISA plates were coated with diluted capture antibody 10 μg/mL and incubated overnight at 4°C. Plates were blocked and then incubated with serum samples overnight at 4°C. HRP conjugated anti-mouse IgM, IgG1, IgG2b, IgG2c, and IgG3 isotypes were added and incubated for 1h at room temperature. The reaction was developed with TMB Substrate Reagent (BD Biosciences), and OD was measured at 450nm using with Infinite® M Nano reader. The concentration was measured with reference to standard curves.

6.7. Cell labelling and Flow cytometry

6.7.1. Surface and intracellular staining

All flow cytometry staining of intracellular and surface-expressed molecules were performed as described. Cell viability was assessed by staining the cell suspension with LIVE/DEAD™ Fixable Near-IR Dead Cell Stain Kit (ThermoFisher #L10119) in PBS for 15' at room temperature. Antibodies (Abs) used are listed in **Table 1**. For analysis of *ex vivo* intracellular cytokine production, the cell suspensions obtained (described above) were in vitro stimulated in complete medium where PMA (50 ng/ml), ionomycin (1

μg/ml) and BFA (1μg/ml) were added and then incubated for 4 hours at 37°C. Surface antigen staining was performed with Brilliant Stain buffer (BD Biosciences #566349) according to manufacturer instructions, intracellular antigen staining was performed using Foxp3/Transcription Factor Staining Buffer set (eBioscience, #00-5523-00), following the manufacturer's instructions. FACS analyses have been done on BD FACSCanto Clinical Flow Cytometry System, BD FACSymphony A5 Cell Analyzer or Cytek Aurora. Flow cytometry data were analysed with FlowJo Software (Treestar).

Antibody	Clone	Source and Identifier
CD45	30-F11	BD Bioscences #564279
CD44	IM7	BD Bioscences #741227
CD33R	RMST2-2	eBioscience #367-9335-82
CD38	90	Biolegend #102728
CD39	24DMS1	Invitrogen #368-0391-82
B220	RA3-6B2	Biolegend #103239
		Biolegend #103248
		Biolegend #103229
		BD Bioscences #612950
CD8a	53-6.7	BD Pharmingen #569279
CD3e	145-2C11	BD OptiBuild #757837
		BD Pharmingen #552774
CD4	GK1.5	BD Pharmingen #568695
		Biolegend #100480
PD1	29F.1A12	Biolegend #135257
		Biolegend #125253
	J43	BD Bioscences #744549
		BD Biosciences #551802
ICOS	15F9	Biolegend #107716
	C398.4A	Biolegend #313537
CTLA4	UC10-4B9	Biolegend #106314
CD25	PC61	Biolegend #102075
		BD Horizon #566120
		BD Bioscences #564023
CD73	eBioTY/11.8	eBioscences #25-0731-82
CD23	B3B4	Biolegend #101608
CD19	1D3	BD Pharmingen #562291
		BD Horizon #612971
		BD Bioscences #749027
	6D5	Biolegend #156527
CD86	GL1	BD Pharmingen #569219

		BD Bioscience #741737
		BD Biosciences #564199
CD138	281-2	BD Biosciences #563147
		Biolegend #142510
		BD Pharmingen #553714
		BD Pharmingen #558626
CD69	H1.2F3	BD Biosciences #612793
		Biolegend #104537
GL-7	GL7	BD Pharmingen #558626
CD80	16-10A1	Biolegend #104738
FAS	Jo2	BD Pharmingen #557653
CD62L	W18021D	Biolegend #161205
	MEL-14	Invitrogen #366-0621-82
		Biolegend #104438
IgD	11-26c.2a	Biolegend #405730
		Biolegend #405749
		Biolegend #405712
IgM	II/41	BD Pharmingen #550676
IA-IE	2G9	BD Biosciences #743876
CXCR3	CXCR3-173	BD Biosciences #740630
	S18001A	Biolegend #155923
CXCR4	L276F12	Biolegend #146517
CXCR5	2G8	Pharmingen #562856
CD11c	N418	Biolegend #117367
	QA18A72	Biolegend #161107
CD107a	1D4B	Biolegend #121628
IFNg	XMG1.2	Biolegend #505830
IL-17A	TC11-18H10	BD Horizon #564169
		BD Pharmingen #562542
TNFa	MP6-XT22	BD Biosciences #563943
IL-2	JES6-5H4	Biolegend #503837
IL-4	11B11	BD Horizon #564006
FoxP3	FJK-16s	Invitrogen #53-5773-82
		eBioscences #12-5773-80
T-bet	4B10	Biolegend #644805
	O4-46	BD Pharmingen #569090
RORgt	AFKJS-9	Invitrogen #61-6988-82
	Q31-378	BD Pharmingen #562683
Bcl-6	K112-91	BD Biosciences #561525
		BD Horizon #568063
Ki-67	SolA15	Thermo Fisher #48-5698-80

		eBioscience # 56-5698-82

Table 1. List of Antibodies

6.7.2. Tetramer preparation

To identify HBs-specific B cells by Flow cytometry, a tetramer was used. HBsAg (ayw, isotype) protein coupled with biotin was kindly provided by Gilead Science. Biotinylated proteins were mixed with Alexa Fluor (AxFl)-647 or 488-fluorescent streptavidin to obtain fluorescent HBsAg-tetramers at 0.5 μg/ml. Briefly, 4M of HBsAg-biotin were mixed with 1M AxFl-647 and -488 streptavidin in FACS Buffer and incubated 30' at room temperature. After that, solutions were centrifuged at high speed, to remove unlabelled biotins. After cell viability staining, the cell suspensions were labelled with HBsAg-tetramers (AxFl647 and AxFl488) in FACS buffer (100 μl/ml) for 30' at 4°C prior surface staining.

Env126 Class-II Tetramer was provided by NIH Tetramer Core Facility as a peptide $HBs_{126\text{-}138}$ loaded tetramer (I-Ab HBsAg). Tetramer staining was performed incubating cell suspensions at 37°C for 1 hour according to manufacturer instructions.

6.8. Histochemistry

For Hematoxylin and Eosin (H&E) staining and HBcAg immunohistochemistry, liver was harvested in Zn-formalin and transferred into 70% ethanol solution after 24 hours. Tissues were then processed, embedded in paraffin and later stained as previously described (Guidotti *et al*, 2015). Bright-field images were acquired through an Aperio Scanscope System CS2 microscope and an ImageScope program (Leica Biosystem) following the manufacturer instructions.

6.9. Purification of viral nuclei acids from serum and qPCR analyses

To isolate viral nucleic acids, serum collected from experimental mice were incubated with IsoHi Buffer (150 mM NaCl, 0.5% NP40, 10 mM Tris pH 7.4), 5 mM $CaCl_2$, 5mM MgCl2, 1 U DNaseI (Life Technologies, Cat #AM1907), 5 U Micrococcal Nuclease (NEB, Cat #MO247S) for 2 hours at 37°C. By adding 20 mM EDTA, pH 8.0, the digestion

was stopped to then purify viral nucleic acid with the QIAmp MiniElute Virus Spin Kit (Qiagen, 57704), according to the manufacturer's instructions. Viremia quantification was performed for HBV envelope (forward: 5′-CCCGTTTGTCCTCTAATTCC-3′; reverse: 5′-GTCCGAAGGTTTGGTACAGC-3′; probe: 5′-CTCAACAACCAGCAC GGGACCA-3′) by absolute qPCR. Reactions were run and analysed on Quant Studio 5 instrument (Life Technologies).

6.10. Antibiotic treatment

Mice received antibiotic cocktail consisting of Vancomycin 0.5 g/L, Neomycin 0.5 g/L, and Metronidazole 0.5 g/L, in drinking water for 3 days *ad libitum* and Clindamycin 0.5 g/L was administered by intraperitoneal injection (IP) on the 4th day. Following competition of antibiotic protocol, the water containing antibiotics was replaced by regular drinking water provided *ad libitum* until the end point of the experiment.

6.11. Faecal microbiota transplant (FMT)

Stool samples from individual mice (3 pellets per mouse) were collected and homogenised in PBS immediately after collection. The homogenised faeces were then centrifuged, and the supernatant was carefully collected. Around 0.2 mL of faecal solution was administered to the each of the experimental mice via oral gavage once a day for 3 consecutive days.

6.12. Murine stool collection and stool culture

Stool samples from individual mice were collected for bacterial culture to assess bacterial levels. Stool samples were collected before starting antibiotic treatment (D0) and after the end of the antibiotic treatment (D5). Freshly collected samples were homogenised with 1mL of PBS and then centrifuged at 300 x *g* for 2'. A 1:1000 dilution of the stool homogenate was straked onto Tryptone Soy Agar (Agar + TSB (BD #211768)) and incubated at 37°C for 48 hours before being observed for growth.

6.13. Biochemical analysis

The extent of hepatocellular injury was monitored by the measuring of plasma alanine aminotransferase (ALT) activity at different time points during the experiments, as previously described (Guidotti *et al*, 2015). ALT activity was measured by an automatic biochemical analyzer (Ilab Aries, provided by Instrumentation Lab Warfen, IT). Normal intervals of sALT activity are comprised between 20 and 80 U/L. Serum HBeAg, HBsAg, and anti-HBsAg Ab were measured by enzyme linked immunosorbent assay (ELISA), as previously described (Tonti *et al*, 2013; Bénéchet *et al*, 2019).

6.14. Statistical analysis

Detailed information concerning the statistical methods used is provided in the figure legends. Statistical analyses were performed with GraphPad Prism software. *n* represents individual mice analysed per experiment. Experiments were independently performed at least in duplicate to control for experimental variation. Results were expressed with ±SEM. Significance is indicated as follows: *P<0.05; **P<0.01; *** P=0.0001, ****P<0.0001. Comparisons are not statistically significant unless indicated.

REFERENCES

7. REFERENCES

Ai W, Li H, Song N, Li L & Chen H (2013) Optimal Method to Stimulate Cytokine Production and Its Use in Immunotoxicity Assessment. *Int J Environ Res Public Health* 10: 3834

Albillos A, de Gottardi A & Rescigno M (2020) The gut-liver axis in liver disease: Pathophysiological basis for therapy. *J Hepatol* 72: 558–577

Arias IM, Alter HJ, Boyer JL, Cohen DE, Fausto N, Shafritz DA & Wolkoff AW (2009) The liver: Biology and pathobiology, fifth edition. *The Liver: Biology and Pathobiology*: 1–1191

Arpaia N, Campbell C, Fan X, Dikiy S, Van Der Veeken J, Deroos P, Liu H, Cross JR, Pfeffer K, Coffer PJ, *et al* (2013) Metabolites produced by commensal bacteria promote peripheral regulatory T-cell generation. *Nature 2013 504:7480* 504: 451–455

Asabe S, Wieland SF, Chattopadhyay PK, Roederer M, Engle RE, Purcell RH & Chisari F V. (2009) The size of the viral inoculum contributes to the outcome of hepatitis B virus infection. *J Virol* 83: 9652–9662

Bäckhed F, Ley RE, Sonnenburg JL, Peterson DA & Gordon JI (2005) Host-bacterial mutualism in the human intestine. *Science (1979)* 307: 1915–1920

Bashford-Rogers RJM, Bergamaschi L, McKinney EF, Pombal DC, Mescia F, Lee JC, Thomas DC, Flint SM, Kellam P, Jayne DRW, *et al* (2019) Analysis of the B cell receptor repertoire in six immune-mediated diseases. *Nature 2019 574:7776* 574: 122–126

Bénéchet AP, De Simone G, Di Lucia P, Cilenti F, Barbiera G, Le Bert N, Fumagalli V, Lusito E, Moalli F, Bianchessi V, *et al* (2019) Dynamics and genomic landscape of CD8+ T cells undergoing hepatic priming. *Nature 2019 574:7777* 574: 200–205

Ben-Moshe S & Itzkovitz S (2019) Spatial heterogeneity in the mammalian liver. *Nature Reviews Gastroenterology & Hepatology 2019 16:7* 16: 395–410

Berland R & Wortis HH (2002) Origins and functions of B-1 cells with notes on the role of CD5. *Annu Rev Immunol* 20: 253–300

Le Bert N, Salimzadeh L, Gill US, Dutertre CA, Facchetti F, Tan A, Hung M, Novikov N, Lampertico P, Fletcher SP, *et al* (2020) Comparative characterization of B cells specific for HBV nucleocapsid and envelope proteins in patients with chronic hepatitis B. *J Hepatol* 72: 34–44

Bertoletti A & Ferrari C (2016) Adaptive immunity in HBV infection. *J Hepatol* 64: S71–S83

Bohne F, Chmielewski M, Ebert G, Wiegmann K, Kürschner T, Schulze A, Urban S, Krönke M, Abken H & Protzer U (2008) T cells redirected against hepatitis B virus surface proteins eliminate infected hepatocytes. *Gastroenterology* 134: 239–247

Boni C, Fisicaro P, Valdatta C, Amadei B, Di Vincenzo P, Giuberti T, Laccabue D, Zerbini A, Cavalli A, Missale G, *et al* (2007a) Characterization of Hepatitis B Virus (HBV)-Specific T-Cell Dysfunction in Chronic HBV Infection. *J Virol* 81: 4215–4225

Boni C, Fisicaro P, Valdatta C, Amadei B, Di Vincenzo P, Giuberti T, Laccabue D, Zerbini A, Cavalli A, Missale G, *et al* (2007b) Characterization of hepatitis B virus (HBV)-specific T-cell dysfunction in chronic HBV infection. *J Virol* 81: 4215–4225

Botha JF, Dusheiko GM, Ritchie MJJ, Mouton HWK & Kew MC (1984) Hepatitis B virus carrier state in black children in Ovamboland: role of perinatal and horizontal infection. *Lancet* 1: 1210–1212

Bouezzedine F, Fardel O & Gripon P (2015) Interleukin 6 inhibits HBV entry through NTCP down regulation. *Virology* 481: 34–42

Brandl K, Kumar V & Eckmann L (2017) Microbiome and Host Interactions: Gut-liver axis at the frontier of host-microbial interactions. *Am J Physiol Gastrointest Liver Physiol* 312: G413

Burton AR, Pallett LJ, McCoy LE, Suveizdyte K, Amin OE, Swadling L, Alberts E, Davidson BR, Kennedy PTF, Gill US, *et al* (2018) Circulating and intrahepatic antiviral B cells are defective in hepatitis B. *J Clin Invest* 128: 4588

Caruso R, Ono M, Bunker ME, Núñez G & Inohara N (2019) Dynamic and Asymmetric Changes of the Microbial Communities after Cohousing in Laboratory Mice. *Cell Rep* 27: 3401-3412.e3

Casola S, Otipoby KL, Alimzhanov M, Humme S, Uyttersprot N, Kutok JL, Carroll MC & Rajewsky K (2004) B cell receptor signal strength determines B cell fate. *Nat Immunol* 5: 317–327

Chai N, Chang HE, Nicolas E, Han Z, Jarnik M & Taylor J (2008) Properties of Subviral Particles of Hepatitis B Virus. *J Virol* 82: 7812

Chassaing B, Etienne-Mesmin L & Gewirtz AT (2014) Microbiota-Liver Axis in Hepatic Disease. *Hepatology* 59: 328

Chen DS (2009) Hepatitis B vaccination: The key towards elimination and eradication of hepatitis B. *J Hepatol* 50: 805–816

Chen Y, Ji F, Guo J, Shi D, Fang D & Li L (2016) Dysbiosis of small intestinal microbiota in liver cirrhosis and its association with etiology. *Sci Rep* 6

Chen Y, Yang F, Lu H, Wang B, Chen Y, Lei D, Wang Y, Zhu B & Li L (2011) Characterization of fecal microbial communities in patients with liver cirrhosis. *Hepatology* 54: 562–572

Chisari F V. & Ferrari C (1995) Hepatitis B virus immunopathogenesis. *Annu Rev Immunol* 13: 29–60

Chu CM & Liaw YF (2007a) HBsAg seroclearance in asymptomatic carriers of high endemic areas: appreciably high rates during a long-term follow-up. *Hepatology* 45: 1187–1192

Chu CM & Liaw YF (2007b) HBsAg seroclearance in asymptomatic carriers of high endemic areas: Appreciably high rates during a long-term follow-up. *Hepatology* 45: 1187–1192

Ciurea A, Hunziker L, Klenerman P, Hengartner H & Zinkernagel RM (2001) Impairment of Cd4+ T Cell Responses during Chronic Virus Infection Prevents Neutralizing Antibody Responses against Virus Escape Mutants. *Journal of Experimental Medicine* 193: 297–306

Corti D, Benigni F & Shouval D (2018) Viral envelope-specific antibodies in chronic hepatitis B virus infection. *Curr Opin Virol* 30: 48–57

Crispe IN (2003) Hepatic T cells and liver tolerance. *Nature Reviews Immunology 2003 3:1* 3: 51–62

Crotty S (2015) A brief history of T cell help to B cells. *Nature Reviews Immunology 2015 15:3* 15: 185–189

Elgueta R, Benson MJ, De Vries VC, Wasiuk A, Guo Y & Noelle RJ (2009) Molecular mechanism and function of CD40/CD40L engagement in the immune system. *Immunol Rev* 229: 152–172

Farci P, Diaz G, Chen Z, Govindarajan S, Tice A, Agulto L, Pittaluga S, Boon D, Yu C, Engle RE, *et al* (2010) B cell gene signature with massive intrahepatic production of antibodies to hepatitis B core antigen in hepatitis B virus-associated acute liver failure. *Proc Natl Acad Sci U S A* 107: 8766–8771

Ferrari C (2015) HBV and the immune response. *Liver International* 35: 121–128

Ficht X & Iannacone M (2020) Immune surveillance of the liver by T cells. *Sci Immunol* 5: 2351

Franz B, May KF, Dranoff G & Wucherpfennig K (2011) Ex vivo characterization and isolation of rare memory B cells with antigen tetramers. *Blood* 118: 348–357

Fumagalli V, Lucia P Di, Venzin V, Bono EB, Jordan R, Frey CR, Delaney W, Chisari F V., Guidotti LG & Iannacone M (2020) Serum HBsAg clearance has minimal impact on CD8+ T cell responses in mouse models of HBV infection. *J Exp Med* 217

Furusawa Y, Obata Y, Fukuda S, Endo TA, Nakato G, Takahashi D, Nakanishi Y, Uetake C, Kato K, Kato T, *et al* (2013) Commensal microbe-derived butyrate induces the differentiation of colonic regulatory T cells. *Nature 2013 504:7480* 504: 446–450

Gago da Graça C, van Baarsen LGM & Mebius RE (2021) Tertiary Lymphoid Structures: Diversity in Their Development, Composition, and Role. *The Journal of Immunology* 206: 273–281

Ganem D & Prince AM (2004) Hepatitis B Virus Infection — Natural History and Clinical Consequences. *New England Journal of Medicine* 350: 1118–1129

Ge X, Ding C, Zhao W, Xu L, Tian H, Gong J, Zhu M, Li J & Li N (2017) Antibiotics-induced depletion of mice microbiota induces changes in host serotonin biosynthesis and intestinal motility. *J Transl Med* 15: 1–9

De Giovanni M, Cutillo V, Giladi A, Sala E, Maganuco CG, Medaglia C, Di Lucia P, Bono E, Cristofani C, Consolo E, *et al* (2020) Spatiotemporal regulation of type I interferon expression determines the antiviral polarization of CD4+ T cells. *Nature Immunology 2020 21:3* 21: 321–330

Grusby MJ & Glimcher LH (1995) Immune responses in MHC class II-deficient mice. *Annu Rev Immunol* 13: 417–435

Guidotti LG & Chisari F V. (2006) Immunobiology and pathogenesis of viral hepatitis. *Annu Rev Pathol* 1: 23–61

Guidotti LG, Inverso D, Sironi L, Di Lucia P, Fioravanti J, Ganzer L, Fiocchi A, Vacca M, Aiolfi R, Sammicheli S, *et al* (2015) Immunosurveillance of the liver by intravascular effector CD8(+) T cells. *Cell* 161: 486–500

Guidotti LG, Matzke B, Schaller H & Chisari F V (1995) High-level hepatitis B virus replication in transgenic mice. *J Virol* 69: 6158–6169

Hardy RR & Hayakawa K (2001) B cell development pathways. *Annu Rev Immunol* 19: 595–621

Harker JA, Lewis GM, Mack L & Zuniga EI (2011) Late Interleukin-6 escalates T follicular helper cell responses and controls a chronic viral infection. *Science* 334: 825

Hartmann P, Seebauer CT & Schnabl B (2015) Alcoholic liver disease: the gut microbiome and liver cross talk. *Alcohol Clin Exp Res* 39: 763–775

Herrscher C, Roingeard P & Blanchard E (2020) Hepatitis B Virus Entry into Cells. *Cells* 9

Hildreth AD & O'sullivan TE (2019) Tissue-Resident Innate and Innate-Like Lymphocyte Responses to Viral Infection. *Viruses* 11

Hoofnagle JH, Gerety RJ & Barker LF (1973) Antibody to hepatitis-B-virus core in man. *Lancet* 2: 869–873

Hsu CL & Schnabl B (2023) The gut–liver axis and gut microbiota in health and liver disease. *Nature Reviews Microbiology 2023 21:11* 21: 719–733

Huttenhower C, Gevers D, Knight R, Abubucker S, Badger JH, Chinwalla AT, Creasy HH, Earl AM, Fitzgerald MG, Fulton RS, *et al* (2012) Structure, function and diversity of the healthy human microbiome. *Nature* 486: 207–214

Iannacone M & Guidotti LG (2015) Mouse Models of Hepatitis B Virus Pathogenesis. *Cold Spring Harb Perspect Med* 5: a021477

Iannacone M & Guidotti LG (2022) Immunobiology and pathogenesis of hepatitis B virus infection. *Nat Rev Immunol* 22: 19–32

Iannacone M, Sitia G, Isogawa M, Marchese P, Castro MG, Lowenstein PR, Chisari F V., Ruggeri ZM & Guidotti LG (2005) Platelets mediate cytotoxic T lymphocyte–induced liver damage. *Nature Medicine 2005 11:11* 11: 1167–1169

Ivanov II, Tuganbaev T, Skelly AN & Honda K (2022) T Cell Responses to the Microbiota. *Annu Rev Immunol* 40: 559–587

Ivetic A, Green HLH & Hart SJ (2019) L-selectin: A major regulator of leukocyte adhesion, migration and signaling. *Front Immunol* 10: 451997

Jenne CN & Kubes P (2013) Immune surveillance by the liver. *Nature Immunology 2013 14:10* 14: 996–1006

Jung MC, Diepolder HM, Spengler U, Wierenga EA, Zachoval R, Hoffmann RM, Eichenlaub D, Frösner G, Will H & Pape GR (1995) Activation of a heterogeneous hepatitis B (HB) core and e antigen-specific CD4+ T-cell population during seroconversion to anti-HBe and anti-HBs in hepatitis B virus infection. *J Virol* 69: 3358–3368

Kawashima K, Andreata F, Beccaria CG & Iannacone M (2024) Priming and Maintenance of Adaptive Immunity in the Liver. *Annu Rev Immunol* 42

Kazankov K, Jørgensen SMD, Thomsen KL, Møller HJ, Vilstrup H, George J, Schuppan D & Grønbæk H (2018) The role of macrophages in nonalcoholic fatty liver disease and nonalcoholic steatohepatitis. *Nature Reviews Gastroenterology & Hepatology 2018 16:3* 16: 145–159

Kespohl M, Vachharajani N, Luu M, Harb H, Pautz S, Wolff S, Sillner N, Walker A, Schmitt-Kopplin P, Boettger T, *et al* (2017) The microbial metabolite butyrate induces expression of Th1- associated factors in cD4+ T cells. *Front Immunol* 8: 28

Kim CY & Tilles JG (1973) Purification and Biophysical Characterization of Hepatitis B Antigen. *Journal of Clinical Investigation* 52: 1176

Kim S, Covington A & Pamer EG (2017) The intestinal microbiota: Antibiotics, colonization resistance, and enteric pathogens. *Immunol Rev* 279: 90–105

Klein SL & Flanagan KL (2016) Sex differences in immune responses. *Nature Reviews Immunology 2016 16:10* 16: 626–638

Knolle PA, Böttcher J & Huang LR (2015) The role of hepatic immune regulation in systemic immunity to viral infection. *Med Microbiol Immunol* 204: 21–27

Kooten C Van & Banchereau J (1997a) Functions of CD40 on B cells, dendritic cells and other cells. *Curr Opin Immunol* 9: 330–337

Kooten C Van & Banchereau J (1997b) Functions of CD40 on B cells, dendritic cells and other cells. *Curr Opin Immunol* 9: 330–337

Kurosaki T, Kometani K & Ise W (2015) Memory B cells. *Nat Rev Immunol* 15: 149–159

Lampertico P, Agarwal K, Berg T, Buti M, Janssen HLA, Papatheodoridis G, Zoulim F & Tacke F (2017) EASL 2017 Clinical Practice Guidelines on the management of hepatitis B virus infection. *J Hepatol* 67: 370–398

Lanzavecchia A (1990) Receptor-mediated antigen uptake and its effect on antigen presentation to class II-restricted T lymphocytes. *Annu Rev Immunol* 8: 773–793

Levrero M & Zucman-Rossi J (2016) Mechanisms of HBV-induced hepatocellular carcinoma. *J Hepatol* 64: S84–S101

Li X, Wu S, Du Y, Yang L, Li Y & Hong B (2020) Entecavir therapy reverses gut microbiota dysbiosis induced by hepatitis B virus infection in a mouse model. *Int J Antimicrob Agents* 56: 106000

Li YG, Yu ZJ, Li A & Ren ZG (2022a) Gut microbiota alteration and modulation in hepatitis B virus-related fibrosis and complications: Molecular mechanisms and therapeutic inventions. *World J Gastroenterol* 28: 3555

Li YN, Kang NL, Jiang JJ, Zhu YY, Liu YR, Zeng DW & Wang F (2022b) Gut microbiota of hepatitis B virus-infected patients in the immune-tolerant and immune-active phases and their implications in metabolite changes. *World J Gastroenterol* 28: 5188

Liaw Y -F, Sheen I -S, Chen T -J, Chu C -M & Pao C -C (1991) Incidence, determinants and significance of delayed clearance of serum HBsAg in chronic hepatitis B virus infection: A prospective study. *Hepatology* 13: 627–631

Linterman MA, Pierson W, Lee SK, Kallies A, Kawamoto S, Rayner TF, Srivastava M, Divekar DP, Beaton L, Hogan JJ, *et al* (2011) Foxp3+ follicular regulatory T cells control the germinal center response. *Nature Medicine 2011 17:8* 17: 975–982

Liu J, Yang HI, Lee MH, Lu SN, Jen CL, Wang LY, You SL, Iloeje UH & Chen CJ (2010) Incidence and determinants of spontaneous hepatitis B surface antigen seroclearance: a community-based follow-up study. *Gastroenterology* 139: 474–482

Liu S, Hou XL, Sui WG, Lu QJ, Hu YL & Dai Y (2017) Direct measurement of B-cell receptor repertoire's composition and variation in systemic lupus erythematosus. *Genes & Immunity 2017 18:1* 18: 22–27

Loder F, Mutschler B, Ray RJ, Paige CJ, Sideras P, Torres R, Lamers MC & Carsetti R (1999) B cell development in the spleen takes place in discrete steps and is determined by the quality of B cell receptor-derived signals. *J Exp Med* 190: 75–89

Long J, Gong J, Zhu H, Liu X, Li L, Chen B, Ren H, Liu C, Lu H, Zhang J, *et al* (2023) Difference of gut microbiota between patients with negative and positive HBeAg in chronic hepatitis B and the effect of tenofovir alafenamide on intestinal flora. *Front Microbiol* 14: 1232180

Loomba R & Liang TJ (2017) Hepatitis B Reactivation Associated With Immune Suppressive and Biological Modifier Therapies: Current Concepts, Management Strategies, and Future Directions. *Gastroenterology* 152: 1297–1309

Luckheeram RV, Zhou R, Verma AD & Xia B (2012) CD4+T Cells: Differentiation and Functions. *Clin Dev Immunol* 2012: 12

Lund FE & Randall TD (2010) Effector and regulatory B cells: modulators of CD4+ T cell immunity. *Nature Reviews Immunology 2010 10:4* 10: 236–247

Madsen L, Labrecque N, Engberg J, Dierich A, Svejgaard A, Benoist C, Mathis D & Fugger L (1999) Mice lacking all conventional MHC class II genes. *Proc Natl Acad Sci U S A* 96: 10338–10343

Maini MK & Burton AR (2019) Restoring, releasing or replacing adaptive immunity in chronic hepatitis B. *Nat Rev Gastroenterol Hepatol* 16: 662–675

Maslowski KM & MacKay CR (2010) Diet, gut microbiota and immune responses. *Nature Immunology 2011 12:1* 12: 5–9

McMahon BJ (2008) Natural History of Chronic Hepatitis B – Clinical Implications. *The Medscape Journal of Medicine* 10: 91

McMahon BJ (2009) The natural history of chronic hepatitis B virus infection. *Hepatology* 49

McMahon BJ, Holck P, Bulkow L & Snowball M (2001) Serologic and clinical outcomes of 1536 Alaska Natives chronically infected with hepatitis B virus. *Ann Intern Med* 135: 759–768

Milosevic I, Vujovic A, Barac A, Djelic M, Korac M, Spurnic AR, Gmizic I, Stevanovic O, Djordjevic V, Lekic N, *et al* (2019) Gut-Liver Axis, Gut Microbiota, and Its Modulation in the Management of Liver Diseases: A Review of the Literature. *Int J Mol Sci* 20

Mitchison NA (2004) T-cell–B-cell cooperation. *Nature Reviews Immunology 2004 4:4* 4: 308–312

Moody MA & Haynes BF (2008) Antigen-specific B cell detection reagents: use and quality control. *Cytometry A* 73: 1086–1092

Morgan DM, Zhang YJ, Kim J-H, Murillo M, Singh S, Loschko J, Surendran N, Sekulovic O, Feng E, Shi S, *et al* (2024) Full-length single-cell BCR sequencing paired with RNA sequencing reveals convergent responses to pneumococcal vaccination. *Communications Biology 2024 7:1* 7: 1–18

De Muynck K, Vanderborght B, Van Vlierberghe H & Devisscher L (2021) The Gut–Liver Axis in Chronic Liver Disease: A Macrophage Perspective. *Cells* 10: 2959

Nagpal R, Wang S, Solberg Woods LC, Seshie O, Chung ST, Shively CA, Register TC, Craft S, McClain DA & Yadav H (2018) Comparative microbiome signatures and short-chain fatty acids in mouse, rat, non-human primate, and human feces. *Front Microbiol* 9: 413720

Nguyen A, Khoo WH, Moran I, Croucher PI & Phan TG (2018) Single Cell RNA Sequencing of Rare Immune Cell Populations. *Front Immunol* 9: 1553

Ni Y, Lempp FA, Mehrle S, Nkongolo S, Kaufman C, Fälth M, Stindt J, Königer C, Nassal M, Kubitz R, *et al* (2014) Hepatitis B and D viruses exploit sodium taurocholate co-transporting polypeptide for species-specific entry into hepatocytes. *Gastroenterology* 146

Palumbo GA, Scisciani C, Pediconi N, Lupacchini L, Alfalate D, Guerrieri F, Calvo L, Salerno D, Di Cocco S, Levrero M, *et al* (2015) IL6 Inhibits HBV Transcription by Targeting the Epigenetic Control of the Nuclear cccDNA Minichromosome. *PLoS One* 10

Papalexi E & Satija R (2017) Single-cell RNA sequencing to explore immune cell heterogeneity. *Nature Reviews Immunology 2017 18:1* 18: 35–45

Papatheodoridis G, Buti M, Cornberg M, Janssen H, Mutimer D, Pol S, Raimondo G, Dusheiko G, Lok A & Marcellin P (2012) EASL clinical practice guidelines: Management of chronic hepatitis B virus infection. *J Hepatol* 57: 167–185

Penna A, Artini M, Cavalli A, Levrero M, Bertoletti A, Pilli M, Chisari F V., Rehermann B, Del Prete G, Fiaccadori F, *et al* (1996) Long-lasting memory T cell responses following self-limited acute hepatitis B. *Journal of Clinical Investigation* 98: 1185

Portugal S, Obeng-Adjei N, Moir S, Crompton PD & Pierce SK (2017) Atypical memory B cells in human chronic infectious diseases: an interim report. *Cell Immunol* 321: 18

Racanelli V & Rehermann B (2006) The liver as an immunological organ. *Hepatology* 43

Ramesh A, Schubert RD, Greenfield AL, Dandekar R, Loudermilk R, Sabatino JJ, Koelzer MT, Tran EB, Koshal K, Kim K, *et al* (2020) A pathogenic and clonally expanded B cell transcriptome in active multiple sclerosis. *Proc Natl Acad Sci U S A* 117: 22932–22943

Rao DA, Arazi A, Wofsy D & Diamond B (2019) Design and application of single-cell RNA sequencing to study kidney immune cells in lupus nephritis. *Nature Reviews Nephrology 2019 16:4* 16: 238–250

Raziorrouh B, Heeg M, Kurktschiev P, Schraut W, Zachoval R, Wendtner C, Wächtler M, Spannagl M, Denk G, Ulsenheimer A, *et al* (2014) Inhibitory phenotype of HBV-specific CD4+ T-cells is characterized by high PD-1 expression but absent coregulation of multiple inhibitory molecules. *PLoS One* 9

Reikvam DH, Erofeev A, Sandvik A, Grcic V, Jahnsen FL, Gaustad P, McCoy KD, Macpherson AJ, Meza-Zepeda LA & Johansen FE (2011) Depletion of Murine Intestinal Microbiota: Effects on Gut Mucosa and Epithelial Gene Expression. *PLoS One* 6: e17996

Ren YD, Ye ZS, Yang LZ, Jin LX, Wei WJ, Deng YY, Chen XX, Xiao CX, Yu XF, Xu HZ, *et al* (2017) Fecal microbiota transplantation induces hepatitis B virus e-antigen (HBeAg) clearance in patients with positive HBeAg after long-term antiviral therapy. *Hepatology* 65: 1765–1768

Renshaw BR, Fanslow WC, Armitage RJ, Campbell KA, Liggitt D, Wright B, Davison BL & Maliszewski CR (1994) Humoral immune responses in CD40 ligand-deficient mice. *J Exp Med* 180: 1889–1900

Robinson MW, Harmon C & O'farrelly C (2016) Liver immunology and its role in inflammation and homeostasis.

Salimzadeh L, Le Bert N, Dutertre CA, Gill US, Newell EW, Frey C, Hung M, Novikov N, Fletcher S, Kennedy PTF, *et al* (2018) PD-1 blockade partially recovers dysfunctional virus-specific B cells in chronic hepatitis B infection. *J Clin Invest* 128: 4573–4587

Sato Y, Silina K, van den Broek M, Hirahara K & Yanagita M (2023) The roles of tertiary lymphoid structures in chronic diseases. *Nature Reviews Nephrology 2023 19:8* 19: 525–537

Schumann A, Lindemann M, Valentin-Gamazo C, Lu M, Elmaagacli A, Dahmen U, Knop D, Broelsch CE, Grosse-Wilde H, Roggendorf M, *et al* (2009) Adoptive immune transfer of hepatitis B virus specific immunity from immunized living liver donors to liver recipients. *Transplantation* 87: 103–111

Schwabe RF & Greten TF (2020) Gut microbiome in HCC – Mechanisms, diagnosis and therapy. *J Hepatol* 72: 230–238

Seeger C & Mason WS (2015) Molecular biology of hepatitis B virus infection. *Virology* 479–480: 672–686

Seto WK, Lo YR, Pawlotsky JM & Yuen MF (2018) Chronic hepatitis B virus infection. *The Lancet* 392: 2313–2324

Seto WK, Wong DKH, Fung J, Huang FY, Liu KSH, Lai CL & Yuen MF (2014) Linearized hepatitis B surface antigen and hepatitis B core-related antigen in the natural history of chronic hepatitis B. *Clinical Microbiology and Infection* 20: 1173–1180

Shi YH & Shi CH (2009) Molecular characteristics and stages of chronic hepatitis B virus infection. *World Journal of Gastroenterology : WJG* 15: 3099

Shin EC, Sung PS & Park SH (2016) Immune responses and immunopathology in acute and chronic viral hepatitis. *Nat Rev Immunol* 16: 509–523

De Silva NS & Klein U (2015) Dynamics of B cells in germinal centres. *Nature Reviews Immunology 2015 15:3* 15: 137–148

Simonetti J, Bulkow L, McMahon BJ, Homan C, Snowball M, Negus S, Williams J & Livingston SE (2010) Clearance of hepatitis B surface antigen and risk of hepatocellular carcinoma in a cohort chronically infected with hepatitis B virus. *Hepatology* 51: 1531–1537

Sironi L, Bouzin M, Inverso D, D'Alfonso L, Pozzi P, Cotelli F, Guidotti LG, Iannacone M, Collini M & Chirico G (2014) In Vivo Flow Mapping in Complex Vessel Networks by Single Image Correlation. *Scientific Reports 2014 4:1* 4: 1–8

Smith PM, Howitt MR, Panikov N, Michaud M, Gallini CA, Bohlooly-Y M, Glickman JN & Garrett WS (2013) The microbial metabolites, short-chain fatty acids, regulate colonic T reg cell homeostasis. *Science (1979)* 341: 569–573

Su J, Brunner L, Ates Oz E, Sacherl J, Frank G, Kerth HA, Thiele F, Wiegand M, Mogler C, Aguilar JC, *et al* (2023) Activation of CD4 T cells during prime immunization determines the success of a therapeutic hepatitis B vaccine in HBV-carrier mouse models. *J Hepatol* 78: 717–730

Sureau C & Salisse J (2013) A conformational heparan sulfate binding site essential to infectivity overlaps with the conserved hepatitis B virus a-determinant. *Hepatology* 57: 985–994

Swain SL, McKinstry KK & Strutt TM (2012) Expanding roles for $CD4^+$ T cells in immunity to viruses. *Nat Rev Immunol* 12: 136–148

Takeuchi T, Nakanishi Y & Ohno H (2024) Microbial Metabolites and Gut Immunology. *Annu Rev Immunol* 42: 153–178

Taneja V (2018) Sex hormones determine immune response. *Front Immunol* 9: 386034

Tonti E, JiménezdeOya N, Galliverti G, Moseman EA, DiLucia P, Amabile A, Sammicheli S, DeGiovanni M, Sironi L, Chevrier N, *et al* (2013) Bisphosphonates target B cells to enhance humoral immune responses. *Cell Rep* 5: 323–330

Trautmann T, Kozik JH, Carambia A, Richter K, Lischke T, Schwinge D, Mittrücker HW, Lohse AW, Oxenius A, Wiegard C, *et al* (2014) CD4+ T-cell help is required for effective CD8+ T cell-mediated resolution of acute viral hepatitis in mice. *PLoS One* 9

Tripathi A, Debelius J, Brenner DA, Karin M, Loomba R, Schnabl B & Knight R (2018) The gut–liver axis and the intersection with the microbiome. *Nature Reviews Gastroenterology & Hepatology 2018 15:7* 15: 397–411

Tu T, Budzinska MA, Shackel NA & Urban S (2017) HBV DNA Integration: Molecular Mechanisms and Clinical Implications. *Viruses* 9

Unanue ER, Turk V & Neefjes J (2016) Variations in MHC Class II Antigen Processing and Presentation in Health and Disease. *Annu Rev Immunol* 34: 265–297

Urbani S, Boni C, Amadei B, Fisicaro P, Cerioni S, Valli MA, Missale G & Ferrari C (2005) Acute phase HBV-specific T cell responses associated with HBV persistence after HBV/HCV coinfection. *Hepatology* 41: 826–831

Vinuesa CG & Cyster JG (2011) How T cells earn the follicular rite of passage. *Immunity* 35: 671–680

Vinuesa CG, Linterman MA, Goodnow CC & Randall KL (2010) T cells and follicular dendritic cells in germinal center B-cell formation and selection. *Immunol Rev* 237: 72–89

Voican CS, Mir O, Loulergue P, Dhooge M, Brezault C, Dréanic J, Chaussade S, Pol S & Coriat R (2016) Hepatitis B virus reactivation in patients with solid tumors receiving systemic anticancer treatment. *Ann Oncol* 27: 2172–2184

Wang H, Luo H, Wan X, Fu X, Mao Q, Xiang X, Zhou Y, He W, Zhang J, Guo Y, *et al* (2020a) TNF-α/IFN-γ profile of HBV-specific CD4 T cells is associated with liver damage and viral clearance in chronic HBV infection. *J Hepatol* 72: 45–56

Wang J, Wang Y, Zhang X, Liu J, Zhang Q, Zhao Y, Peng J, Feng Q, Dai J, Sun S, *et al* (2017) Gut microbial dysbiosis is associated with altered hepatic functions and serum metabolites in chronic hepatitis B patients. *Front Microbiol* 8: 2222

Wang L & Wan YJY (2019) The role of gut microbiota in liver disease development and treatment. *Liver Res* 3: 3–18

Wang R, Tang R, Li B, Ma X, Schnabl B & Tilg H (2020b) Gut microbiome, liver immunology, and liver diseases. *Cellular & Molecular Immunology 2020 18:1* 18: 4–17

Wang X, Chen L, Wang H, Cai W & Xie Q (2020c) Modulation of bile acid profile by gut microbiota in chronic hepatitis B. *J Cell Mol Med* 24: 2573

Warren A, Le Couteur DG, Fraser R, Bowen DG, McCaughan GW & Bertolino P (2006) T lymphocytes interact with hepatocytes through fenestrations in murine liver sinusoidal endothelial cells. *Hepatology* 44: 1182–1190

Webster GJM, Reignat S, Maini MK, Whalley SA, Ogg GS, King A, Brown D, Amlot PL, Williams R, Vergani D, *et al* (2000) Incubation phase of acute hepatitis B in man: Dynamic of cellular immune mechanisms. *Hepatology* 32: 1117–1124

Wieland SF, Spangenberg HC, Thimme R, Purcell RH & Chisari F V. (2004) Expansion and contraction of the hepatitis B virus transcriptional template in infected chimpanzees. *Proc Natl Acad Sci U S A* 101: 2129–2134

Wisse E, Braet F, Luo D, De Zanger R, Jans D, Crabbé E & Vermoesen A (1996) Structure and function of sinusoidal lining cells in the liver. *Toxicol Pathol* 24: 100–111

Wu X, Su Z, Cai B, Yan L, Li Y, Feng W & Wang L (2018) Increased Circulating Follicular Regulatory T-Like Cells May Play a Critical Role in Chronic Hepatitis B Virus Infection and Disease Progression. *Viral Immunol* 31: 379–388

www.who.int/news-room/fact-sheets

Xu J, Foy TM, Laman JD, Elliott EA, Dunn JJ, Waldschmidt TJ, Elsemore J, Noelle RJ & Flavell RA (1994) Mice deficient for the CD40 ligand. *Immunity* 1: 423–431

Yan H, Peng B, He W, Zhong G, Qi Y, Ren B, Gao Z, Jing Z, Song M, Xu G, *et al* (2013) Molecular Determinants of Hepatitis B and D Virus Entry Restriction in Mouse Sodium Taurocholate Cotransporting Polypeptide. *J Virol* 87: 7977–7991

Yang PL, Althage A, Chung J, Maier H, Wieland S, Isogawa M & Chisari F V. (2010) Immune effectors required for hepatitis B virus clearance. *Proc Natl Acad Sci U S A* 107: 798–802

Yuen MF, Chen DS, Dusheiko GM, Janssen HLA, Lau DTY, Locarnini SA, Peters MG & Lai CL (2018) Hepatitis B virus infection. *Nat Rev Dis Primers* 4

Zeng Y, Chen S, Fu Y, Wu W, Chen T, Chen J, Yang B & Ou Q (2020) Gut microbiota dysbiosis in patients with hepatitis B virus-induced chronic liver disease covering chronic hepatitis, liver cirrhosis and hepatocellular carcinoma. *J Viral Hepat* 27: 143–155

Zhao M, Jiang J, Zhao M, Chang C, Wu H & Lu Q (2021) The Application of Single-Cell RNA Sequencing in Studies of Autoimmune Diseases: a Comprehensive Review. *Clin Rev Allergy Immunol* 60: 68–86

Zheng D, Liwinski T & Elinav E (2020) Interaction between microbiota and immunity in health and disease. *Cell Research 2020 30:6* 30: 492–506

Zheng M, Yu J & Tian Z (2013) Characterization of the liver-draining lymph nodes in mice and their role in mounting regional immunity to HBV. *Cellular & Molecular Immunology 2013 10:2* 10: 143–150

Zhu Q, Xia P, Zhou X, Li X, Guo W, Zhu B, Zheng X, Wang B, Yang D & Wang J (2019) Hepatitis B Virus Infection Alters Gut Microbiota Composition in Mice. *Front Cell Infect Microbiol* 9: 377

